THE ROLE OF THE GLYCOPROTEIN BCLB IN THE EXOSPORIUM OF *BACILLUS ANTHRACIS*.

by

BRIAN M. THOMPSON

B.S., Kansas State University, 2002

AN ABSTRACT OF A DISSERTATION

Submitted in partial fulfillment of the requirements for the degree

DOCTOR OF PHILOSOPHY

Department of Diagnostic Medicine/Pathobiology
College of Veterinary Medicine

KANSAS STATE UNIVERSITY
Manhattan, Kansas

2007

ABSTRACT

Anthrax is a highly fatal disease caused by the gram-positive, endospore-forming, rod-shaped bacterium *Bacillus anthracis*. Spores, rather than the vegetative bacterial cells, are the source of anthrax infections. The spores of *B. anthracis* are enclosed by a prominent loose-fitting structure called the exosporium. The exosporium is composed of a basal layer and an external hair-like nap. The filaments of the hair-like nap are made up largely of a single collagen-like glycoprotein called BclA. A second glycoprotein, BclB, has been identified in the exosporium layer. The specific location of this glycoprotein within the exosporium layer and its role in the biology of the spore are unknown. We created a mutant strain of *B. anthracis* ΔSterne that carries a deletion of the *bclB* gene. Immunofluorescence studies indicated that the mutant strain produced spores with increased amounts of the BclA glycoprotein expressed on their surface. Differences in exosporium composition between the mutant and wild-type spores were identified. The mutant was also found to possess structural defects in the exosporium layer of the spore (visualized by electron microscopy, immunofluorescence, and flow cytometry) resulting in an exosporium that is more fragile than that of a wild-type spore and is easily lost. The resistance properties of the mutant spores were unchanged from that of the wild-type spores. The *bclB* mutation did not affect spore germination or kinetics of spore survival within macrophages. BclB plays a key role in the formation and maintenance of a rigid and complete exosporium structure in *B. anthracis.* BclB plays a key role in the formation and maintenance of the exosporium structure in *B. anthracis.*

.

THE ROLE OF THE GLYCOPROTEIN BCLB IN THE EXOSPORIUM OF *BACILLUS ANTHRACIS*.

by

BRIAN M. THOMPSON

B.S., Kansas State University, 2002

A DISSERTATION

Submitted in partial fulfillment of the requirements for the degree

DOCTOR OF PHILOSOPHY

Department of Diagnostic Medicine/Pathobiology
College of Veterinary Medicine

KANSAS STATE UNIVERSITY
Manhattan, Kansas

2007

Approved by:

Major Professor
George C. Stewart

COPYRIGHT

THE ROLE OF THE GLYCOPROTEIN BCLB IN THE EXOSPORIUM OF *BACILLUS ANTHRACIS*

BRIAN M. THOMPSON

2007

Table of Contents

Materials and Methods

Results

Additional Results

List of Tables

Table

List of Figures

Figure

Acknowledgements

I would like to thank Dr. George Stewart for advising me and supporting me over the last few years, Dr. T.G. Nagaraja for assisting in my transition between colleges, and Dr. Roman Ganta for starting me off in science. I would also like to thank Matt Kuntsman and Katie Spears for helping me stay sane all these years.

Literature Review

Introduction

"For neither might the hides be used, nor could one cleanse the flesh by water or master it by fire. They could not even shear the fleeces, eaten up with sores and filth, nor touch the rotten web. Nay, if any man donned the loathsome garb, feverish blisters and foul sweat would run along his fetid limbs, and not long had he to wait ere the accursed fire was feeding on his stricken limbs."

Virgil: The Georgics III, 30 B.C.

Bacillus anthracis, a spore-forming gram positive bacterium, is the etiological agent of anthrax. The anthrax disease has been described in history as early as the book of Genesis in the 15th century as the 5th plague that killed the cattle of the Egyptians (160). Greek, Roman, Hindu, and European literature all contain reports of anthrax outbreaks. Major outbreaks occurred in Germany in the 14th century and in Russia during the 17th century. The diseased animals were buried in deep pits to avoid spreading of the contagion to the human populations and other cattle in the area. Centuries later the spore-ridden pit could be unearthed by an unsuspecting farmer plowing a field and exposing his whole herd to the ages-old anthrax spores. Most of the more modern outbreaks occurred among those with occupations related to livestock and livestock byproducts. Wool workers were very susceptible to the disease due to the large numbers of spores inhaled each day from the contaminated wool, and in many areas the disease became known as "woolsorter's disease."

Anthrax, although uncommon in developed countries, is still a threat among developing countries. Anthrax is endemic in Central America, the Caribbean, Spain, Greece, the Middle East, and much of Africa. West Africa is the most affected region in the world with continuous outbreaks among both wildlife and humans, with the largest reported outbreak in 1979-1980 consisting of 10,000 cutaneous anthrax infections. Annually there are roughly 20,000 to 100,000 cases of anthrax worldwide (161).

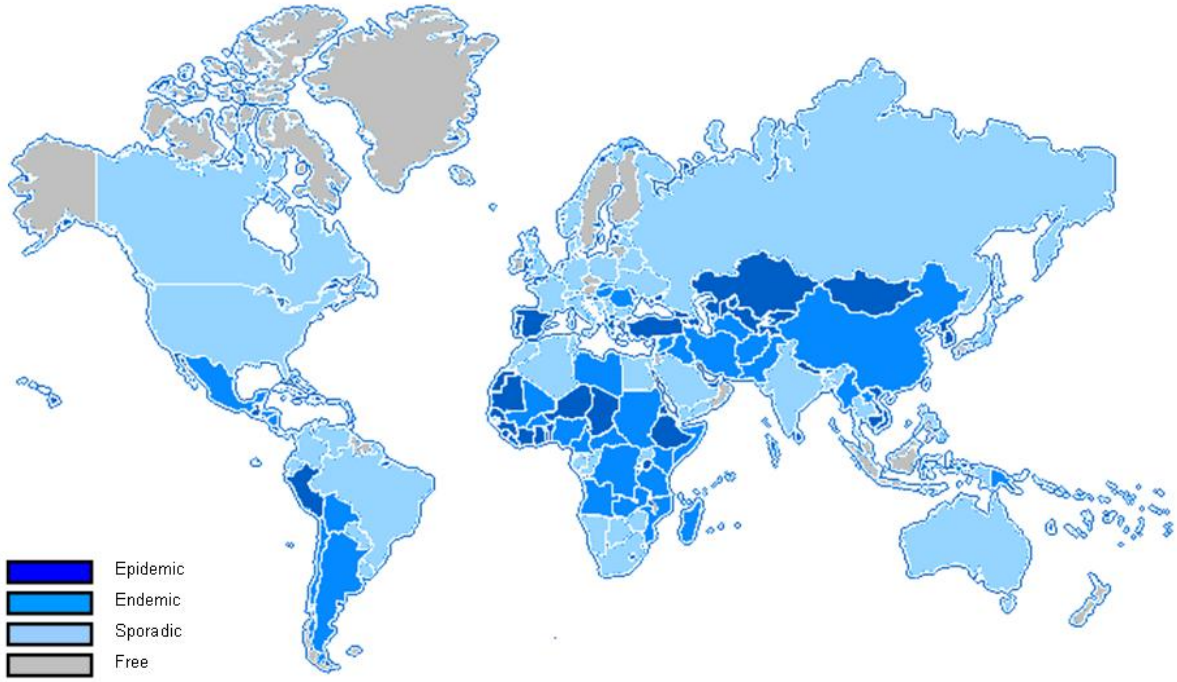

Figure 1: Incidence of Bacillus anthracis outbreaks. Adapted from the History Magazine, 2002

Bacillus anthracis was first described by Davaine, a French parasitologist in 1850. Robert Koch and Louis Pasteur, two founding fathers of modern medical microbiology, both worked on the ancient pathogen. In 1888, Koch first described the complete sporulation to germination life cycle of *anthracis* and other spore-formers (1). Louis Pasteur observed that leaving cultures of *B. anthracis* in the sun caused them to become avirulent. The cultures threw off their virulence plasmids due to the increased temperature, leading Pasteur to develop the concept of attenuation and the creation of weakened bacterial vaccines. These discoveries led to the concepts and vaccine design strategies which have saved millions of lives over the years.

Although most human cases of anthrax are among people who come in contact with animals and animal byproducts, recently some new cases are due to the development of anthrax as a biological weapon. It is an ideal bioterrorism agent, able to be produced in mass quantities and covered in a resistant coat to allow it to remain stable, not require refrigeration for storage, and maintain virulence for hundreds of years. Aerosolization of the spores as a means of dissemination could have dire consequences, infecting unknown thousands with flu-like symptoms and leading to heavy mortality rate. The World Health Organization estimates that 50 kg of weapons grade anthrax released by an aircraft over an urban population of 5 million would result in 250,000 cases of predominantly inhalation anthrax, and at an economic impact of 26.2 billion dollars per 100,000 exposed (125).

Anthrax has been listed as a category A select agent, along with tularemia, smallpox, plague, and other pathogens. The USA, USSR, France, and England have all developed anthrax as a weapon of war. In 1937, the Japanese used *B. anthracis* spores as a weapon against the Chinese, and did extensive testing of the bacterium on Chinese prisoners. Recently, Iraq has also

admitted to having an active biological warfare program including anthrax. The tragic release of huge stockpiles of biological weapons grade spores at the Russian town of Sverdlovsk in 1979 led to 64 deaths in the surrounding populace. The recent Amerithrax letters in the US lead to 18 cases of anthrax, 11 inhalational cases of which 5 died, and 7 cutaneous cases. The development of better vaccines to anthrax has been a top priority in many countries over the last few years.

General Phenotype/Genotype

Bacillus anthracis is a Gram-positive, non-motile, aerobic spore former. It is primarily a pathogen of ruminants, but occasionally infects humans. This rod-shaped bacterium contains a low G+C DNA content. When nutrients are scarce, the bacterium produces a centrally located, hardy spore that can resist many environmental insults and survive until the environment is again suitable for stable growth. The bacterium contains a unique amino acid based capsule. *Bacillus anthracis* is one of the few bacteria that contain group II introns; novel genetic elements that have properties of both catalytic RNAs and retroelements. They encode reverse transcriptase and are either active retroelements, or are derivatives of retroelements, and are able to self-splice (60). Whether the *B. anthracis* spore is able to germinate and subsequently thrive in the soil is still under debate, but a recent study has shown that it can germinate and grow in the rhizosphere of some grassy plants (68).

Many advances have occurred in the last 30 years in the study of the *Bacillus* pathogens. Although there are numerous *Bacillus* species, only three have been identified as major pathogens. *Bacillus anthracis* is primarily a pathogen of ruminants, and its infection is initiated upon access of the spores into the body. *Bacillus cereus*, genetically related to *anthracis*, is a major food poisoning agent and causal agent of endopthalmitis. *Bacillus thuringiensis* is a major pathogen of insects with its insecticidal toxins and is currently used as an insect control agent. The major difference between *B. anthracis* and *B. cereus* remains the presence of two virulence plasmids in the *B. anthracis* strains. Other than the presence of the two virulence plasmids, there are about 150 genes that have been shown to differ between *B. cereus* and *B. anthracis*.

Differentiation of Strains

The *Bacillus cereus* group is one of the most taxonomically similar groups of eubacteria (147). In fact, DNA-DNA hybridization and pulse field electrophoresis have shown great homology among *B. anthracis*, *B. thuringiensis*, and *B. cereus* (33). A recent multilocus enzyme electrophoresis study has concluded that the members of this group belong to one species (51). Although traditionally the presence of the *anthracis* plasmids pX01 and pX02 were enough to differentiate the species from others of the *B. cereus* family, recent reports of pX01 and pX02-like plasmids in *B. cereus* have led these plasmids to not be reliable in differentiation studies (126). Analysis of the RNA polymerase B subunit genes can partially differentiate *B. anthracis* from its sister species (50). Differentiation between *B. cereus* and *B. anthracis* has also been attempted by searching for gamma phage specific for one species of the *B. cereus* family. The presence of the crystal insecticidal toxins helps differentiate *B. thuringiensis* from the others

strains. Some strains of *Bacillus cereus* and *Bacillus thuringiensis* spores have filamentous appendages (48, 57). Differentiation between strains has also been tried using variability in optical chromatographic readings, although this may be due to some of the differences in exosporium filaments which are not present in all the species and strains of the various members of the *Bacillus cereus* family (59). Polymorphism in the BclA exosporium gene has also led to the development of a PCR-based test to differentiate *Bacillus cereus* family members (99).

Virulence Factors

The pX01 plasmid

The first of the two virulence plasmids in *B. anthracis* is pX01. This 181 kb plasmid encodes approximately 143 ORFs, including the genes for the production of the three toxin components that make up the two anthrax toxins. The genes responsible for the production of the anthrax toxins are *pagA* (encoding protective antigen), *lef* (containing lethal factor), and *cya* (encoding edema factor) genes. Although the GC content of 33% would suggest that it is a natural *Bacillus* plasmid the pX01 plasmid contains a pathogenicity island of 44 kb which is surrounded by two insertion elements and several genes predicted to be the result of horizontal transfer. pX01 also encodes *gerX*, a germination operon that is essential for virulence in mice (40, 45). The anthrax toxin genes have also been found, albeit rarely, in *B. cereus* respiratory infection isolates that contain pX01-like plasmids (126). These strains have also been found to contain polysaccharide capsule clusters on a separate virulence plasmid.

Anthrax produces two binary toxin combinations, consisting of a binding component and a effector component. The first aspect of the toxin entry into host cells is the binding of protective antigen (PA) to a receptor. It is known as protective antigen because antibodies produced against PA protect the animal during experimental infection by blocking access of toxins into the cells. There are actually two anthrax toxin receptors, ANTXR1 and ANTXR2 (32). ANTXR1 corresponds to anthrax receptor/tumor endothelial marker 8, and ANTXR2 corresponds to capillary morphogenesis protein 2. After the PA binds to one of the receptors on susceptible cells it combines into a heptamer in lipid rafts upon the cell membrane (132). The PA precursor is a protein of 83,000 molecular weight (PA83). After insertion into the target cell membrane the PA83 heptamer is cleaved by furin or other furin-like proteases to produce a 63,000 molecular weight protein (PA63) (162). The PA63 heptamer now contains a binding domain to facilitate the binding of lethal factor and edema factor. Both lethal factor (LF), the product of the *lef* gene, and edema factor (EF), product of the *cya* gene, have a common N-terminal domain that binds to the cleaved PA63 heptamer. The binding of the PA63 heptamer to the lethal or edema factor leads to the complex being brought into the cell by receptor-mediated endocytosis by a clathrin-dependent process (133). As the pH of the endocytic vesicle decreases, this acidic environment leads a change in conformation and formation of a pore by the heptamer, releasing the edema factor and lethal factors into the cell cytoplasm. The combination of PA and LF, called lethal toxin (LT), leads to death in high doses in experimental animals (56). The combination of PA and EF, called edema toxin (ET), leads to production of edema in the skin of animals (56). None of the components alone are toxic, as lethal factor and edema factor can not access the cell without PA, which by itself causes no pathology.

Lethal Toxin

Lethal Toxin is a zinc metalloprotease whose target is the N-terminus of MAPKKs, MEK1, and MEK2 (196). It is capable of cleaving all of the various MAPKKs except MEK5, and these cleavage events lead to rapid cell lysis by apoptosis in murine macrophages. It is believed that the majority of cellular toxicity associated with anthrax infection is due to this intracellular hydrolysis of important host protein substrates (163). Lethal Factor can also lead to the collapse of vasculature and hypoxia. The characteristic pleural effusions and necrosis of the liver, spleen, and bone have all been attributed to the hypoxia-mediated damage due to LT (56).

Edema Toxin

The action of the edema toxin (ET) is dependent upon the host calcium-binding protein calmodulin. ET efficiently converts intracellular ATP into cAMP. The edema factor adenylate cyclase is at least 1,000 fold more active than any of the host adenylate cyclases in cAMP production, and leads to large amounts of secreted fluid in cells (56, 112, 164). Purified ET has been shown to inhibit the chemotactic response of polymorphonuclear leukocytes and their subsequent phagocytosis (165, 166). Highly-purified ET can cause death in a BALB/c mouse at very low doses and is more lethal than LT. Purified ET leads to accumulation of fluid in the intestines, hemorrhaging of the ileum and adrenal glands, lesions in the lymphoid organs, bone, bone marrow, GI mucosa, heart and kidneys; and multiorgan failure (56). *In vitro*, ET inhibits adhesion of neutrophils, stimulates their apoptosis, and blocks proliferation of lymphocytes (112).

In the host it is likely that the two toxins act in synergy to produce all the symptoms of anthrax. Both are produced by 3 hrs after germination and suppress superoxide and NO production (118). In later stages of the disease, lethal levels of toxins induce the development of the cytokine-independent shock-like death associated with anthrax (56, 112, 136). EF and LF deficient strains are greatly attenuated. The cleavage of MEK 1, 2, and 3 *in vitro* by LF leads to activation of macrophages and related signaling would produce cytokines such as TNFα, IL-1, and IL-6 (163). ET inhibits not only induced TNFα secretion but also inhibits phagocytosis and oxidative burst activities. The two toxins function together to induce shock in a rat model (112). Mice deficient in macrophages are resistant to LF challenge (124). Both toxins cause hypotension (112). LT leads to high extravasation of fluid and ET leads to increased cAMP levels in cardiac pacemaker cells and decreased heart rate (112). More on the actions of the two toxins, as well as their role in modification of the immune system can be found in the **Disease Progression** section below.

The pX02 plasmid

The second virulence plasmid in *B. anthracis* is the 96 kb plasmid pX02, which contains the *capA, capC, capB*, and *capD* genes responsible for the production of the characteristic poly-D-glutamic acid capsule. This capsule is produced and surrounds the cell after outgrowth *in vivo*, or *in vitro* in the presence of bicarbonate, hindering phagocytosis and perhaps playing a role in adherence. The weakly antigenic capsule may act to hide the cells from the adaptive immune system. In addition to the capsule genes, pX02 encodes Dep, a capsule degradation enzyme, and

several global regulators of virulence. The first of these regulators is AcpA, which interacts with and turns on the capsule biosynthesis genes (129). The second, AcpB, also turns on the capsule biosynthesis genes. Both the AcpA and AcpB regulators are turned on by the master regulator, AtxA. AtxA is encoded on pX01, and *atxA* mutants are avirulent (127). The pX02 plasmid is often spontaneously lost, especially during growth at elevated temperatures, such as 42ºC (30).

Virulence Regulation

Control of virulence gene expression in *B. anthracis* is highly dependent upon *atxA*, a global virulence regulatory gene located on the virulence plasmid pX01. In fully virulent strains, containing both the pX01 and pX02 plasmids, AtxA acts as a global regulator controlling expression of the pX02-encoded capsule biosynthesis genes, *capBCAD*; as well as the toxin structural genes *pagA*, *lef*, and *cya* on the pX01 plasmid (127, 128). AtxA also controls expression of a number of other genes on the chromosome (131). PagR is a major regulator of the *pagA*, *cya*, and *lef* genes. PagR has also been found to affect transcription of the S-layer genes and biases the cells in the presence of CO_2 to produce the Ea1 S-layer protein over the Sap S-layer protein during infection (130). Regulation of PagR is controlled by AtxA (130, 127). This effect may not be direct and is likely the result of intermediate factors (67). CapD (Dep) is a degradative enzyme which can break down the capsule into small D-glutamic acid fragments that are secreted from the cell. AtxA, in the current Koehler model, regulates the capsule genes through the pX02 encoded genes *acpA* and *acpB* (131). *acpA* and *acpB* isogenic mutants have no effect on capsule production, but an *acpA/acpB* double mutant is completely devoid of capsule (129). AcpA and AcpB share substantial amino acid and functional similarities. For

many AtxA-regulated genes, including *acpA, acpB*, and the toxin genes, expression is greatly induced under conditions of high CO_2 or bicarbonate. This effect (*acpA*, 23-fold and *acpB*, 59-fold) is greater than can be explained by the bicarbonate induction of *atxA* alone (2.5-fold), suggesting that another regulator or bicarbonate itself upregulates the *acpB* and *acpA* promoters (66, 131, 129).

This reason for bicarbonate and temperature induction of toxin and capsule genes may be from recognition of host surroundings and the necessary induction of toxin production to survive and thrive in the host environment. The concentration of bicarbonate for optimal expression is the same concentration that is found in the bloodstream, 48 mM. Toxin production is also regulated by the sporulation regulator Spo0A, which exerts its effect through the regulator AbrB; and recently been reported to be regulated by GerH, potentially through Spo0A (155).

S-layer and Capsule

In addition to the usual peptidoglycan and cytoplasmic membrane of most Gram-positive bacteria, *B. anthracis* encodes two other surface layers. The first layer is formed at the outermost point of the cell wall. A single protein polymer is assembled in a large crystalline sheath that surrounds the entire bacterium (7). The S-layer may play a role in involvement of cell shape maintenance, protection from complement, interactions with host macrophages, and in molecular sieving (5). The S-layer is comprised of one of two proteins depending on the growth phase of the bacterium. The protein Sap (surface array protein) is first assembled into the S-layer during growth, and is slowly replaced during stationary phase with the Ea1 protein

(Extractable antigen 1) (6). The S-layer proteins can comprise 5-10% of the total cell protein (5). S-layer proteins have not been found to be important in virulence, as the LD_{50} in mice doesn't change in the absence of the S-layer, however, they may confer increased resistance to complement pathway-mediated defenses. Along with the EA1 and Sap S-layer proteins, other putative S-layer proteins have recently been found (61). These S-layer proteins are able to be recognized by the immune system as potential vaccine candidates (61).

Surrounding the entire bacterium is the capsule, composed of polymers of poly-D-glutamic acid (5, 154). An amino-acid composed capsule is rare, but it has also found on the related species *Bacillus licheniformis*. The two most important virulence factors are considered to be the capsule and toxins.. The capsule is encoded on the pX02 plasmid by the *capB, capC*, and *capA* genes. The role of the capsule in pathogenesis is to interfere with phagocytosis of the bacterium and to surround the bacterium in a poorly immunogenic polymer to help hide the bacterium cell membranes from the immune system (5). Both survival of the bacterium in the blood stream and progression to septicemia are also enhanced by the presence of the capsule. During germination and outgrowth in the presence of serum and elevated levels of CO_2, the capsule is released through openings on the vegetative cell surface. The formation of the capsule is exterior to the S-layer, but does not require the S-layer for its attachment to the cell surface (5, 6, 7). The capsule genes are essential for virulence in a mouse model of inhalational anthrax (119).

Other Virulence Factors

Bacillus anthracis encodes for a number of other virulence factors. Recently it has been found that if *B. anthracis* is grown under anaerobic conditions, it can induce production of the anthrolysins (62). The anthrolysins consist of Anthrolysin O and three phospholipases C. These four anthrolysins have overlapping function, but are essential for virulence in an inhalational model of anthrax in mice (35, 36). Expression of the anthrolysins occurs in the early stages of infection, as they are turned on when the spores are engulfed by macrophages (62). In fact, mutations in the phospholipases C lead to the inability of spores to grow in association within macrophages. The hemolysin Anthrolysin O is secreted by vegetative cells and is lethal to human leukocytes, monocytes, and lymphocytes *in vitro*, in addition to lysing erythrocytes (148). Activity of Anthrolysin O is hindered by the presence of cholesterol, as minute quantities of cholesterol or sera leads to inactivation of the hemolysin (148).

Bacillus cereus and *Bacillus thuringiensis* control a number of secreted hemolysins by the regulon PlcR (63). The PlcR regulon in *B. anthracis* has been reported to be silent due to a *plcR* gene truncation (63). But under strict anaerobic conditions the anthrolysins are active, suggesting that the truncated PlcR of *B. anthracis* is active under these conditions (62). The PlcR regulon has been reported to inhibit sporulation and is incompatible with the AtxA-controlled virulence regulon (64). It was originally predicted to have been evolutionarily silenced due to this incompatibility (64). All the anthrolysin determinants in *B. anthracis* have PlcR binding sites. Transcription of *plcR* is activated during stationary phase in *B. cereus* and is autoregulated. PlcR activates at least 15 genes encoding proteases, phospholipases, and two enterotoxin complexes (65, 63).

Other virulence factors include the sortase genes, *srtA* and *srtB,* which play a role in the interaction of the vegetative bacterial cells and the macrophages. This role may be indirect, as the sortase mutants are not able to fully localize bacterial proteins to the exterior layers of the cells. These mistranslocated proteins are likely the effector molecules that allow the bacterium to survive inside the host cells (37). *Bacillus anthracis* also requires the presence of siderophores for growth in macrophages and for virulence, and like other pathogens, need this continual uptake of iron to be able to replicate efficiently enough to maintain an infection (38, 46). *B. anthracis* has two distinct siderophore gene clusters (38). Due to the dramatic growth of *B. anthracis* in the host, it is understandable that *anthracis* would need siderophores to obtain sufficient iron at an optimal rate for maximal growth. This increased growth is essential for virulence as the bacteria overruns the host immune system.

Two putative collagen binding adhesions have been identified and are expressed on the surface of *B. anthracis* vegetative cells (52). These adhesions may help the bacterium bind to the extracellular matrix and help protect them from attack from the immune system. The Gram-positive cell surface is composed of many macromolecules, including peptidoglycan, techoic and lipotechoic acids (LTAs), S-layer, and cell surface proteins. The teichoic and lipoteichoic acids give the bacterium an overall negative charge. This negative charge on the teichoic acids becomes a major attractant for positively charged antibacterial compounds (93). Many Gram-positive organisms have developed the means of coating the negative charges on the LTA with D-alanine. In *B. anthracis* this is accomplished by the products of the *dltABCD* operon. *dltA* encodes a D-alanine:D-alanyl carrier protein ligase which covalently attaches D-alanine to the 4' phosphopantetheine prosthetic group found on the D-alanyl carrier protein Dcp encoded by *dltC*

(93). DltB is a transmembrane channel and DltD is a chaperone protein ensuring the fidelity of the D-alanine ligation to Dcp. Loss of function of any of the four *dlt* genes is sufficient to terminate the entire pathway (93). Addition of D-alanine to LTA in outgrown *B. anthracis* led to complete resistance to lysozyme and β-defensin-1 (produced by endothelial cells), and moderate resistance to $sPLA_2$, HNP-1, and HNP-2 (defensins produced by phagocytic cells) (93). Addition of D-alanine to the LTA also allowed the vegetative cells to better survive engulfment by macrophages and afforded better resistance to positively-charged antibiotics (93). *Staphylococcus aureus* and *Listeria monocytogenes* strains lacking the *dltABCD* operon are less virulent in their respective mouse models (73, 90).

The exosporium of the endospore of *B. anthracis* contains an arginase (141). Many bacterial pathogens are killed by efficient production of NO and other free radicals by macrophages. The arginase in spores of *B. anthracis* can compete with the macrophage for arginine, inhibiting its ability to be modified into NO (141).

Diseases

The symptoms and outcomes of persons infected with *B. anthracis* differ based upon the route of infection. Spores gain entry into the body either thru open wounds in the skin, by ingestion, or by inhalation of the spores into the lungs. Infection by all three routes can lead to serious and lethal systemic infection.

One of the most common routes of infection in humans is entry of spores into abrasions in the skin. The incubation period ranges from 1-12 days. The cutaneous form is first characterized by the formation of a black pustule at the site of entry as the bacteria produces edema and lethal factors. This painless eschar leads to significant edema of the surrounding areas, and in some cases the bacterium can gain access to the bloodstream, leading to systemic anthrax (29). The mortality rate of cutaneous anthrax infections is about 20% without antibiotic treatment, but cases of progression to systemic anthrax can be up to 95% lethal.

The second route of infection, although fairly rare, is gastrointestinal anthrax. This is usually caused by ingestion of undercooked meat from an infected animal, and this was last reported in the USA in Minnesota in 2000 (30). The incubation period is 1-7 days. Symptoms include bloody diaherria, severe abdominal pain, fever, and nausea. This can be a common route of infection in herbivores, as the spores can be ingested along with associated plant matter. This is predicted to be the main lifecycle of *B. anthracis*, as some experts point out that *B. anthracis* probably does not maintain a full lifecycle in the soil. In humans the mortality rate of ingestional anthrax is about 25-60%, even with appropriate antibiotic therapy (29).

The last, and by far the most lethal route of infection, is inhalational anthrax. This is the most serious concern regarding anthrax, as an aerosolized attack using *Bacillus* spores could be potentially devastating if unleashed on a naïve population. Disease is rarely recognized before bacteremia and toxemia develop. It is difficult to diagnose, as it produces non-descript flu-like symptoms early in the course of infection. The Department of Defense estimates the LD_{50} in humans to be about 8-10,000 spores to cause infection, although that number varies greatly from

report to report. After a short time, the bacteria flood the bloodstream and the patient becomes septic, leading to shock, fever, and respiratory failure. The patient usually succumbs within 24 hours of the beginning of sepsis. At this late stage the bacteria are very resistant to treatment, and the mortality rate is as high as 95% (29). It is important that antibiotic therapy in cases of inhalational anthrax be continued for up to 60 days, as spores can persist in the lungs and cause repeat infection after the usual 14 day antibiotic therapy (167, 170).

Very rare reports of meningitis due to *B. anthracis* are usually a complication that arises from infection elsewhere in the body and dissemination after bacteremia and is extremely fatal (approaching 100%) (29). Renal anthrax and ophthalmic anthrax have also been described, but are extremely rare.

Treatment

Treatment of cutaneous anthrax is intramuscular administration of 1 million units of procaine penicillin every 12-24 hours for 5-7 days (26). In serious illness, usually septic or pulmonary anthrax, 2 million units of penicillin G per day is administered intravenously or 500,000 units administered intravenously through a slow drip every 4-6 hours. Streptomycin, in conjunction with penicillin, has a synergistic effect in 1-2 g doses per day. Some penicillin-resistant strains of *B. anthracis* have been found (168). Unfortunately, the strain used in the Amerithrax letters and in many historic outbreaks produces an inducible β-lactamase (169). It appears to be highly sensitive *in vitro*, but *in vivo* in patients with high bacterial loads the bacteria may induce β-lactamase production and penicillin resistance. There are published

reports of strains resistant to penicillin *in vitro* and *in vivo* (29). Ciproflaxin at 400 mg intravenously twice daily is the new recommended treatment for those infected with anthrax (26). The recommended regimen in inhalational anthrax is ciproflaxin plus 1-2 additional antibiotics (26). The duration of treatment should be 60 days for inhalational anthrax, as ungerminated spores may germinate after prolonged stay in the lungs post-treatment and emerge into fatal infection (170).

Disease Progression

Inhalational anthrax always initiates with the entry of spores into the pulmonary cavity. Soon after entry, the spores are taken up by resident alveolar macrophages and lung dendritic cells (LDCs) (39, 41, 42, 92, 116, 122, 134). Alveolar macrophages consist of the major phagocytic population in the lungs, although LDCs are more efficient at phagocytosis of spores than alveolar macrophages. Spores and germinated vegetative cells are able to be internalized by fibroblasts and epithelial cell lines *in vitro* as well (34). Alveolar macrophages are the primary site of spore germination *in vivo* (22, 40, 41). Spores germinate in the phagolysosome of the macrophages while in the lungs or en route to the mediastinal lymph nodes (39). Germination within macrophages is dependent on the *gerH* germination operon and the presence of germinants L-alanine and adenosine found inside the macrophages (22). There is little if any germination inside the lung mucosa itself (77). Alveolar macrophages are thought to act as a "Trojan horse," delivering the bacteria to the unsuspecting lymph nodes. LDCs also sample lung environments and could potentially deliver the spores to the mediastinal lymph nodes as well. Both macrophages and LDCs express sporocidal activities *in vitro* (2, 28, 49, 92, 115, 122, 171).

There is roughly a 10-fold decrease in CFU of engulfed spores in the first 2.5 hours *in vitro*. The roughly 10% that do persist begin to multiply and overtake the macrophages. Macrophages play a critical role in the mouse model of infection, whereas PMNs play just a minor secondary role (124, 138). A macrophage-deficient mouse model was more susceptible to infection, showing a role of the macrophage in resisting infection and not just as a "Trojan horse" (124).

Many spore and vegetative cell motifs are recognized by host pattern recognition receptors through MyD88-dependent and –independent processes. Vegetative cells signal through TLR2, most likely due to the presence of lipotechoic and techoic acids in the cell wall, and Anthrolysin O signals through TLR4 (27). NOD protein signaling, which recognizes bacterial peptidoglycan components, leads to upregulation of inflammatory cytokines and activation of macrophages. *Bacillus* spp. have been found to be the most stimulatory of all bacteria tested in their ability to activate NOD1 (27). *Bacillus* spp also activate NOD2, but these cell wall recognition receptors are not species specific (2). NOD1 recognizes iE-DAP dipeptide and related structures found in all Gram-negative and some Gram-positive bacteria and NOD2 recognizes muramyl dipeptide (MDP). Most of the stimulatory activity of these receptors is found in the supernatant of growing cultures, suggesting that released modified pieces of peptidoglycan are the actual stimulants (2).

Bacillus anthracis can induce an immunostimulatory response to both spores and vegetative cells during *in vitro* and *in vivo* infection. Alveolar macrophages and LDCs coming into contact with spores produce TNFα, IL-1β, IL-6, and IL-8 (2, 28, 116). The IL-1β response can be induced *in vivo* with as little as 100 spores (116). IL-1β production leads to macrophage

expression of NO. The NO spore-killing response of macrophages is critically dependent on the internalization of spores, presumably due to internal recognition receptors (28, 141). IL-1β and TNFα activate and recruit phagocytes, promoting clearance and destruction of ungerminated spores in the lungs (28). Mouse strain susceptibility to *B. anthracis* spores was due to the presence of a gene locus involved in inflammation that leads to the production of IL-1β and IL-18 (107, 175). Spores themselves induce the production of IFN-β and activation of alveolar macrophages (2, 28, 116). IL-6 induces B-cell antibody formation and recruitment (28, 116). Although many studies have shown the immunostimulatory effects of spores and vegetative cells of *B. anthracis*, in the context of host infection in a fully virulent strain, the host defenses begin to be shut down by the bacteria as soon as outgrowth and induction of virulence factor gene expression begins.

Human dendritic cells exposed to *B. anthracis* spores have been shown to trigger reprogramming of their chemokine expression from the tissue homing receptors CCR2 and CCR5 to the lymph node receptor CCR7 (115). This reprogramming would greatly help the spores by directing them to the regional lymph nodes and to their optimal destination more efficiently. The engulfed spores germinate, multiply, escape the phagolysosome, and are released *en route* and during arrival of the macrophages and LDCs to the mediastinal lymph nodes (39, 49). During this process *B. anthracis* upregulates and produces many of its virulence factors, including the toxins, capsule, and other virulence factors mentioned above. PA and other toxin genes are produced in the germinating cells in as little as 1 hour after infection, concurrently with spore-laden macrophage arrival in the perivascular and peribronchiolar lymph node channels in a guinea pig model of infection (43, 114). Lysis of the macrophages and the

release of the bacteria are dependent on an *atxA*-regulated gene that is not a toxin gene, but another gene product encoded on the pX01 plasmid (39). The escape of the cells from the macrophages has also been linked to toxin secretion and InhA1 (140).

At 4 hours post-infection in a guinea pig model spores and vegetative cells were found in and around phagocytes in the peristial lymph nodes (114). In rhesus monkey and chimpanzee models of inhalation anthrax infectious spores were taken up and delivered to the mediastinal lymph nodes within 6-18 hours post-infection (114). Once in the lymph nodes, the bacteria multiply rapidly and produce copious amounts of the toxins. These toxins offset any immunostimulatory effects described earlier and lead to local immunosuppression within the infected lymph nodes.

Initial immunosuppression by the *B. anthracis* toxins begins soon after germination of the spores in the alveolar macrophages and LDCs. LT has been reported to abolish the secretion of proinflammatory cytokines by macrophages (118, 134) and LDCs (115, 120, 172). LT can induce apoptosis of macrophages *in vitro* through the inhibition of p38 MAPK and its anti-apoptotic signals (135, 138). ET cooperates with LT in the suppression of early cytokine expression and inhibition of other phagocytic cell types. The combination of ET and LT inhibits priming and activation of PMNs and their ability to produce sporocidal NO. It also inhibits chemotaxis of PMNs to the lymph nodes and inhibits interferon production (139). Exogenous interferon therapy blocks the apoptosis of macrophages, promotes activation, and leads to more effective spore killing (139). LT disrupts the production of PLA_2 in pulmonary phagocytes, which was found to be critical in anthrax spore killing (173). After inhibition of PMNs and

alveolar macrophages, monocytes remain the sole defender left in the fight against *B. anthracis*, but to no avail, as LT inhibits the differentiation of monocytes into macrophages *in vitro* and therefore inhibits their ability to fight off invaders (174, 175). Cholesterol-dependent anthrolysin O is lethal to human PMNs, monocytes, lymphocytes, and lytic to RBCs (148).

Although the association of *B. anthracis* with antigen presenting cells such as alveolar macrophages and LDCs in the lymph nodes would suggest a potential for activation of an adaptive immune response, this is unlikely due to the short time course of infection owing to the rapid replication and toxin production by *B. anthracis* in inhalational cases. In other forms of anthrax, the adaptive immune system may have time to be mobilized, but the adaptive immune response is also inhibited by the anthrax toxins. LT has been shown to inhibit the expression of co-stimulatory molecules, which in the presence of bacterial antigen presentation may lead to not only the inability to mount a response to the antigens but likely the induction of tolerance (120). Tolerance to bacterial antigens may lead to the development of protective T regulatory cells to hinder future adaptive immune responses to *B. anthracis* epitopes and lead to a poor response to future infections. Additionally, LT and ET abolish T-cell activation and cytokine secretion including IL-2 induction of T-cell proliferation (177, 178). LT also acts as an inhibitor of the humoral response through action MKKs important in B-cell proliferation and IgM production (120, 137). ET induces a Th2 shift and diverts the immune system into a poor anti-bacterial response (114, 176, 179). Major players in the adaptive immune response are inhibited by the *B. anthracis* duo of toxins, and phagocytes are killed or deactivated leading to the unchecked proliferation of the bacteria in the lymph nodes.

After a series of multiplications, immune cell death, and recruitment in the lymph nodes; the lymph node begins to swell. As the mediastinal lymph node expands, the bacteria soon gain access to the bloodstream and begin to stream out. The bacteria will also spread to adjacent lymph nodes through the lymphatics. Massive bacterimia ensues, followed shortly by toxemia as the cells secrete the toxins. Some phagocytic cells have toxin-induced resistance to the circulating toxins, but the presence of the capsule protects the bacteria from the resistant macrophages and complement and is essential for dissemination throughout the body (119, 121).

The last stage of the disease is characterized by the distant actions of the toxins at sites throughout the body, and usually begins at roughly 24 hours post-infection in a guinea pig model. The toxins lead to vascular injury with edema, hemorrhages, and thrombosis, through several mechanisms that lead to the death of the host. LT acts on the major endothelial barrier by action on the central actin fibers and modification of endothelial cell distribution (112, 114, 163, 182). LT's actions on the VE-cadherins and induction of endothelial cell apoptosis induce bleeding, hypotension, and cardiac distress (123, 180, 181). ET causes necrosis throughout the body in zebrafish, and rapidly kills mice (56, 112, 114, 183). ET also leads to hypotension by action on cardiac pacemaker cells (112, 114, 183). The two toxins' attack on the circulatory system leads to hypotension, vascular collapse, and hypoxia throughout the body. The lack of adequate blood flow and hypoxia plus action of ET and LT leads to massive damage of the internal organs (136). The PA subunit and Anthrolysin O activity together lead to hemolysis of the remaining RBCs (138). LT and ET are linked to disruption of platelet function and aggregation, leading to worsening of the leakage in the blood vessels (182, 183). The massive

vascular leakage leads to pleural effusion and this fluid buildup is usually the cause of death by asphyxiation. As the host dies and nutrients become limited the bacteria becomes dormant. Once the bacilli become exposed to oxygen by opening of the remains by bloating gases, trauma, or autopsy, the bacilli quickly sporulate and can spread to the surrounding environment, starting the infection cycle anew.

Disease in Animals

Endemic anthrax cases usually begin by ingestion of food or water that is contaminated with anthrax spores. An animal dying of anthrax produces an enormous amount of spores, and when the carcass is exposed to air by escape of bloated gases the bacilli sporulate rapidly. The majority of outbreaks occur after heavy rains following a period of drought, as spores from the environment become distributed in the water.

The disease in animals usually takes one of 3 forms: peracute, acute, and chronic. The peracute form is most often seen in cattle and other ruminants (26). Disease onset is rapid and death ensues quickly due to cerebral hypoxia. The subacute and acute forms are frequent in cattle, horses, and sheep. Symptoms of the subacture/acute phases consist of fever, a stop in rumination, periodic depression, respiratory difficulty, convulsions, and eventually death. Bloody discharges from the natural orifices as well as edemas in various parts of the body are sometimes observed (26).

Outbreaks in less susceptible species like pigs, and sometimes cattle, horses, and dogs are usually of the chronic form, although some animals will succumb to the acute form. The main symptom of the chronic form is pharyngeal edema. Frequently, a foamy bloody discharge can be seen coming from the sides of the mouth. The animals die from asphyxiation. The chronic form can also present itself as intestinal anthrax (26). Under necropsy, the acute animals will display rapid decomposition and bloated carcasses. Hemorrhaging and splenomegaly, as well as enlarged kidneys, liver, and lymph nodes are often seen. The initial stage of every infection involves the spores gaining access into the body and germinating.

Germination

In order to initiate germination and restore vegetative growth when conditions favor outgrowth, the spore must be able to monitor the outside environment. The germination receptors, located in the spore cytoplasmic membrane, encounter the germination signals as they pass through the external spore coat layer. Early events in germination begin as the spore membrane increases in fluidity (184, 185). Cations from the spore coat are released into the environment, including H^+, K^+, and Ca^{2+}. One of the major releases of cations is dipicolinic acid (DPA). DPA release leads to degradation of the spore's peptidoglycan cortex (17). This is followed by release of Ca^{2+} ions and activation of lytic enzymes, like CwlJ and SleB. These lytic enzymes start the degradation of the peptidoglycan and spore coat layers, leading to water uptake and the start of metabolism and increase in ATP synthesis (9, 11). The SASPs (small acid soluble proteins) that coat and protect the spore DNA are degraded by germination proteases and any damaged DNA is repaired. Degraded SASPs proteins are used as a nutrient source for

the emerging spore (8). The current dogma is that different germinants bind to tricistronic encoded germination receptors on the inner membrane, like the well characterized GerA receptor of *B. subtilis* (16).

The GerA family of germination receptors react to different stimuli (21). High concentrations of alanine (100 mM), or low concentrations (1 mM) with the presence of His, Pro, Trp, or Tyr can induce significant germination in 1 hour (16). D-alanine can inhibit germination by L-alanine (187). The GerS germinant receptor family recognizes aromatic ring structures. The presence of purines (inosine, adenosine, or guanosine [weaker]) with many amino acids (A, C, H, M, F, P, S, W, Y, V) can induce germination (16). This induction was inhibited in the *gerS* mutant spores, which were unreactive to inosine and alanine-induced germinants (16). No purine alone will cause germination in *B. anthracis*, but can in *B. cereus* (186).

GerX, another of the GerA family of receptors, is located on the pX01 plasmid of *B. anthracis*. *gerX* mutants are attenuated for virulence in a mouse model (41). GerH also plays a role in germination of endospores in macrophages *in vitro* (22). Different *Bacillus* species react to differing germination stimuli (11). *B. cereus* and *B. anthracis* germinate most efficiently in the presence of alanine or inosine and cofactors. The presence of other cofactors greatly increases the ability of the germination receptors to signal. Anti-spore polyclonal antibodies significantly hinder the ability of spores of *B. anthracis* to germinate, potentially by blockage of access of germinates to germination receptors or by blocking lytic digestion of the spore coat layers (20).

Vaccination

Anthrax was the first disease in which the principle of bacterial vaccination was found to be effective. 1881, in Pouilly Le Fort, the Pasteur strain of *B. anthracis* was the first attenuated bacterium used successfully as a vaccine. In 1937 the Sterne strain of *B. anthracis* was isolated. It is cured of the pX02 plasmid, rendering it unable to produce the antiphagocytic capsule. The Sterne strain is used as a live vaccine to this day, but only in a veterinary capacity. It induces great protection in many studies and is utilized as a livestock vaccine in anthrax-endemic regions (30, 105). Since it is a live vaccine and has potential to harm the animal with its other virulence factors, it has not been considered safe for use on humans. However, it was utilized as a human vaccine during the cold war years in the former Soviet Union. Several new vaccine candidates have been proposed and/or tried in animals over the last half-decade.

Human vaccines based on cell-free filtrates of nonencapsulated strains of *B. anthracis* were developed in several Western countries in the 1950s. PA and other secreted proteins were absorbed from cell supernatants using aluminum hydroxide gel (Alum), and this cell-free cocktail was given to humans. This newer vaccine, name AVA for Anthrax Vaccine Adsorbed requires doses at 0, 2, and 4 weeks as well as at 6, 12, and 18 months, followed by annual boosters. Annual booster shots are necessary, as the vaccine is only protective for roughly a year (105). The vaccine confers poor protection from challenge with aerosolized spores in a number of animal models (106, 108). AVA vaccines also provide less protection than the live spore Sterne strain vaccine and have a number of side effects (105, 189). Reaction to the AVA vaccine is not just to PA, although it is the major factor responsible for protection. Approximately 69

proteins of *B. anthracis* react to antiserum generated by the AVA vaccine, which may not constitute the full gambit of protective antigens (31, 104). Full protection against anthrax infections may require the use of multiple immunogens.

A laboratory study has shown that inclusion of formaldehyde-inactivated spores to AVA or other PA-based vaccines results in total protection in both mice and guinea pigs (3). Even the newer recombinant PA-based vaccines provide less protection than the live Sterne spore vaccines, but have fewer side effects than AVA (30). The addition of better adjuvants to the AVA vaccine has been show to increase its efficacy (101). A recombinant PA vaccine bound to alhydrogel has been found to protect rhesus monkeys from an aerosolized dose of virulent *B. anthracis* spores (98). Production of antibodies by other more efficient vaccine delivery methods may also be helpful in future vaccine strategies (102).

Ideally a vaccine could be developed necessitating fewer doses and conferring better protection than the currently used AVA vaccine, and with the potency of the Sterne vaccine without the hazards. PA is the basis for many of the new vaccine designs. Other immunogens, for instance the capsule (103), could be beneficial additions to the AVA or other recombinant PA vaccine strategies. Antibodies to PA offer protection by neutralization of the LT and ET toxins (98). High-affinity monoclonal antibodies produced against PA protect animals during *B. anthracis* infections (100). Laboratory animals used in the development of vaccines include mice, guinea pigs, and rabbits, with the use of rhesus monkeys as a non-human primate model. Mice are very susceptible to anthrax, with the presence of only either the capsule or the toxins being necessary to produce lethal infections (107).

Production of anti-spore antibodies and anti-spore IgG inhibits the germination of *B. anthracis*. Antibodies against both germinated and ungerminated spores have the same neutralizing effect (20). Anti-PA antibodies have the ability to stimulate phagocytosis of spores by macrophages and inhibit some spore germination *in vitro* (43). The ability of anti-spore antibodies to inhibit germination is not a consequence of overall binding, but correlates to which epitopes are bound. There is no association between agglutination and abililty to inhibit germination (20). One proposed mode of action is the blocking of the pores that allow germinants to enter the spore by the anti-spore antibodies (20). GerH is necessary for the germination of spores in macrophages (22). The use of *gerH* mutant spores may allow the use of a spore vaccine to illicit an anti-spore response without the fear of germination and infection. Some protection afforded by spore vaccines is accomplished by stimulation of IFNγ producing $CD4^+$ T lymphocytes (197).

The addition of BclA, a potent immunogen in the exosporium of the spore, to a recombinant PA DNA vaccine leads to better protection than PA alone (53). Other spore antigens may increase the protection as well. Antibodies to recombinant PA lead to delayed germination of spore and a modest increase in uptake by macrophages and spore killing. (43) The tetrasaccharide of the BclA glycoprotein may also be an effective vaccine addition that can illicit a response and be added to future vaccines (82).

Sporulation

Most of the known literature on sporulation has been derived from studies of *B. subtilis*. *Bacillus subtilis* is genetically best characterized member of the genus *Bacillus*. Sporulation of *B. anthracis* has not been studied in detail and general extrapolations can be dangerous, as *B. anthracis* has over 1000 genes with no known homology to *B. subtilis*. *B. anthracis* also contains an extra spore layer (the exosporium) and some homologs of *B. subtilis* sporulation genes have been shown to play different roles in *B. anthracis*.

Under conditions of nutrient starvation and in the presence of oxygen, cells of the *Bacillus* spp. undergo the process of sporulation. Sporulation allows production of a dormant spore which can survive adverse conditions and allow the bacteria to reemerge when the environment is more suitable to sustained growth. The production of endospores allows *Bacillus* spp. to become resistant to UV rays, ionizing radiation, pressure, heat, desiccation, high salinity levels, pH, and chemical agents. This dormant and highly resistant endospore allows the survival of the bacteria in contaminated soil for many years. Many researchers have argued that *B. anthracis* does not grow in the soil and persists only as endospores. The presence of nitrate in the soil leads to sporulation and killing of any vegetative cells (4). In a more recent study, *B. anthracis* spores were found to germinate and multiply in the rhizospheres of several grass species (68). The centrally located spore has virtually no detectable levels of metabolism, little to no ATP and NADH, and no enzyme activity (192). Cells remain in this metabolically inactive form until the presence of inosine and/or alanine and co-factors leads to initiation of germination and outgrowth.

During the process of sporulation, groups of genes are sequentially activated and silenced in an 8-10 hour period that leads the nutrient-deprived cell through a series of developmental stages (110). This process is broken down into a series of time points denoted using the Roman numerals 0-VII (47). Each Roman numeral signifies the hour in which the events each event occurs. Gene mutations which are essential at each timepoint are denoted by the addition of the respective Roman numeral and order that they are important, i.e., the sporulation mutant Spo0A is active during the 0 hour time point (end of exponential growth).Sporulation is initiated at Stage 0 with the master sporulation regulator Spo0A. During Stage I DNA replication initiates at an axial filament in the center of the vegetative cell. Stage II denotes the time point where the spore septum begins to be formed to initiate the unequal cell division and formation of two compartments, the larger *mother cell* compartment and the much smaller *forespore* compartment.

The forespore is engulfed by the mother cell membrane, leading to the forespore being encased by two bilipid membranes. This is the hallmark of the third stage of sporulation (Stage III). During Stage IV, a thick layer of carbohydrate and spore-specific peptidoglycan is layered between the two forespore membranes. This layer is known as the cortex. The outer membrane of the forespore is layered with sequential layers of spore coat proteins and calcium dipliconate during Stage V of sporulation. Addition of the final spore coat layers, which provide several of the inherent resistance properties that protect the endospores, and the final exosporium formation are accomplished during Stage VI. The outermost exosporium layer is synthesized during Stage VI in *Bacillus anthracis*, *cereus*, and *thuringiensis* (18, 191). The final stage of sporulation,

Stage VII, is marked by the lysis of the mother cell and release of the mature spore into the environment (47). Figure 2 outlines the general process.

Sporulation gene transcription in *B. anthracis* has been found to occur in 5 semi-distinct waves (54, 88). Interestingly, the spore associated proteins are produced much earlier than they are incorporated, and these proteins are predicted to be inherently more stable than their vegetative cell counterparts, leading to increased concentration of spore related proteins and a decrease in shorter lived vegetative cell proteins (54, 88). Sporulation-specific sigma factors are transcribed in a defined series that has been well characterized in *B. subtilis*, and in part attribute to the waves of sporulation gene transcription (146).

Regulation of Sporulation and Sigma factors

Regulation of gene expression in bacteria occurs primarily at the level of transcription. DNA-binding proteins can significantly affect the efficiency of transcription, but the specificity of the transcription reaction depends on the interactions between the RNA polymerase (RNAP) and the DNA promoter sites with which they recognize. RNAP is most commonly found in two parts, the core RNAP, which catalyzes the polymerization of ribonucleotides into a RNA complementary copy of a DNA template, and the holoenzyme complex, which contains subunits of the RNAP core complex (β, β', and two α) plus an additional protein subunit called the sigma factor. The sigma factor determines the specificity of the RNAP for target gene promoters and dissociates from the core RNAP when transcription from the sigma-specific promoter is initiated.

During the life cycle of a bacterium, it shuffles different sigma factors to modify its gene expression to best suit its current environment and various stresses. *Bacillus subtilis* has had its cascade of sigma factors well characterized. Alternative sigma factor usage in *B. subtilis* can be used as a model for alternate sigma usage in *B. anthracis*, but some care must be taken, as sporulation target genes and recognition sequences are not identical between the two species.

Sigma A is the primary sigma factor in the vegetative cell. It is responsible for transcription of the housekeeping genes and genes involved in very early sporulation. It is by far the most abundantly utilized sigma factor, involved in expression of most genes utilized during growth in rich media (110). The σ^A-dependent transcripts include DNA damage response genes, heat shock response genes, genes responsible for stationary phase degradative enzyme synthesis, and the development of bacterial competence. The sigma factor σ^A is critical for the initiation of sporulation and directs the transcription of several of the *spo0* genes, most notably Spo0A. Spo0A is a DNA binding protein that acts as the transcriptional activator/repressor that initiates a cascade of events leading to sporulation. σ^A has been found to be act on sporulation-related genes through at least Stage II of sporulation (activation of SpoIIG and SpoIIE; 110).

The sigma factor σ^B regulates the expression of stress responses, including responses to heat shock, O_2 limitation, and exposure to high salt or ethanol (110). It is also activated when *Bacillus* enters into the stationary phase of growth. Although σ^B plays a role in the response to these stresses, it is not essential, as a σ^B-null mutant is not more susceptible to environmental stressors (110). σ^B plays no significant role in transcription of sporulation related genes.

The extremely low abundance of σ^C has limited its study, and it has no major effects of regulation of transcription of genes to date (110). σ^D is involved in flagellar gene expression, secretion machinery, and chemotactic protein sensors (110, 113). Both σ^C and σ^D play no major roles in sporulation, despite σ^D's upregulation during the exponential and stationary phase of growth. σ^L likewise does not play a role in sporulation, with just a minor role in expression of amino acid degradative enzymes (110, 113).

σ^H expression is controlled by early stage sporulation factors. σ^H is essential for sporulation, but it is also present during exponential growth where it may play a role in transcription of vegetative genes (110, 113). Most sporulation gene transcripts are also enhanced by the activity of Spo0A related enhancers of transcription. σ^H also plays roles in competence, TCA cycle enzyme synthesis, and DNA repair enzymes (110). σ^H has been recently found to be involved in toxin gene expression in *B. anthracis* (113).

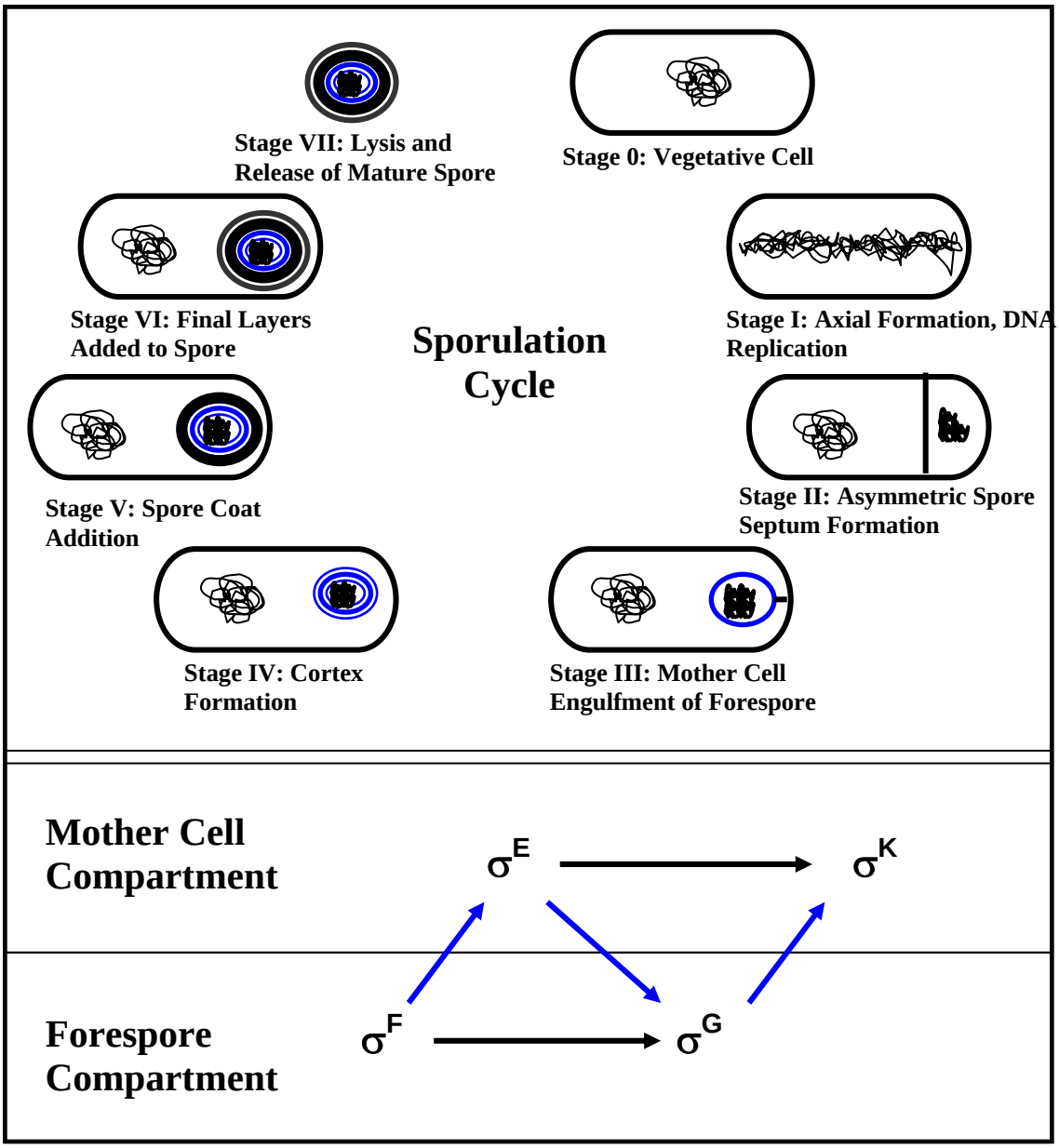

Figure 2. Top panel denotes a representation of the sporulation cycle of B. subtilis. The bottom panel demonstrates the interactions between sporulation specific sigma factors, with direct effects denoted by black arrows and indirect effects denoted by blue arrows. Adapted from Hilbert *et al.* (111)

Both σ^E and σ^K are mother cell-specific transcription factors. They direct early and late phase transcription of genes, respectively, and transcribe genes essential to addition of spore coat and exosporium proteins. The σ^E sigma factor becomes active during Stage II of sporulation and into later stages. Seventeen known genes in *B. subtilis* are under the regulation of the σ^E (110, 113). σ^E-dependent transcripts are responsible for spore septum formation, forespore engulfment, peptidoglycan and cortex formation, and layering of some of the early spore coat proteins, including CotE. σ^E-dependent products are also involved in the cleavage of pro-σ^K into active σ^K (110). This cleavage is tightly regulated, and delays production of active σ^K until its products are ready to be assembled into the spore over the initial layering of the σ^E transcribed products. σ^K expression initiates between the third and fourth stage of sporulation, and the pro-σ^K is cleaved to its active form during late stage IV. This may rely on processing by a protein that is dependent on σ^G expression in the forespore (110, 113). σ^K-controlled genes include germination receptors, genes involved in DPA accumulation and synthesis, and most of the genes that encode proteins in the spore coat and exosporium. σ^K, by virtue of its replacement of other sigma factors, also acts to inhibit production of early stage sporulation genes (111).

The sporulation genes that are transcribed in the forespore compartment utilize σ^F- and σ^G-specific promoters. *SigF* is transcribed during stage II of growth. σ^F activation in the forespore compartment is due to cleavage of the pro-σ^F into the active form (110). σ^F is activated after production of the spore septum between the mother cell and the forespore. σ^F transcribed genes include those encoding the enzymes and other products necessary for protein cleavage and efficient nutrient acquisition in the germinating spores. σ^F also plays a role in the cleavage of the

pro-σ^E protein into its active form by an unknown mechanism. σ^G is a forespore specific sigma factor. It is active during the third and fourth stages of sporulation. σ^G transcribed genes include those encoding the SASP proteins, which are involved in protection and packaging of the spore DNA. A σ^G-encoded protein acts by an unknown mechanism to cleave pro-σ^K into σ^K (111). These sporulation-specific sigma factors are sequentially linked and act upon one another to precisely regulate the assembly of the spore in different compartments in a phase-dependent manner (109). This ensures an ordered, complete structure is constructed, leading to the ability of the spore to survive many environmental challenges. The interactions between the spore-specific sigma factors are demonstrated in **Figure 2**. **Table 1** summarizes the sigma factors expressed in B. subtilis, their roles, and their putative binding sites.

Sigma Factor	Genes	Function	Promoters -35	Promoters Spacer	Promoters -10
Vegetative Sigmas					
σ^A	*sigA, rpoD*	Housekeeping/early sporulation	**TTGACA**	**17**	**TATAAT**
σ^B	*sigB*	General stress response	**RGGXTTRA**	**14**	**GGGTAT**
σ^C	Unknown	Postexponential gene expression	**AAATC**	**15**	**TAXTGYTTZTA**
σ^D	*sigD, flaB*	Chemotaxis/flagellar gene expression	**TAAA**	**15**	**GCCGATAT**
σ^H	*sigH, spoOH*	Postexponential gene expression, Competence and early sporulation	**RWAGGAXXT**	**14**	**HGAAT**
σ^L	*sigL*	Degradative enzyme gene expression	**TGGCAC**	**5**	**TTGCANNN**
Sporulation Sigmas					
σ^E	*sigE, spoIIGB*	Early mother cell gene expression	**ZHATAXX**	**14**	**CATACAHT**
σ^F	*sigF, spoIIAC*	Early forespore gene expression	**GCATR**	**15**	**GGHRARHTX**
σ^G	*sigG, spoIIIG*	Late forespore gene expression	**GHATR**	**18**	**CATXHTA**
σ^K	*sigK, spoIVCB:spoIIIC*	Late mother cell gene expression	**AC**	**17**	**CATANNNTA**

Table 1: Summary table of sigma factor target genes, sequences, and role in sporulation. H=A or C, N= A,G,T,or C, R=A or G, W=A, G, or C, X= A or T, Y=C or T, and Z= A or G. Adapted from Haldenwang *et al.* 1995 (110)

Spore Structures

The spore is the infectious agent of *B. anthracis*. The *B. anthracis* endospore is formed in several steps. Assymetric septation of the nutrient-starved vegetative cell produces the large mother cell and small forespore compartments. The mother cell then engulfs the forespore, encasing it with two distinct membranes. The first step in assembly of the spore is the packaging of the DNA, ribosomes, tRNAs, and other cellular components into the core of the forespore. Newly-packaged DNA and enzymes are protected by the production of the thick layer of modified spore-specific peptidoglycan, called the spore cortex, between the two forespore membranes (11). DNA is condensed by small acid soluble proteins (SASPs), low molecular weight proteins that surround the DNA and protect them from UV, radiation, heat, and other chemicals (58). SASPs are synthesized late in sporulation. They bind and alter the DNA structure and properties dramatically. The low water content of the core inactivates the enzymes present in the core and helps induce dormancy.

This low percentage of water in the core (27-55% in spore versus 75-80% in growing cells) and the low amount of free water in the core restricts the flow of macromolecules and enhances the resistance properties of the spore due to freezing and desiccation. Also in great abundance in the spore core is pyridine-2,6-dipicolinic acid (DPA). DPA consists of 5-15% of the spore dry weight and is chelated mostly by Ca^{2+}. This molecule is secreted in the first moments of spore germination in conjunction with the influx of large amounts of water. DPA plays a large role in the reduction of the water content of the spore core (58).

External to the cortex is found a series of proteins that form a lattice called the spore coat. The spore coat is made up of proteins synthesized in the mother cell and layered onto the outermost of the two forespore membranes. The spore coat consists of greater than 50 proteins in *B. subtilis* (10). Surrounding the spore coat, and presumably the last layer placed on the outside of the spore, is the loose balloon-like structure known as the exosporium. The exosporium is also synthesized within the mother cell. After a final stage of maturation the mother cell lyses to release the mature spore. See Figure 3.

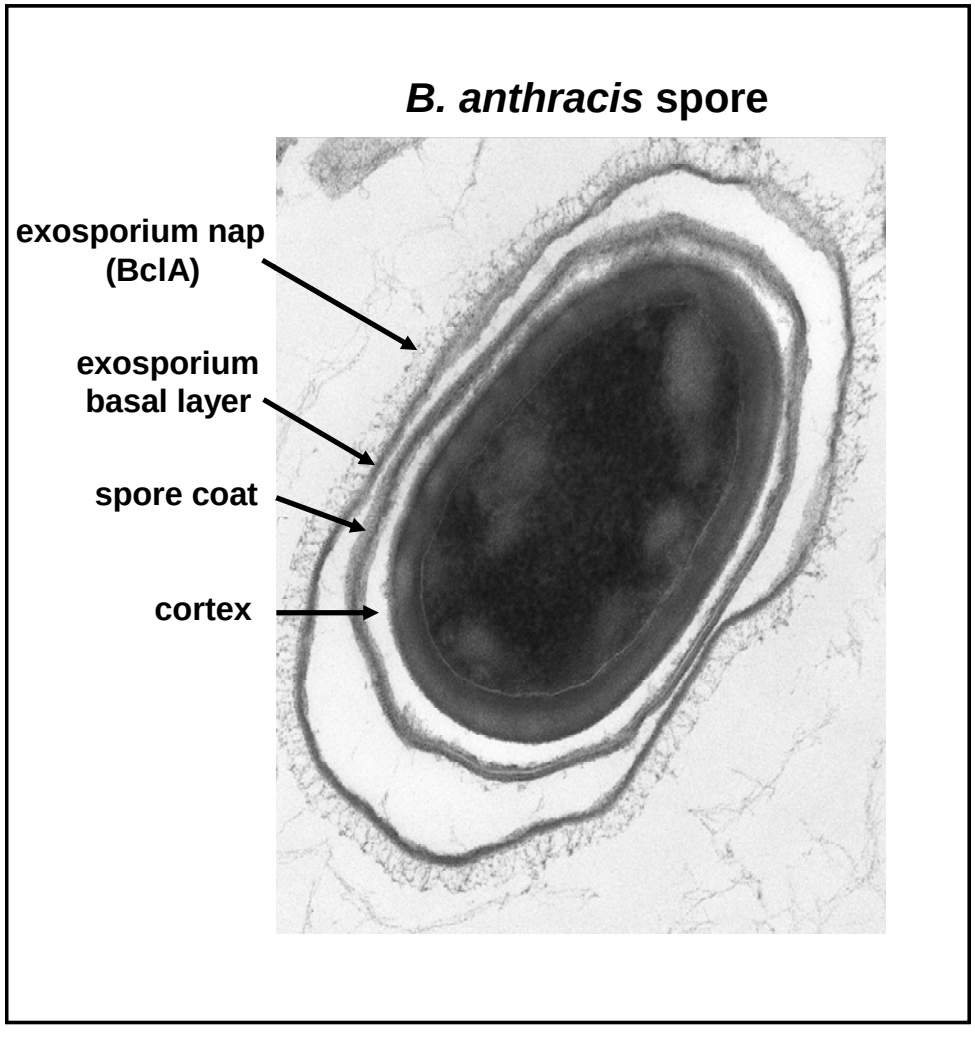

Figure 3: Layers of the *B. anthracis* spore

The Spore Coat

In the well characterized *B. subtilis*, the spore coat contains a complex mixture of at least 24 proteins which can be resolved into two or three morphological layers (55, 87). Coat assembly requires regulatory proteins and key morphogeneic factors. The coat also plays a role in germination, perhaps by providing access for germinants to the germinant receptor proteins located in the cytoplasmic membrane (24). Lytic peptidoglycan hydrolase enzymes may also be located in the spore coat, which are involved in lysis of the spore cortex during germination (188). The spore coat proteins undergo extensive crosslinking, with many of the spore coat proteins containing multiple cysteine residues. The crosslinked spore coat is involved in some spore resistances: like exogenous lytic enzymes that can degrade the spore cortex, UV light, hydrogen peroxide, and can protect the spore from predation from protozoa, but has little to no role in spore resistance to heat, radiation, and other chemicals (58, 158).

Although *B. anthracis* and *B. subtilis* have similar numbers of predicted spore coat proteins and a few common coat proteins, the outer coat layers vary significantly (55). The *B. subtilis* spore coat is a relatively thick structure with a distinctly light inner layer and a darker outer layer (87). In contrast, the *B. anthracis* spore coat,appears thin and compact (87). It is also separated by a gap, sometimes called an interspace, from the exosporium, not present in *B. subtilis*. In most cases, the precise function of various spore coat proteins has been difficult to determine, since gene disruptions had no measurable phenotypic effects.

Coat assembly in *B. subtilis* is a complex multistep process. One early event in coat assembly is the essential localization of SpoIVA to the outer membrane of the forespore on the mother cell side (110, 113). SpoIVA marks the exterior of the outer membrane as the site of all future coat protein assembly and directs the layering of the initial spore coat layers. A layer of coat proteins are assembled around SpoIVA. A *spoIVA* mutant in *B. anthracis* failed to progress past the early stages of sporulation and never produced mature spores (87). These mutant spores lacked the cortex, and the mother cells were filled with swirls of electron dense coat material (87). SpoIVA appears to have a role in *B. anthracis* similar to that in *B. subtilis*, namely marking and directing assembly of the spore coat layers on the outside of the forespore. The outermost part of the initial coat layer contains the coat protein CotE (87). In the final stage of coat assembly, the inner and outer coat layer appears between the CotE and the SpoIVA layers (87). The CotH protein, directed by the CotE protein in *B. subtilis*, directs deposition of several other coat proteins.

The *B. anthracis cotE* mutant was found to lack attachment of the exosporium, and also had detached spore coat layers (87). Examination of the *cotE* mutant spores under AFM revealed a loss of the typical pole to pole ridges found in *B. anthracis* spores (12). These data show that the CotE protein is essential for anchoring the coat layers and exosporium to the core and that it also plays a role in the proper construction of the spore coat. Proteomic studies did not find CotE in the exosporium, so its role in anchoring of the exosporium occurs within the spore coat, or it plays an indirect role (87). CotE may play a role in stability of the exosporium, as it may control ExsY and CotY assembly, since these genes are homologs of the CotZ protein of *B. subtilis*, which is controlled by CotE (87).

The ExsA proteins of *B. cereus* and *B. anthracis* have been found to be vital in proper assembly of the spore coat and the exosporium (81). Obvious defects in the spores were evident under transmission electron microscopy (TEM). Mutant spores became extremely sensitive to lysozyme, were unstable, and tended to lyse when subjected to freezing and thawing. The spore coat layers and exosporium were misformed, and remained free and unattached to the spore core (81).

A *cotY* mutation in conjunction with an *exsY* mutation leads to spore coats that are very thin, with a decrease in resistance to lysozyme, phenol, chloroform, and toluene (86). The double mutant has difficulty constructing an exosporium, and CotY as well as CotE may play a role in maintaining an ordered structure upon which an exosporium can be constructed (86, 87).

A major coat protein has been identified in all of the *B. cereus* family members, and it has been named CotA. This 13 kDa protein has 6 cysteine residues and is likely to crosslink with many other coat proteins (24). CotA confers resistance to lysozyme. The *cotA* determinant has a consensus σ^K promoter element, consistent with the appearance of the CotA antigen at stage IV of sporulation. TEM studies reveled that a *cotA* mutant lacked the majority of the spore coat as well as had an increased sensitivity to chloroform, phenol, and bleach. AFM studies show the coat of *B. anthracis* and *B. cereus* spores are covered in ridges that run along the long axis of the spore, and that presence of the exosporium hides these features (12). These ridges may be reflective of the dehydration state of the spore core at the time of imaging (14).

Exosporium

The outermost layer of the *B. anthracis* spores is the exosporium. *Bacillus subtilis*, the best characterized spore-former, does not possess a defined exosporium, consequently, many of the mechanisms involved in its construction are unknown and currently under investigation. Scanning electron microscopy has revealed the exosporium contains a paracrystalline basal layer and a hair-like outer layer called the nap (142, 143). Several proteins of the exosporium are related to the morphogenetic and outer spore coat proteins of *B. subtilis*, but many of them have no known homology to any known proteins outside the *B. cereus* family. A proteomic analysis of exosporium proteins revealed the presence of 137 exosporium-predicted proteins, but the extract used in this study was not pure exosporium, and contained contaminating spore coat and other proteins (88).

The primary permeability barrier and source of spore antigens is the exosporium (15, 23). The exosporium may also play a role in interactions with the soil environment, binding to immune cells in the mammalian host, and evasion of host defenses. It helps protect underlying epitopes from recognition by the innate immune system and also allows the spores to be more resistant to killing by host macrophages *in vitro* (28, 39). This exosporium layer is chemically complex; consisting of protein, amino and neutral polysaccarhides, and lipids (190). Exosporium antigens first show up at stage III of sporulation. The exosporium has been speculated to be the reason for the extreme hydrophobicity of the spore, and therefore might play a role in adhesion (78).

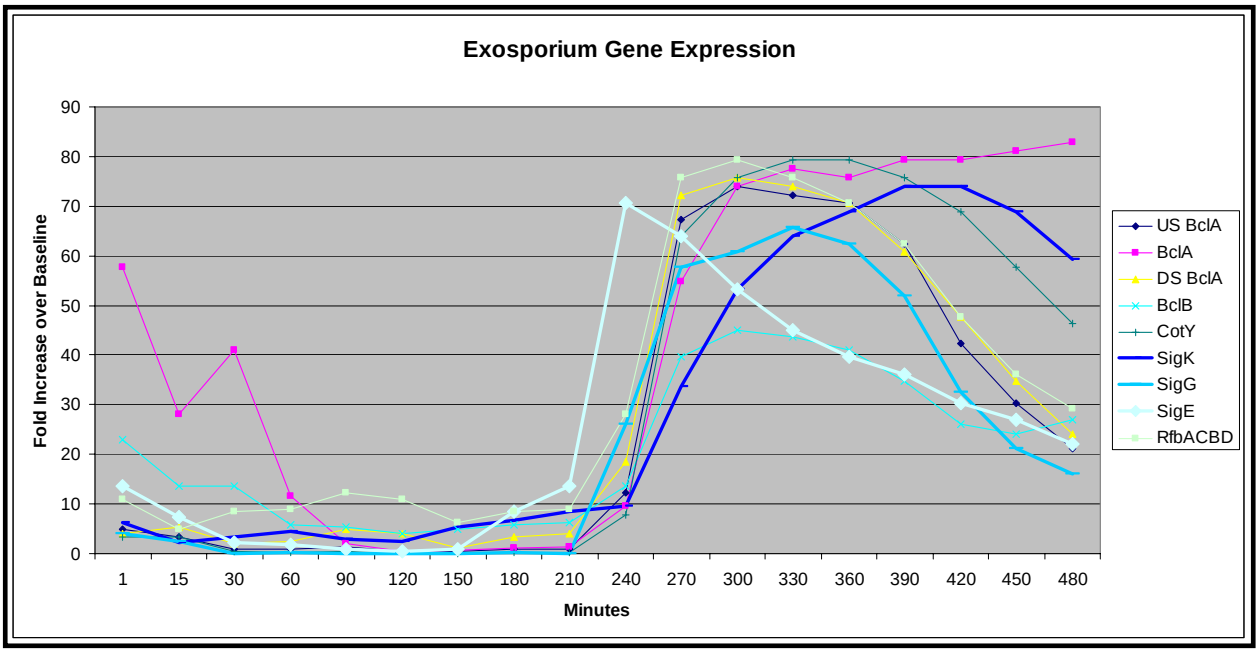

Figure 4: Expression of late sporulation genes, adapted from Bergman *et al.* (54)

Characterization of exosporium proteins extracted from *B. cereus* has recently identified more than 10 proteins (79). These included ExsB, ExsC (not expressed in *anthracis*), ExsD, ExsE, BxpB/ExsF, ExsG and ExsJ. Only the *exsJ* and *bxpB* genes have been further characterized to date. ExsJ is a glycoprotein that migrates at a mass of 72 kDa and 205 kDa. This most likely represents the monomer and trimer versions of the protein, as is found in the similar BclA and BclB proteins of *B. anthracis* (79). The *exsJ* gene has high homology (>88%) to the *exsH* gene found elsewhere in the chromosome, and the major differences between the two proteins are found in the N-terminal regions of the two proteins. In both *B. anthracis* and *B. cereus*, the presence of an exosporium operon is apparent. Following the *bclA* determinant is a series of glycosylation biosynthesis genes (glycosyltransferases and methyltransferases) followed by a rhamnose gene cluster. The spore carbohydrate glycosylation machinery is predicted to

place the sugar residues on the BclA and BclB proteins. The glycosylation machinery determinants are transcribed concurrently with *bclB*, *bclA*, and other σ^K-directed genes, consistent with late sporulation mother cell expression. Beyond the rhamnose determinants is a series of genes that sequence similar to *B. subtilis* coat genes. Among this group of genes is the gene encoding the basal layer protein BxpB/ExsF, ExsY (a CotY homolog), and CotY proteins. This region is conserved among the *B. cereus* family members, but only parts of the operon are present in the *B. subtilis* chromosome (79). **See Figure 5.**

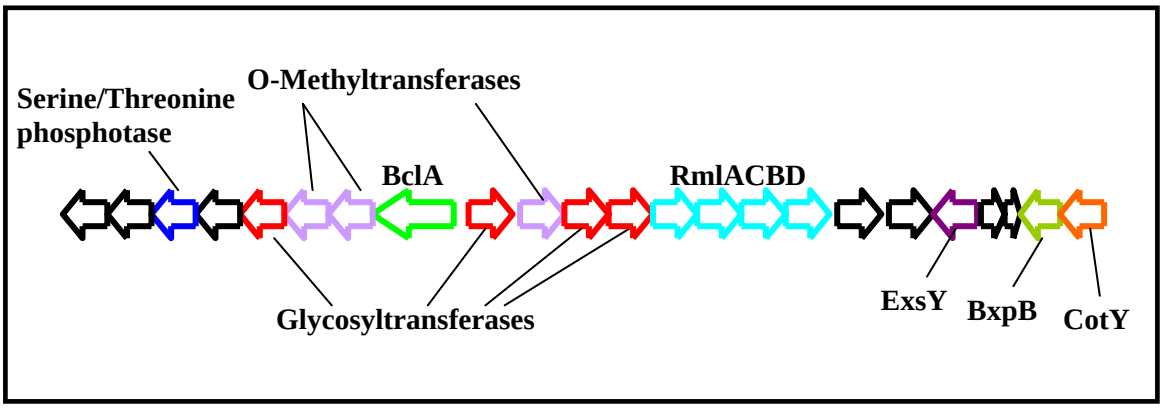

Figure 5. The *bclA* operon and adjacent spore-associated operons**.**

Several proteins have been isolated from the exosporium of *B. anthracis*. Alanine racemase and nucleoside hydrolase were isolated and identified, as well as the CotY and ExsY components (13). S-layer proteins were also found, but these are likely a contaminant (13). The BxpB protein was identified in the *B. anthracis* exosporium (13). BxpB/ExsF, ExsY, and BclA were all found in a high molecular weight grouping of proteins migrating at greater than 250 kDa (13). A novel new protein, ExsK, was also found in the *B. anthracis* exosporium, but has not been identified as an exosporium protein yet in *B. cereus* (13). The *B. anthracis* exosporium contains an arginase which maycompete with macrophages for free arginine, limiting their ability to produce NO and other free radicals to attack the germinating cells (141).

Very little is known about the basal layer and its associated proteins. The basal layer consists of four paracrystalline sheets, each exhibiting a hexagonal perforate lattice structure (142, 143, 159). The basal layer is comprised of many proteins, including BxpB (25). BxpB, along with BxpA, BxpC, and ExsK; are all currently predicted to be basal layer proteins (25). The *bxpB* determinant encodes a 17 kDa protein found to be located in the basal layer by immunogold labeling. This protein forms strong covalent complexes with BclA and other basal layer/nap proteins, including ExsY and CotY. ExsY and CotY are homologues of CotZ, which are CotE-controlled spore coat proteins of *B. subtilis* (87).

When BxpB is SDS-extracted from spores, it is isolated as both a monomer and in high molecular weight complexes with BclA and possibly ExsY and CotY. *bxpB* mutants cannot assemble a hairlike nap, although BclA is still synthesized at normal levels (25). The lack of BxpB leads to expedited spore germination and outgrowth, potentially due to easy access of

germinants into the spore (25). CotY, ExsY, CotB-1, and CotB-2 may be associated with the basal layer or outer coat protein layers (25). Also incorporated into either the basal layer or the nap is alanine racemase, superoxide dismutase, and inosine-uridine-preferring nucleoside hydrolase. These enzymes could protect the spore from reactive oxygen species during infection, and suppress premature germination by less than optimal levels of germinants (13, 79, 187). The major germinants of *B. cereus* spores are alanine and inosine (9, 11, 16). Alanine racemase converts L-alanine to D-alanine, a competitive inhibitor of germination. A nucleoside hydrolase would degrade inosine, preventing germination by minute quantities of inosine.

The immune inhibitor A protein (InhA) protein has been found in all three species of the *B. cereus* family in various degraded and native forms (18). This protein, best characterized in *B. thuringiensis*, is a zinc metalloprotease and degrades proteins of the immune system (18). It is highly toxic to Drosophila. It migrates as a band of about 72 kDa and as several smaller bands of 46, 22, and 18 kDa (18). The protein is secreted throughout the life cycle of the vegetative cell, but a homolog is found associated with, or is a contaminant of, exosporium preparations. InhA is a major component of the exosporium of *B. cereus* and *B. thuringiensis*, but is only found in minor quantities in *B. anthracis* (13, 79, 140). The InhA metalloprotease allows *B. cereus* spores to escape from macrophages and may play a small role in macrophage escape by *B. anthracis* as well (140).

Formation

Exosporium antigens appear as early as stage III of sporulation (191). *B. cereus*, *B. anthracis*, and *B. thuringiensis* all contain specific glycoproteins on the surface layer of the exosporium (18, 99, 19). The major glycoprotein in *B. anthracis* is BclA which is highly immunogenic (19). It is the major component of the hair-like nap that forms the outermost layer of the exosporium. Many proteins of the exosporium have recently been described, but the overall function of the exosporium has yet to be determined (13). This loose balloon-like structure is made up of at least 20 proteins (13, 18, 79). Most of this layer is made up of protein, but many of these proteins are glycosylated and potentially lipidated. The exosporium can bind to lectins, which may bind to the many glycosylated proteins found in the exosporium (193). The exosporium is 2% of the mass of the spore and is about 50% protein, 20% lipid, 20% neutral polysaccharides, and 10% other components (190).

The BxpA and BxpB/ExsF proteins have been isolated from the exosporium (15). The Gln-rich BxpA protein is predicted to form sheaths, as it shares homology with filarial sheath proteins (15). A *bclA* mutant allows antibody access to basal layer proteins, suggesting the BclA protein inhibits the ability of antibodies to access the basal layer. The sugarless *rmlD* mutant, responsible for glycosylation of BclA, also allows access of antibodies to the basal layer. This suggests the glycosylation of BclA leads to inhibition of antibody entry (15). Anti-BxpA antibodies bind BxpA more efficiently in the glycosylation-deficient Δ*bclA* and Δ*rmlD* strains (84). The BxpB protein does not contain a repeat region and is associated with BclA and other high molecular weight exosporium proteins. The *exsFA* and *exsFB* map to different parts of the

B. anthracis chromosome, but are homologs of each other, sharing 78% identity with the majority of the differences occurring at the N-termini of their protein products. The basal layer proteins ExsFA and ExsFB (BxpB and homolog) proteins are also involved in exosporium integrity and the incorporation of BclA into the nap (80). Loss of ExsFA leads to a decrease in BclA incorporation in the nap, and a double knockout of ExsFA and ExsFB leads to no incorporation of BclA in the nap (80). ExsFA and ExsFB are found in high molecular weight complexes co-migrating with BclA, BxpB, ExsY, and CotY (80).

Nap

A major component of the exosporium is the hair-like nap, which is mostly comprised of BclA (15, 19). The nap and the associated hair-like filaments were first described on the exosporium of *B. anthracis* in 1966 (144). Truncations of the BclA CLR also lead to a decrease in the size of the hair-like filaments on the outer surface of the spore; further evidence that this protein is BclA (75, 83). Proteins of the nap are likely to be the first proteins seen by the innate immune system in interactions with the spores (83, 19). The hair-like nap differs in length from species to species, and even from strain to strain (15, 83). The nap does not play a role in the resistance of the spore to various insults (19).

BclA also comprises the major species seen on blots on an exosporium extraction when using a polyclonal anti-spore antibody (15, 19). Antibodies both to the BclA protein or the carbohydrate portion of BclA can be produced (15). Ruthenium red allows the visualization of the nap under TEM by binding to the glycoprotein moities (156). A 715 Da tetrasaccharide and a

324 Da disaccharide are linked to BclA by GalNAC (19, 23). Many copies of the tetrasaccharide are linked to the collagen-like region of BclA, but the disaccharide most likely is attached outside the collagen-like region (CLR) (23). The nap extends from the exosporium for 600A^{o} (15, 83). Deletions in the CLR lead to a decrease in the glycosylation with the tetrasaccharide, but not the disaccharide. This was discovered by hydrazinolysis and led to the discovery of a *B. anthracis* specific sugar identified as anthrose (23). The BxpB protein plays a role in incorporation of the BclA glycoprotein into the exosporium (25).

Also reported to be in the exosporium and likely the nap is the protein InhA (immune inhibitor A). It is reported to be the major antigen on the outside of *B. cereus* spores. The BclA protein is coated with sugars, a major portion comes from the *rmlACBD* operon adjacent to the *bclA* operon on the chromosome (92). The *rmlACBD* operon encodes enzymes necessary for rhamnose biosynthesis. Although spores from a *rmlD* mutant were more efficiently taken up by macrophages and bound more efficiently to macrophages, they were not more virulent in a guinea pig model (92). Interestingly, macrophages can recognize and internalize collagen via the mannose receptor, and this may recognize the collagen-like proteins of the nap (145).

The Cap and ExsY

ExsY is required for complete formation of the exosporium of *B. anthracis* (85). Assembly of the exosporium in an *exsY* mutant is halted after partial formation of a polar exosporium-like structure termed the "cap" (85). The exosporium cap produced could readily be stripped off under growth in liquid media (85). The *exsY* mutant grown on solid media retained

the cap structure. An *exsY* mutant also appears to lack BxpB, showing a relationship between the two proteins. The mutant spores ruptured a novel sac-like structure in the exosporium during germination and outgrowth (85, 86). This sac was still evident when Δ*exsY* spores were grown in solid media. ExsY is found not only incorporated into high molecular weight complexes with the BclA protein, but also found in monomers, dimers, and trimers (85, 86). BclA is not assembled into the exosporium but rather is secreted into the supernatant in an *exsY cotY* double mutant, further suggesting an interaction between the two proteins. ExsY has a consensus σ^K promoter, consistent with its expression during the spore coat/exosporium assembly phase of sporulation.

The presence of the cap has led to the development of the bottle cap model for spore germination (97). According to this model, ExsY plays a role in the development of the exosporium beyond the cap. This cap may be the first structure of the exosporium to be assembled, since it appears first under TEM analysis. Alanine racemase, an enzyme commonly found in the exosporium, was shown to only be localized in the three quarters of the exosporium that is not part of the cap (97). This suggests that the assembly of the cap and the assembly of the rest of the exosporium are sequential and separate, and their formation discontinuous. During germination and outgrowth, the emerging cell bursts through the exosporium and underlying layers, and this always appears to be at the end of the spore that corresponds to the cap (97). This led to the prediction that the cap is designed to facilitate the emergence of the outgrowing cell.

BclA

BclA (*Bacillus* collagen-like protein of *anthracis*) has been found in all the *B. cereus* family members. The BclA protein is comprised of distinct N-terminal and C-terminal domains, with a series of collagen-like GPT repeats comprising the extensive middle portion of the protein. Several aspects of the BclA protein are similar to collagen, and lead to the prediction that BclA can form a triple helical structure. A glycine residue occupies every first amino acid in the repeating GXX triplet sequence. 39% of the non-glycine residues in the repeat are prolines, which are essential for triple helix stabilization by limiting rotation of the polypeptide chains (69, 94, 194). Computer modeling predicts that BclA exists in a coiled conformation (19). rBclA naturally forms a triple helical structure upon heating and cooling the protein (75). The native BclA protein confers exceptional stability, and may act as a protective shield to the spore.

The BclA N-terminus domain is similar in structure to members of the TNF family, and its role is currently unknown. N-terminal sequencing of the protein extracted from spores has shown that the first 19 residues of the protein are processed to remove 19 aa from the N-terminus (15, 19). The N-terminus also faces towards the basal layer in the orientation of the exosporium (19).

The internal repeat region is hydrophobic with 70 collagen-like triplet repeats (GXX) and 54 GPT triplets (19). The hydrophobic nature of BclA may explain the general hydrophobicity of the entire spore (78). Between residues 41-232 is the repeat of $((GPT)_5GDTGTT)_2$ known as the BclA repeat (15). Variations in the BclA repeat, as well as parts of the N and C termini

displaying sequence polymorphisms, allow species and strain discrimination (99, 83). Differences in the number of repeats also correspond to the length of the hair-like nap on the exosporium (83). Mutants of *bclA* are apparently devoid of a visible nap on the outer surface of the exosporium (19).

The 134 aa C-terminal domain (CTD) is essential for forming the triple helical structure of the BclA protein. The CTD itself can naturally form a heat stable triple helix (75). This domain also faces away from the spore in the exosporium, and is the most external part of BclA. Recombinant BclA is resistant to many proteases, but is highly susceptible to collagenases, whereas the native glycosylated BclA is resistant to both (75, 72). Collagenase treatment of the rBclA leads to digestion of the amino terminal of the collagen like region, but the CTD remains resistant (72). BclA also has a dissociation constant equivalent to a triple helix when examined by circular dichroism (75). This CTD most likely acts as the stabilizing point, to which the rest of the BclA protein is folded. rBclA will spontaneously refold into a triple helix, starting with the CTD (75). BclA is predicted to have a lollipop structure, with the collagen-like region containing the stalk and the CTD forming a triple helical head of the globular protein (69). The globular CTD domain is strikingly similar to the C1q protein of compliment and tumor necrosis factor. Both BclA and C1q have been shown to be capable of interacting with the SP-C component, a major part of the lung alveolar surfactant layer (69).

The structure and role of BclA in the pathogenesis of *B. anthracis* is just now being elucidated. BclA electrophoretically migrates at >70 kDa, which is much greater than the 34 kDa expected from its amino acid sequence. This is potentially due to the large content of prolines, which have been shown to modify the migration of collagen-like proteins (15, 194). These collagen-like proteins are extremely rare in prokaryotes (19, 94). The repeated threonine residues throughout the repeat may serve as multiple sites of O-linked glycosylation (83). These proteins can form triple helical structures, without the need for hydroxyprolines that eukaryotes use in their collagen triple helices. Threonines can substitute by making direct hydrogen bonds to neighboring carbonyls to stabilize the structure (195). This stabilization can be enhanced by glycosylation of the threonines. Glycosylation of threonine residues in worm collagen greatly stabilize the triple helices (195). The glycosylation of BclA may lead to resistance to protease activity. The ability of bacterial collagen-like proteins to form triple helices *in vitro* has been recently shown with the streptococcal collagen-like proteins (95, 96). They too contain a long collagen-like internal region and may be involved in adhesion.

Two O-linked oligosaccharides, a 715 kDa tetrasaccharide and a 324 kDa disaccharide are released from spore- and exosporium-associated BclA after hydrazinolysis treatment (19, 23). Each oligosaccharide is probably attached to BclA by a GalNAc linker. The tetrasaccharide is found in multiple copies in the collagen-like region of BclA, and the disaccharide is most likely attached outside this region (74). The disaccharide is composed of a rhamnose residue and a component identified as 3-O-methyl-rhamnose. The tetrasaccharide is 2-O-methyl-4-(3-hydroxy-3-methyl-butamido)-4,6-dideoxy-β-D-glucopyranosyl-(1→3)-α-L-rhamnopyransol-(1→3)-α-L-rhamnopyranosyl-(1→2)-L-rhamnopyranose. The terminal end sugar is 2-O-methyl-

4-(3-hydroxy-3-methylbutamido)-4,6-dideoxy-D-glucose. This terminal sugar has been named anthrose. The anthrose sugar moiety is not found in the other members of the *B. cereus* family, although they all contain the BclA protein. This sugar could be exploited as a novel target of diagnostic kits (74). These sugars have been synthesized *in vitro* (70, 71).

Synthetically synthesized GPT repeats also are stabilized by glycosylation (69). Recombinant BclA expressed in *E. coli* hosts is not glycosylated. BclA is rarely found without being glycosylated, hinting at a linked production/glycosylation pathway (19). When the native protein in the spore is extracted and treated with trifluoromethanesulfonic acid (TFMS) to remove the glycosylation, the protein still retains a small portion of the sugar moieties (15, 19). A *bclA* mutant sporulates and germinates with kinetics similar to wild-type strains (19). The *bclA* gene has a putative σ^K promoter upstream of the open reading frame, consistent with sporulation stage expression of proteins produced in the mother cell. This open reading frame is followed by two inverted repeats after the termination codon.

The highly glycosylated nature of BclA may play a role in binding of the spores by carbohydrate recognition molecules of antigen-presenting cells (APCs; 19). This glycosylation also may protect the protein coat and spore from enzymatic cleavage and help exclude some molecules from gaining access to the spore. It may also play a role in adherence, as several other collagen-like proteins in prokaryotes have been predicted to be adhesins (95, 96, 152). *bclA* mutant spores presented no significant change in virulence in a mouse model of infection (77) but the course of disease was modified (personal communication). BclA is a major immunodominant antigen of the spore. This response is not to the extensive glycosylation of the

spore, which can elicit an immune response, but is to the protein component (15). Using a live or irradiated spore vaccine, an immune response to the tetrasaccharide itself can be made, and is another potential target for future vaccines (82, 76). BxpB, ExsFA, and ExsFB play a role in BclA being incorporated into the nap layer of the exosporium (80).

BclB

Recently, a second collagen-like spore glycoprotein of *B. anthracis* was identified (89). This new glycoprotein was named BclB for *Bacillus* collagen-like protein B. Other exosporium glycoproteins, ExsJ and ExsH, have been identified in *B. cereus* and *B. thuringiensis*, but have not been found in *B. anthracis*. Both ExsJ and ExsH have been found to migrate during electrophoresis as a >205 kDa species. ExsJ has been found to contain rhamnose, galactosamine, and a third unidentified sugar. ExsH has a region of collagen-like repeats, like ExsJ, but the carbohydrate composition has not been identified (89). The *bclB* determinant was predicted to have been formed from a unique crossover event between ExsH-like or ExsJ-like genes derived from *B. cereus* or *B. thuringiensis* (89).

Upon urea extraction of spores of *B. anthracis*, two high molecular weight glycoproteins were identified (89). One was the well characterized BclA protein, and the second, migrating at 205 kDa, was the newly identified BclB protein. When deglycosylated, BclB migrated as a band of about 83 kDa, suggesting that it has a collagen-like triple helix structure similar to BclA or is an extensively glycosylated protein. Using GC-MS analysis, 3-O-methyl rhamnose, rhamnose, and galactosamine were found to be part of the BclB glycoprotein, all three of which are also

present in BclA (89). BclB contains a repeated GXX motif, GITGVTGAT, which has been named the BclB repeat. The role of BclB in the *B. anthracis* spore was unknown and the subject of this research project.

Materials and Methods

Bacterial Strains

The bacterial strains used in this study are listed in Table 2. All *E. coli* strains were cultivated in L Broth or Tryptic Soy Broth (TSB, Oxoid). All *Bacillus anthracis* strains were grown in Brain Heart Infusion broth (BHI, Difco), with or without 0.5% glycerol, or L Broth, unless otherwise noted. Agar plates were made by mixing the above broths with 1.5% agar prior to autoclaving. Antibiotic selection was used for the maintenance and selection of plasmids and recombination events, and was used at the concentrations noted in Table 3.

Table 4 contains a table of the plasmids used in this study. Frozen stocks of all clones and constructs was made by heavily inoculation of freshly grown cultures into BHI broth containing 20% glycerol and placed on dry ice. After quick freezing on dry ice, the cryo-tubes were placed at -80^{o}C for long term storage and recorded in the Stewart Laboratory stockbook.

Strain	Genotype	Marker
E. coli		
DH5α	F- φ80lacZΔM15 Δ(lacZYA-argF)U169 deoR recA1 endA1 hsdR17(rk-, mk+) phoA supE44 thi-1 gyrA96 relA1 λ-	
GM48	F- λ- dam-3 dcm-6 thr-1 leuB6 ara-14 tonA31 lacY1 tsx-78 glnV44(Am) galK2(Oc) galT22 thi-1	
M15	see Qiagen manufacturer's specifications	
Able K	lac(LacZω-) [Kanr McrA- McrCB- McrF- Mrr- HsdR(rK-)] [F′ proAB lacIqZΔM15 Tn10 (Tetr)]	Kan^R
B. anthracis		
ΔSterne	7702 pX01- pX02-	
MUS1692	ΔSterne Δ*bclB* Kan::*bclB*	Kan^R
CTL292	ΔSterne Δ*bclA* 63-907	Kan^R

Table 2: Bacterial Strains used in this study.

	Chloramphenicol	Kanamycin	Erythromycin	Neomycin	Ampicillin	Gentamicin
E. coli	10 μg/ml	25 μg/ml	250 μg/ml	N/A	100 μg/ml	N/A
B. anthracis	10 μg/ml	50 μg/ml	5 μg/ml	25 μg/ml	N/A	2.5 μg/ml

Table 3: Antibiotic Concentrations

Plasmids	Description	Markers
pREP4	Qiagen LacI inducible repression plasmid	Kan^R
pQE30	Qiagen protein expression vector	Amp^R, Cm^R
pBT3571	BclA protein expression vector, pQE30 BclA ORF	Amp^R, Cm^R
pBT3642	BclB protein expression vector, pQE30 BclB ORF	Amp^R, Cm^R
pUTE583	Koehler *B. anthracis* cloning vector	Cm^R, Ery^R
pGS3632	Recombination vector with BclB flanking regions and KanR marker	Amp^R, Kan^R, Ery^R

Table 4: Plasmids used in this study

DNA Manipulations

Plasmid DNA from *E. coli* was isolated by following the Wizard Plus SV Plasmid DNA purification system (Promega) protocol or by the procedure of Birnboim and Doly (149). Quantification of the purified plasmid DNA was spectrophotometrically determined using the Nano-Drop ND-1000 spectrophotometer. Restriction endonuclease digestions were performed under the conditions set forth by the manufacturers. A characteristic digestion would be 10 µl of plasmid DNA at a concentration of 150 ng/µl; combined with 17 µl ddH_20, 3 µl of the corresponding restriction digestion buffer, and 1 µl of the restriction enzyme.

Clean up of plasmid and chromosomal DNA, ligation reactions, and PCR products was accomplished by extraction with an equal volume of TE-saturated phenol (pH 8.0) followed by extraction with an equal volume of chloroform. One final centrifugation (time and rpm or g value) was performed to fully remove any residual phenol/chloroform from the samples. A 0.1 volume of 3M Na acetate (pH 5.0) was added to the DNA, followed by 2.5 volumes of 95% chilled ethanol. The mixture was incubated on ice for 10 minutes, followed by a final spin of 10 minutes in a Marathon 16Km microcentrifuge (Fisher Scientific). The ethanol supernatant was decanted, and the remaining DNA pellet was placed in a Centrivap Concentrator (Labconco) for 20 minutes to remove any residual ethanol from the samples. The dried DNA pellet was resuspended in 20 µl of ddH_20. If the product was to be ligated post-precipitation, the two digested products would be mixed at the appropriate ratio prior to precipitation with ethanol.

Screening of isolated plasmid DNA or digested restriction products was accomplished by electrophoresis in a 1% agarose gel containing ethidium bromide (EtBr, 0.5 µg/ml) in tris-acetate electrophoresis buffer. The DNA was premixed with 3 µl DNA loading buffer (Promega) and loaded into individual wells of the gel.

Gel purification of DNA was accomplished using the procedure provided by the Quantum Prep Freeze N' Squeeze DNA gel purification kit (BioRad) or the Qiaquick Gel Extraction Kit (Qiagen). DNA ligations were performed at 16˚C using T4 DNA ligase in a 20 µl volume. When the DNA recovery rates were especially low due to low-copy plasmids or loss of samples, DNA pellets after ethanol precipitation were resuspended in 9 µl of dH_2O and added to 1µl 10x T4 DNA ligase buffer and 0.5 µl T4 DNA ligase. Ligations were usually performed with a ratio of insert to vector of 3:1. Ligation was allowed to continue overnight (14-20 hours) at 16^oC in a Microcooler II constant temperature chamber (Boekel Scientific).

Transformation of *E. coli*

Frozen competent cells were thawed on ice. 5-10 µl of ligated DNA or 1-2 µl of pure plasmid DNA was added to 50 µl of cells and allowed to sit on ice for 10 minutes. The cell-DNA mixture was heat-shocked by incubation of the mixture in a 37°C water bath for 5 minutes. Immediately after heat shocking, 250 µl of L broth was added to the mixture, and the cells were incubated for 60 min. at 37°C with shaking at 250 rpm. After a hour of incubation the broth was plated in 100 µl aliquots on plates containing the appropriate antibiotic, or resuspended in 5 ml of L broth with antibiotics and incubated overnight at 37°C.

PCR

All primers were obtained from IDT technologies (Coralville, IA). Primers were resuspended in 1 ml ddH_20. Aliquots of primers diluted to 25 ng/µl were prepared and stored frozen at -20°C. PCR reactions were performed using Ex-Taq polymerase as outlined by the manufacturer (Takara). A typical reaction would be: 10 µl 10X reaction buffer, 8 µl dNTPs, 3 µl primer 1 (25 ng/µl), 3 µl primer 2 (25 ng/µl), template DNA (2 µl of chromosomal miniprep DNA, 0.2 µl if plasmid DNA), 0.5 µl Ex-Taq enzyme, 73.5 µl ddH_20 for a total of 100 µl per reaction. Reactions were allowed to continue for 35 cycles, at T_Ms appropriate for the primers used. Extension times were set conservatively, corresponding to approximately 1 minute per kb of expected PCR product size.

Primers	Sequence
BclB KO Construction	
bclB 5pK	ggtaccgcagaaggaaaattaagttcg
bclB 3pS	gtcgacactaattcatctcgctttaac
bclB soeFB	aacaaaggatccctcattccacatttttgtttcctaattaac
bclBsoeRB	caaaaatgtggaatgagggatcctttgttacaatgttaatagg
BclA KO Screening	
5pbclAXh	aactcgagctgaaggcaatgtatc
3pbclAXh	aactcgagcaattctctcctctag
qbclA5pB	cgggatccatgtcaaataataattatt
qbclA3pS	agcgtcgacttaagcaacttttttcaat
Backbone Screening	
pute5p	cgataccgtcgacctcg
pute3p	aacaaaagctgggtacc
Intact BclA screening	
bclA5pXm	aacccgggctgaaggcaatgtatc
bclA3pS	agcgtcgaccaattctctcctctag
Intact BclB screening	
bclB5pK	ggtaccgcagaaggaaaattaagttcg
bclB3pS	gtcgacactaattcatctcgctttaac
BclA protein	
qbclA5pB	cgggatccatgtcaaataataattatt
qbclA3pS	agcgtcgacttaagcaacttttttcaat
BclB protein	
qbclB5pB	cgggatccatgaaacagaatgacaaattatg
qbclB3pS	agcgtcgacttagacgatattaagacctgc

Table 5: Primers used in this study

PCR products were cloned into either the Invitrogen pCR Topo 2.1 TA or the Stratagene pSCα-1 cloning vectors in accordance with the supplier's protocol. DNA inserts were sequenced using the M13 upstream and downstream primers on an Applied Biosystems 3730 DNA Analyzer using Applied Biosystems Prism BigDye Terminator cycle sequencing chemistry, and the sequences compared to the TIGR sequenced genome of the *Bacillus anthracis* Sterne strain.

Electroporation conditions

An overnight culture of *Bacillus anthracis* was grown in BHI broth with 0.5% glycerol with appropriate antibiotics. 0.5 ml of this overnight culture was used to inoculate 100 ml of BHI + 0.5% glycerol in a 500 ml Erlenmeyer flask. The flask was allowed to incubate at 37°C with shaking until the OD_{600} reached 0.6. The culture was then passed thru a disposable Analytical Test Filter Funnel apparatus with a pore size of 0.45 μm (Nalgene). The cells were then washed with 25 ml of ice cold Electroporation buffer, and this step was repeated three times. After the third wash, the filtered cells were recovered in 5 ml of ice cold Electroporation buffer and placed on ice.

1 mm electroporation cuvettes were loaded with 100 μl of cells and 1 μg of high quality plasmid DNA obtained from a *dam*$^-$ host. After loading, the cuvettes were pulsed at 25 μFD, 100 Ohms, at 2.5 kV. Immediately after pulsing, the cell/DNA mixture was resuspended in 1 ml of BGGM. After incubation at 37°C for 1 hour, aliquots were plated onto BHIA plates with the appropriate antibiotics and allowed to incubate overnight at 37°C.

Isolation of Chromosomal DNA.

B. anthracis strains were cultured in 10 ml TSB with appropriate antibiotic selection at 37ºC. The cells were harvested by centrifugation, washed with 10 ml TE buffer (0.01 mM Tris-HCl, 0.001 mM EDTA, pH 8.0), and the cell pellets frozen at -25ºC for several hours to overnight and then thawed, resuspended with 0.1 ml TE, and incubated at 37ºC for 30 minutes to induce autolysis. The cell lysate was treated with RNaseA (25 μg) and N-lauryl sarcosine (0.8%). Proteinase K (25 μg) was then added and the sample incubated at 60ºC for 1 hr. The sample was then cooled on ice and sequentially extracted with TE-saturated phenol and chloroform. The DNA was either dialyzed against distilled water at 4ºC overnight or precipitated with ethanol as described above and then resuspended in sterile distilled water.

Preparation of Competent *E. coli*.

Cells from an *E. coli* competent cell stock was streaked onto a prewarmed L agar plate and incubated overnight at 37°C. One colony was picked and inoculated into 5 ml L broth in a 15 ml polypropylene conical centrifuge tube (Fisher Scientific) and incubated overnight with shaking at 37°C. 1L of prewarmed L broth (with appropriate antibiotics) was inoculated with 1 ml of the overnight culture and incubated at 37˚C with shaking. Growth was allowed to continue until absorbance at 600 nm reached 0.2 for *recA*$^+$ strains or 0.6 for *recA*-negative strains. The culture was then chilled on ice for 10 minutes. The culture was dispensed into 6-250 ml centrifuge bottles, and centrifuged at 3,000 *g* for 10 minutes. After discarding the supernatant the pellets were resuspended in 50 ml of 0.1 M $CaCl_2$ (4°C). The bottles were placed

in an ice bath for 10 minutes, followed by another spin at 3,000 *g* for 10 minutes. The supernatant was again decanted and the pellets were resuspended in 10 ml of 0.1 M $CaCl_2$ and pooled. The pooled competent cells were kept on ice for 20 hours. After 20 hours, 2.5 ml of sterile glycerol were added, and the competent cells were aliquoted into sterile microcentrifuge tubes, quick-frozen on dry ice, and then stored at -80^{o}C for future use.

Protein Production

The ORFs of selected genes were PCR amplified and cloned into the plasmid pQE30 (Qiagen), to allow for inducible expression in *E. coli* by the addition of IPTG. These plasmid constructs were transformed into either GM48 or Able K strains of *E. coli* bearing the pREP4 plasmid that encodes the lacI repressor, to minimize basal transcription of the cloned ORF. A 5 ml overnight culture of the plasmid-containing bacteria was inoculated into 1 liter of prewarmed LB broth containing antibiotics and incubated with shaking for several hours at 37^{o}C. When the $O.D._{600}$ reached 0.6, 2 ml of 0.5 M IPTG was added to the flask to induce expression of the His-tagged protein. After 1 hour of induction, the culture was centrifuged for 10 minutes at 5,000 rpm using centrifuge bottles in a GSA rotor in a Sorvall RC5B Plus centrifuge. Cell pellets were frozen at -80^{o}C until the protein purification procedure was carried out .

Purification of proteins was done using a His-Spin Protein Miniprep purification kit (Zymo Research). Each cell pellet was resuspended with 1 ml of Zymo His-Binding Buffer, for a total of roughly 2-3 ml per culture. 1g of .1 mm glass beads (Biospec) was added into bead-beating tubes along with 1 ml of the resuspended cell pellet. The bead-beating tubes were bead-beat for 4-1 minute pulses, and centrifuged for 5 minutes in a microcentrifuge at 10,000 *g* to

remove the beads and cell debris. The supernatant was removed and the His-tagged proteins purified over the his-purification columns as per the manufacturer's suggested protocol. The eluted fractions were pooled and then dialyzed twice against PBS or distilled water at 4^{o}C overnight. Protein concentrations were determined using a Nano-Drop ND-1000 spectrophotometer and protein stored at -80^{o}C until use. Purity of the protein was assessed by SDS PAGE

Production of Rabbit Polyclonal Antibodies

A vial of Ribi adjuvant plus MPL + TDM + CWS Emulsion (Corixa) was warmed up to 42^{o}C for 10 minutes. 1 ml of sterile saline was added to the emulsion with a 21 gauge needle and vortexed vigorously for 3-4 minutes. 250 μg of purified protein was mixed with saline to a volume of 500 μl. This mixture was added to 500 μl of the adjuvant emulsion for a final volume of 1 ml. This immunogen sample was mixed vigorously by vortexing. Six subcutaneous injections were given and the rabbit was boosted after 3, 6 and 9 weeks. Prior to each boost, a bleed of 10 ml was performed. The resulting serum was tested for reactivity to recombinant protein by Western Blot analysis. When the desired antibody titer was reached, the rabbit was sacrificed and a terminal bleed was obtained.

The collected blood was allowed to clot at 4^{o}C for 1 hour. A swab was used to remove adherent material from the top of the tube. Tubes were centrifuged for 10 minutes at 5,000 rpm in a SM-24 rotor (Sorval). Clear sera were removed and aliquoted into labeled cryo-freeze tubes (Corning). These were then frozen and stored at -80^{o}C until use.

Sporulation Assays

An overnight TSB culture of *B. anthracis* was used to inoculate fresh media to an initial OD_{600} of 0.2. For sporulation in broth, 1 ml of culture was added to 9 ml broth and put in a 30°C or a 37°C shaker overnight. For sporulation on agar plates, 2 swabs of culture were distributed evenly across the surface of a 100 x 15 mm plate and then incubated at 30°C or 37°C. At various time points, cells were collected and split into two even aliquots. One aliquot of spores went in a 65°C water bath for 30 minutes to obtain a spore count (resistance to heat killing). The other half was diluted directly and plated for total viable CFUs.

Production of Spores

To obtain large quantities of spores, a 5 ml exponential phase culture was grown under antibiotic selection. Swabs of the culture were then inoculated evenly and heavily onto nutrient agar plates and incubated at 30°C for 5 days. Samples were taken and examined under phase contrast microscopy to assay the ratio of spores:vegetative cells. When greater than 95% of the samples were released spores, sterile swabs dipped in PBS were used to gently harvest the spores off the surface of the nutrient agar plates. The collected spores were pelleted in a microcentrifuge, and the supernatant discarded. The spore pellet was washed 3x in PBS to remove residual cell debris. Storage of the spores was done at room temperature or at 4°C.

Resistance Properties of *B. anthracis* Spores

Heat resistance. Spores from the wild-type and mutant strains were resuspended in PBS at a concentration of 10^8 cfu/ml in tightly capped tubes (to prevent evaporation volume loss) and placed in a 65°C water bath. Samples were removed at hourly intervals, dilutions prepared in sterile PBS, and plated on BHIA plates which were then incubated overnight at 37˚C for viable count determinations.

Resistance to ultraviolet irradiation. Spores were resuspended in PBS at a concentration of 10^6 spores/ml, placed in a sterile glass petri dish, and irradiated with a UV germicidal lamp (dose of 700 erg/mm^2). Samples were removed at 30 sec intervals diluted in sterile PBS, and plated on BHIA plates for viable count determinations.

Resistance to organic solvents (chloroform and ethanol). 50 µl of chloroform was added to 0.45 ml of spores in a 1.5 ml polypropylene microcentrifuge tube, vortexed vigorously, and incubated at room temperature for 10 min. An aliquot was then removed, serially diluted in PBS, and plated on BHIA plates for viable count determinations. For resistance to ethanol, 50 µl of the spores were added to 0.45 ml of 70% ethanol in a 1.5 ml polypropylene tube, vortexed, incubated, diluted, and plated.

Resistance to disinfectants. Spores were tested for resistance to phenol, bleach (sodium hypochlorite), and a quaternary ammonium salt disinfectant (Roccal-D [Upjohn]). To determine the level of resistance to these disinfectants, 50 µl of the spores were added to 0.45 ml of 5%

(w/v) phenol, bleach (1:32 dilution of bleach [5.25% sodium hypochlorite]), or 1:200 dilution of Roccal-D (stock was 20% alkyl dimethyl benzyl ammonium chloride) in 1.5 ml polypropylene microcentrifuge tubes. The samples were vortexed vigorously and kept at room temperature. After 10 minutes, aliquots were removed from each, serially diluted in PBS, and plated on BHIA plates for viable count determinations.

Germination Assay

To assay germination, $1x10^4$ spores in 100 µl were added to 900 µl of DMEM + low glucose, or 900 µl DMEM + low glucose (**NOTE:** define low glucose) and 10% FBS. After 1 hour, the sample was divided and half placed at 65°C for 30 minutes and plated on BHIA to obtain a plate count of ungerminated spores, and the other half was directly plated on BHIA to obtain a total CFU count. The difference between the two counts was equivalent to the number of spores germinated.

Macrophage Infection Assay

10^5-10^6 RAW 264.7 Mφ were dispensed into 24-well tissue culture plates (Falcon) and were incubated overnight in Dulbecco's Modified Eagle Media (DMEM) with low glucose plus 10% heat inactivated [65ºC for 1 hr] fetal bovine serum (FBS). Endospores were diluted in DMEM with 10% FBS and then immediately added to wells at an MOI of 1:1 or 10:1 spores:macrophages. To maximize the number of endospores interacting with Mφ, the plate was centrifuged at 1,000 rpm for 5 min in a Sorvall 6000D tabletop centrifuge (Sorvall Instruments)

equipped with a Sorvall H100B rotor that was prewarmed to 37°C. After centrifugation, the plates were incubated for an additional 30 min at 37°C in an H_2O saturated atmosphere with 5% CO_2 to allow for germination and outgrowth of endospores. The culture medium was aspirated from each well, the Mφ were washed and the medium was replaced with fresh medium supplemented with 50 μg/ml gentamicin and incubated for 30 min at 37ºC to eliminate any unphagocytosed germinated endospores and extracellular vegetative cells. The medium was removed and the cells washed twice with fresh antibiotic-free DMEM and resuspended in fresh prewarmed medium. Intracellular bacterial numbers were then quantified by dilution plating after Mφ from triplicate wells were lysed with distilled water (lysis was observed under light microscopy). The bacteria were serially diluted in PBS and plated on BHIA plates directly (total viable counts) or after heating for 30 minutes at 65ºC (ungerminated spore counts).

SDS PAGE

10 mg (wet wt) of spores were either extracted by boiling the spores in a urea buffer (50 mM Tris-HCl, pH 10, 8 M urea, 2% 2-mercaptoethanol) or by boiling the spores in SDS sample buffer (50 mM Tris-HCl, pH 6.8, 4% SDS, 10% glycerol, 2% B-mercaptoethanol, 0.02% bromophenol blue) for 10 minutes. The extracted spores were pelleted at 10,000 *g* for 10 minutes at room temperature. The supernatant was removed and used to load individual lanes of a 4-20% gradient Tris-HCl protein gel (Bio-Rad) and electrophoresed in Tris-glycine-SDS buffer. Gels were stained with coomassie brilliant blue.

Analysis of Glycoproteins and Phosphoproteins

Proteins separated on 4-20% Tris-HCl gradient SDS PAGE gels were stained with glycoprotein stain (Pierce) or Pro-Q Phosphoprotein stain (Invitrogen) as per the suggestions of the supplier. Images of the phosphoprotein stained gels were taken at 340 nm.

Western Blots

After proteins were resolved by SDS PAGE, the gel was washed twice with cold transfer buffer. The gel was transferred onto a nitrocellulose (NC) membrane using a BioRad transfer cassette apparatus. The NC membrane was removed and placed in blocking buffer with StartingBlock (Pierce) for 1 hr with gentle shaking. The blocking reagent was discarded, and1-3 µl of primary rabbit polyclonal antiserum was added in wash buffer to the blot and placed on a gyrotary shaker for 1 hour at room temperature. After two quick washes in wash buffer, the blot was washed 6X for 5 minute intervals with wash buffer.

The wash buffer was discarded, and 1 µl of goat anti-rabbit IgG-alkaline phosphotase conjugate (Vector) was added in wash buffer and allowed to shake for 1 hour. After two quick washes in wash buffer the blot was washed 8x in 5 minute intervals with wash buffer. Development of the blot was performed using the AP Conjugate Substrate kit (BioRad) to the manufacturer's instructions and allowed to develop for 10 minutes. The blot was blotted dry with a paper towel.

Protein Identification Via MALDI-TOF MS Analysis

Coomassie stained gel bands were excised from the gel using a razor blade, transferred to a microcentrifuge tube, and minced to approximately 1-2 mm^3 pieces. The gel pieces were first equilibrated for 15 minutes in 500 µl 100 mM ammonium bicarbonate solution at RT with gentle mixing. Bands were then destained with 3-15 minute washes in 500 µl of 50/50 acetonitrile/100mM ammonium bicarbonate wash. Gel pieces were then dehydrated for 20 minutes in a fresh aliquot of acetonitrile. The acetonitrile was replaced with 150 µl 10 mM DTT in 100 mM ammonium bicarbonate. Gel bands were then rehydrated and reduced at 56^{o}C for 30 minutes. The reducing agent was removed and the protein bands were alkylated in-gel with 100 µl 50 mM iodoacetamide in 100 mM ammonium bicarbonate for 30 minutes in the dark. The gel pieces were then rinsed with wash solution before a final round of dehydration in acetonitrile.

Protein bands were rehydrated for 2 hours at 4^{o}C in a 20 µg/ml solution of modified TPCK-treated porcine trypsin (Promega) At the end of the rehydration period the trypsin solution was replaced with 40 mM ammonium bicarbonate/10% acetonitrile and the proteins digested overnight at 37^{o}C The digested protein solution was recovered from the protein gel pieces and transferred into 600/300/100 acetonitrile/water/10% TFA acid. The gel pieces were then extracted twice for 10 minutes in the same solution. The pools were frozen with liquid nitrogen and lyophilized. Dried digests were reconstituted in 990/10 water/88% formic acid for desalting with a micro C18 Ziptip (Millipore). Each sample was cycled in and out of a Ziptip 15 times for peptide loading onto the column. The Ziptip loaded with protein were washed 5 times with the water/formic acid solution, followed by elution with a 700/290/10 acetonitrile/water/88% formic acid solution.

0.6 µl of the elution was mixed with 0.6 µl of alpha-cyano-4-hydroxycinnamic acid (CHCA) matrix solution. A 0.4 µl aliquot of the mixture was deposited on a polished stainless steel target and allowed to crystallize. Mass Spectra were acquired using an Applied Biosystems Inc. 4700 MALDI TOF/TOF MS with a 355 nm Nd:YAG laser (200 Hz) in the positive ion delayed extraction reflector MS or positive ion MS/MS mode. The eight most intense ions were selected for analysis for MS/MS. Database searches were performed in the automated batch mode with Applied Biosystems' GPS Explorer (version 3.6). Data were submitted to Matrix Science's Mascot search engine for queries against the NCBI nr bacteria protein database.

Transmission Electron Microscopy

To the buffer-washed spores, 1 ml of a 2% glutaraldehyde, 0.1 M sodium cacodylate solution containing 0.1% ruthenium red (Electron Microscopy Sciences, Fort Washington, PA) was added and incubated for 1 hour at 37°C. Each pellet was then washed in cacodylate buffer and fixed for 3 h at room temperature in a 1% osmium tetroxide (Electron Microscopy Sciences), 0.1 M sodium cacodylate solution containing 0.1% ruthenium red. A negative control was treated identically, but ruthenium red was omitted from these two steps. Spores were washed in buffer and embedded in 3% agar (EM Science, Gibbstown, NJ). Dehydration involved sequential treatment with 25, 50, 75, 95, and 100% acetone. Polymerization was carried out at 60°C in Epon/araldite resin. Electron microscopy sections were cut at 85 nm thickness and put on 200 mesh carbon-coated copper grids and then stained with a 2% uranyl acetate solution (Electron Microscopy Sciences) for 40 min at 37°C. The sections were then treated with Sato's Triple Lead for 3 minutes, washed in ultrapure water, and stained again for 18 minutes in 5% uranyl acetate,

followed by one final wash and were observed by transmission electron microscopy with a JEOL 1200EX electron microscope.

Immunogold labeling of embedded spores was performed after fixation of spores in a 2% gluteraldehyde and 2% formaldehyde PBS solution. After dehydration and embedding as listed above, the cut grid sections were blocked in a 1% BSA solution for 30 minutes. The grids were thrice washed in PBS, and the primary antiserum was added to the grids at a concentration of 1:25 in Incubation buffer (Aurion). Following a one hour incubation at room temperature, the grids were washed 6X in Incubation buffer, and were incubated with 1:25 goat anti-rabbit secondary conjugate with 15 nm colloidal gold (Aurion) and incubated for two hours. After a series of washes in PBS, the grids were post-fixed in 2% gluteraldehyde on 0.1 M PBS for 5 minutes followed by washes in PBS and distilled water.

Scanning Electron Microscopy

B. anthracis spores were fixed overnight at 4°C in 20 volumes of modified Karnowsky's fixative (2% paraformaldehyde, 2.5% glutaraldehyde, 1.7 mM $CaCl_2$ in 0.1 M cacodylate buffer [pH 7.4]). After the spores were fixed, they were washed twice in 0.1 M cacodylate buffer (pH 7.4) and post-fixed in 1% osmium tetroxide in 0.1 M cacodylate buffer overnight at 4°C. After the cells were washed twice in double-distilled water, they were resuspended in double-distilled water, mounted on coverslips coated with poly-L-lysine, and dehydrated in a series of alcohol solutions (25, 50, 70, 95, and 100%). Dehydrated samples were treated for 5 min with hexamethyldisilazane (Electron Microscopy Supplies, Ft. Washington, Pa.), dried, mounted, and

sputter coated with gold (S150A sputter coater). Samples were viewed in a Hitachi H-300 electron microscope with a 3010 scanning image accessory.

For SEM immunogold labeling, spores were attached to poly-L-lysine coverslips and allowed to adhere for 30 minutes. They were then rinsed in PBS with 50 mM NH_4Cl, followed by a PBS blocking solution (1% BSA and 1% goat serum) for 5 minutes. Anti-BclA rabbit polyclonal antiserum was diluted in PBS blocking solution (1:50) and added to the coverslips for 30 minutes at room temperature. Two 5 minute washes in PBS plus 0.1% BSA followed. 15 nm colloidal gold conjugated goat anti-rabbit IgG antibodies (Aurion) were diluted 1:20 in PBS plus 0.01% fish gelatin and applied to the spores for 30 minutes at room temperature. Three washes in PBS were performed, followed by fixation in 2% gluteraldehyde in PBS for 1 hour. The coverslips were then washed twice in PBS buffer, and three times in distilled water. The spores were then dehydrated and treated as above.

NO Assay

50 µl of media from each well of the infection study was taken at various intervals and placed in a 96-well plate. To each well 50 µl of sulfanilamide solution (.33% w/v in 2.5% Phosphoric acid) and 50 µl of (.03% w/v in 2.5% Phosphoric acid) N-(1-Naphthyl)ethylenediamine dihydrochloride solution were added to each sample. Measurements were made using a Bioluminometer (Bio-Tek Synergy HT) at 500 nm. The results of the assay were compared against a dilution standard of sodium nitrite.

Epi-fluorescence Microscopy

5 mg of spores (wet wt.) were resuspended in StartingBlock (Pierce) and incubated at room temperature for 45 minutes with occasional mixing. The spores were then pelleted and resuspended in StartingBlock. Rabbit anti-BclA or anti-BclB polyclonal antiserum (1:250 dilution) was then added and incubated at room temperature for 45 minutes with occasional mixing. The spores were washed 3X in StartingBlock and then incubated with (amount) FITC-Protein A conjugate (Sigma Chemical Co.) and incubated for 45 minutes at room temperature with occasional mixing. The spores were subsequently washed 3X with StartingBlock, resuspended in PBS, and then examined by epi-fluorescence microscopy using a Nikon E600 microscope.

Spore Analysis by Flow Cytometry

10 mg of spores were resuspended in 500 μl of 4% paraformaldehyde in PBS and incubated for 2 hours at room temperature. The spores were then washed 4X with PBS and then resuspended in StartingBlock and incubated with mixing at room temperature for 45 minutes. The spores were then pelleted and resuspended in StartingBlock. Rabbit polyclonal antiserum (1:250 dilution) against BclA or BclB was then added and incubated with mixing at room temperature for 45 minutes. The spores were then washed 3X in StartingBlock PBS and then incubated with mixing with FITC-Protein A conjugate (Sigma Chemical Co.) and incubated for 45 minutes at room temperature. The spores were subsequently washed 3X with StartingBlock, followed by 2X with PBS and then processed on a FACScan flow cytometer using a 488 nm

argon laser (Beckton Dickinson Biosciences). Data were analyzed using Cell Quest analysis software (Beckton Dickinson). For the ethanol-treated spores, the spores were resuspended in 50% ethanol for 10 minutes and then pelleted and resuspended in StartingBlock. The treated spores were then exposed to the antiserum and FITC-Protein A as described above.

Results

Mutant Strain Construction

A precise in-frame deletion of the *bclB* determinant was created utilizing the splicing by overlapping extension (SOE) procedure (150, 151). Primers bclB 5pK (ggtaccgcagaaggaaaattaagttcg), bclB 3pS (gtcgacactaattcatctcgctttaac), bclB soeFB (aacaaaggatccctcattccacatttttgtttcctaattaac), and bclBsoeRB (caaaaatgtggaatgagggatcctttgttacaatgttaatagg) were obtained from Integrated DNA Technologies, Inc. (Coralville, IA) and used to amplify a DNA fragment consisting of the 1 kb sequence immediately upstream of the *bclB* open reading frame and the 1 kb sequence immediately downstream of this determinant. Flanking the PCR fragment are unique *Kpn*I and *Sal*I sites incorporated into the outer primers and a unique *Bam*HI site at the position of the deleted *bclB* determinant. The cloned PCR fragment was verified by DNA sequence analysis at the University of Missouri DNA Core Facility. The ΩKan2 cassette (152) was inserted as a *Bam*HI fragment into the unique BamHI site of the SOE product. The Gram-positive replication region and erythromycin resistance marker from pUTE583 (153) was subcloned into the plasmid to create the mutagenic shuttle plasmid pGS3632 (Figure 6). The pGS3632 plasmid was passaged through the *dam*-negative *E. coli* host GM48 and electroporated into the ΔSterne strain of *B. anthracis* by the method of Green *et al.* (154). Allele replacement mutants were obtained as described by Saile and Koehler (155). Electrotransformants were screened for resistance to kanamycin (50 μg/ml) and neomycin (25 μg/ml) and sensitivity to the vector encoded erythromycin resistance (5 μg/ml).

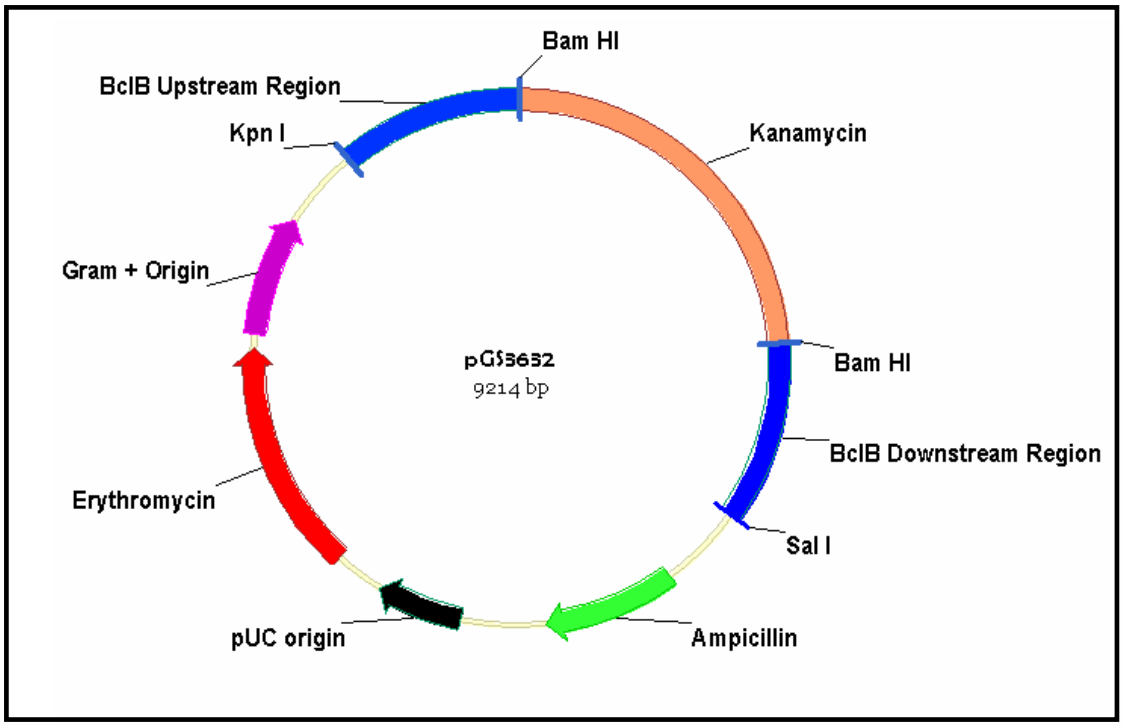

Figure 6: *bclB* knockout vector pGS3632

Verification of the *bclB* mutant and the CTL292 *bclA* mutant.

DNA was isolated from clones with the correct antibiotic-resistance phenotype and screened by PCR for the presence of the plasmid backbone (using primers pute5p cgataccgtcgacctcg and pute3p aacaaaagctgggtacc), an intact *bclA* region (primers bclA5pXm aacccgggctgaaggcaatgtatc and bclA3pS agcgtcgaccaattctctcctctag), and the *bclB* region (primers bclB5pK ggtaccgcagaaggaaaattaagttcg and bclB3pS gtcgacactaattcatctcgctttaac).

A precise deletion of the *bclB* determinant was introduced into *B. anthracis* ΔSterne-1 to create strain MUS1692. PCR analysis confirmed that the 1.1 kb *bclB* open reading frame was

successfully deleted and replaced with the 2.2 kb kanamycin resistance cassette as evidenced by the upward shift of the PCR amplicon (size increase of 1.1 kb.) (Figure 7) Sequence analysis of the MUS1692 amplified DNA fragment confirmed its identity as the deletion allele.

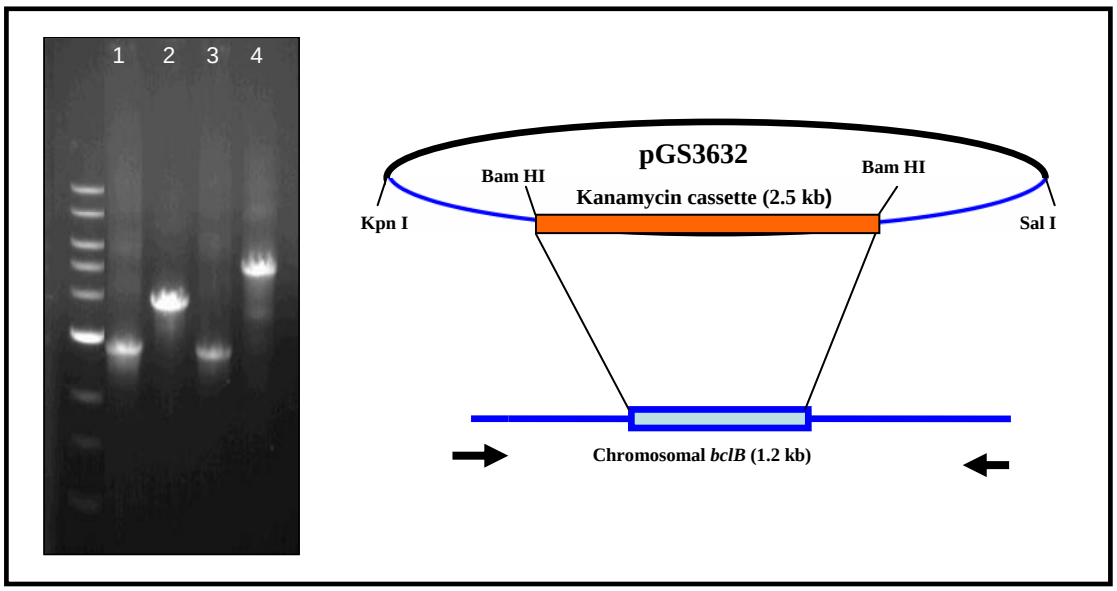

Figure 7: Left Panel: PCR analysis of the *bclB* null mutant of *B. anthracis*. Primers were designed to amplify a 2.9 kb fragment containing *bclA* (as a control; lanes 1 and 3) or a 4.0 kb fragment containing *bclB*. Lanes 1 and 2 are products from the ΔSterne wild-type strain and lanes 3 and 4 represent products from strain MUS1692. The 5.2 kb band in lane 4 corresponds to the replacement of the 1.1 kb open reading frame with a 2.2 kb kanamycin resistance cassette. Right panel: Demonstration of the replacement of the *bclB* gene with the kanamycin cassette.

Chromosomal DNA was isolated from the *bclA* mutant strain CTL292 (a gift from Charles Turnbough, Jr, 75) and PCR amplification was carried out with the primer pair 5pbclAXh (aactcgagctgaaggcaatgtatc) and 3pbclAXh (aactcgagcaattctctcctctag) to amplify a DNA fragment whose ends were external to the deletion, and the primer pair qbclA5pB (cgggatccatgtcaaataataattatt) and qbclA3pS (agcgtcgacttaagcaacttttttcaat) to amplify internal to the *bclA* open reading frame. The internal deletion and the presence of the kanamycin cassette were verified by PCR and the shift of the amplicon from 2.8 kb to 3.9 kb in length. The junction of the deletion was also verified by the presence of a 120 bp product versus the 1.1 kb wild-type *bclA* ORF length, demonstrating the deletion of the collagen-like region (CLR) of *bclA*. (Figure 7)

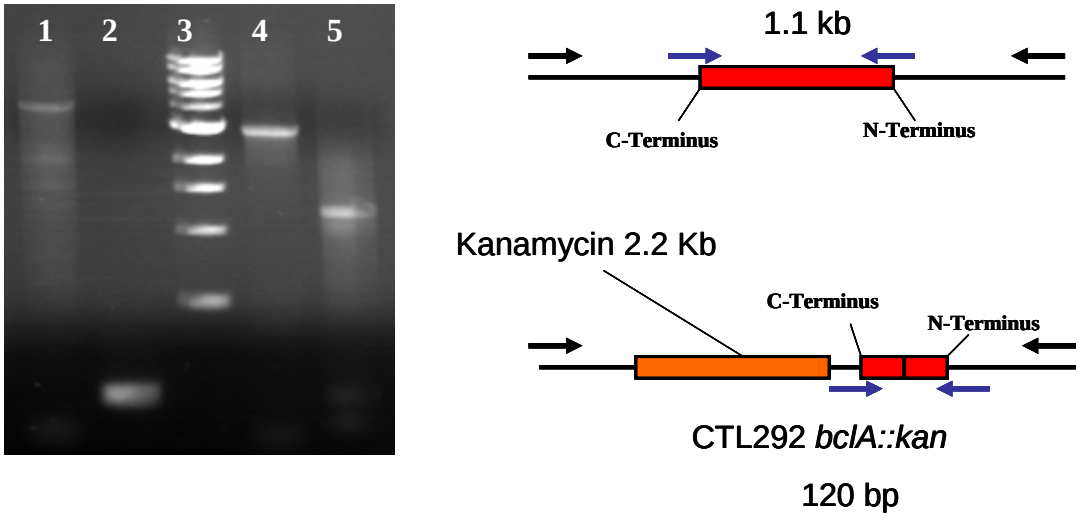

Figure 8: PCR analysis of the bclA mutant CLT292. Left, PCR gel: Lane 1, CTL292 bclA flanking regions,Lane 2, CTL292 bclA, Lane 3, DNA ladder, Lane 4, ΔSterne bclA flanking regions, Lane 5, ΔSterne bclA. Right: Representative map of the bclA gene in CTL292. Blue arrows denote internal primer locations, Black, primers amplifying flanking regions

Electron microscopic examination of the spores lacking the BclB glycoprotein.

Transmission electron microscopy revealed that the Δ*bclB* spores comprised a mixed population of spores. Many of the spores were morphologically identical to the parental strain spores (Fig. 9A). However, a number of spores with damaged exosporia were evident. The majority of these had ruptures of the exosporium layer, usually at one pole of the elliptical spore (Fig. 9B, 9C and 9F). In addition, empty exosporia were evident in the mutant spore preparation (Fig. 9B, 9D and 9E), but were not present in the spores prepared from the wild-type parental strain. A large amount of debris that visually resembled exosporium material was abundant in spore preparations from the mutant strain, but not from the wild-type parent. (Fig 10A, 10B) Ruthenium red staining of the spores, which allows visualization of the glycoprotein outer nap layer of the exosporium (156), revealed that the surface glycoprotein, thought to be predominantly BclA, was present in both the mutant and wild-type spores. This dye also stained the debris material, supporting the idea that this material was shed exosporia. (Figure 10)

Over two hundred spores from the ΔSterne-1 and MUS1692 strains were examined from electron micrographs and the numbers of spores with an intact exosporium were calculated (Table 6). In a typical spore preparation, 95% of the wild-type spores appeared normal, whereas only 60% of the BclB-negative spores had a normal architecture. The remainder of the BclB-negative spores displayed a damaged exosporium. The defect was either minor, with the damage usually at one pole of the spore, or severe with the spore either devoid or largely devoid of an exosporium layer. In addition, free exosporia are evident in the spore fields from the *bclB* mutant but were not observed in spore preparations from the wild-type spores. It appears that a

consequence of a lack of BclB production is the assembly of spores with a more fragile exosporium layer.

Strain	No. of spores examined	Normal morphology	Major exosporium damage	Minor exosporium damage	No. of empty exosporia[b]
ΔSterne	345	326 (94.5%)	0	19 (5.5%)	0
bclB-negative	230	138 (60%)	34 (15%)	58 (25%)	38

Table 6: Intact spores from electron micrographs were counted and characterized. Minor damage is defined as an obvious rupture of the exosporium layer but with ≥50% of the exosporium remaining associated with the spore coat surface; major damage is defined as loss of more than half of the exosporium layer and includes the exosporium-negative spores.

b: Free exosporia numbers not included in the spore numbers or the damaged spore categories.

To determine the distribution of the BclB protein in the spore, immunogold labeling of the TEM samples was performed using goat-anti rabbit antibodies labeled with 15 nm colloidal gold particles. Anti-BclB antibodies bound to the exosporium, as well as in the spore coat and spore cytoplasm (Fig. 11A). Further analysis of the controls, where preimmune sera (Fig. 11B) or sera raised to a non-bacillus immunogen was used (data not shown), showed a low level of non-specific binding in the cytoplasm and spore coat. Non-specific binding was consistently found, but was always localized to the spore core and inner spore coat layers, and was not seen in the exosporium. This supports the contention that the immunogold labeling of the exosporium was specific binding to the BclB protein. The presence of an increased amount of immunogold label in the coat and core of the wild-type spores when compared to the control sera-treated spores suggested that BclB was present in those parts of the spore as well, and was not just localized to the exosporium. Further evidence that BclB may also play a structural role in the spore coat was the appearance of what resembled sloughed off spore coat in the *bclB* mutant. (Fig 10B).

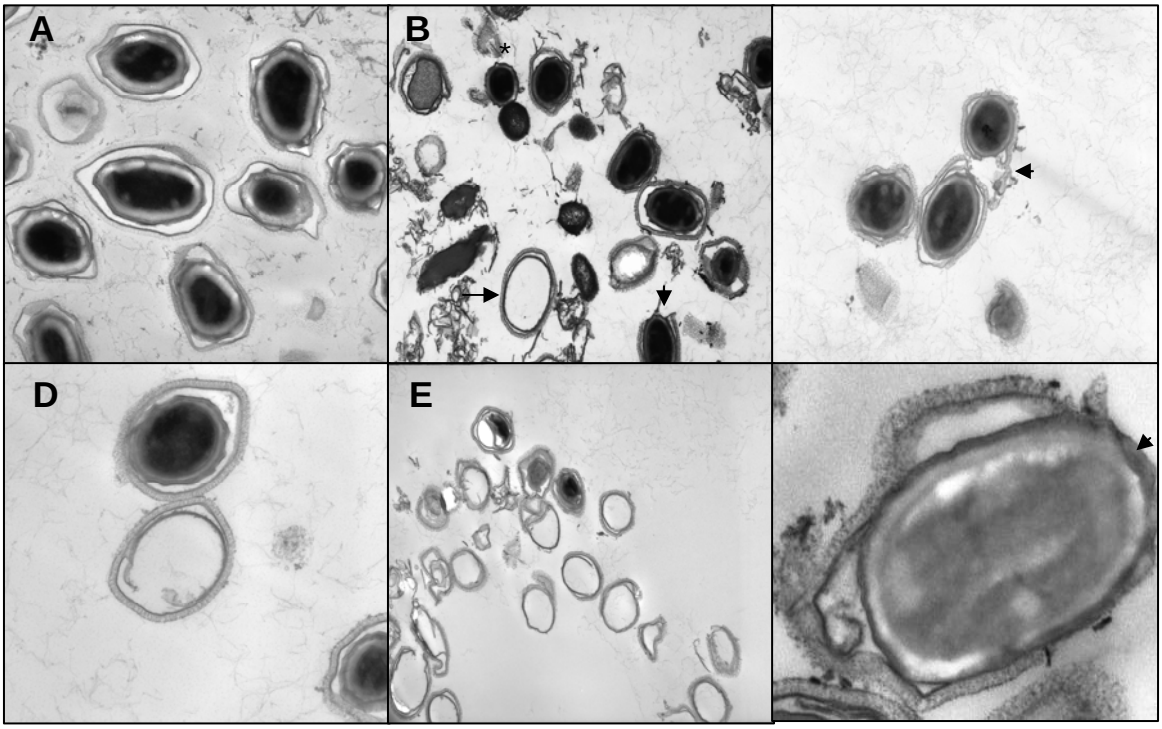

Figure 9: Transmission electron micrographs of spores from the ΔSterne strain (panel A) and the *bclB*-negative strain (panels B-F). In panel B, defects typical of a BclB-negative phenotype are illustrated including an exosporium-less spore (asterisk), ruptured exosporium (arrowhead) and empty exosporium (arrow). Panel C shows damaged exosporia and panels D and E (lower magnification) show the empty exosporia. Panel F is a higher magnification of a spore displaying typical damage to the exosporium which appears to be sloughing off the spore.

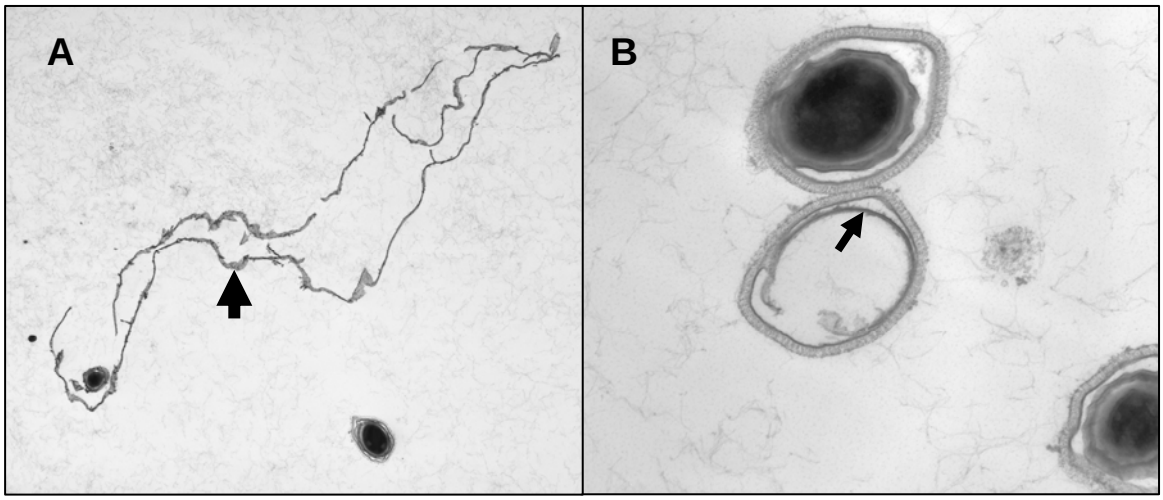

Figure 10: TEM depictions of the free spore material. Panel A: Arrow points to free exosporium-like debris. Panel B: Arrow points to sloughed off material inside free exosporium, potentially spore coat.

To further characterize the exosporium of the *bclB*-mutant spores and also to determine if the debris present in the BclB-negative spore samples was exosporium, immunogold labeling was performed with polyclonal anti-BclA sera. In both the ΔSterne and the BclB-negative spores, significant binding of the immunogold particles was found in the nap layer of the exosporium of the anti-BclA labeled spores (Fig. 11C, 11D). Both strains, when stained with anti-BclA and anti-BclB antibodies, displayed an increase in the labeling of the spore coat and cytoplasm relative to the immunogold labeling observed with the control sera. Although other studies have not shown the presence of BclA in the spore coat and cytoplasm (75, 25), the use of a polyclonal antiserum (instead of monoclonal antibodies used in other studies) may explain the differences seen in these micrographs, as more epitopes can be recognized by the multivalent sera. In

addition, the ruthenium red-stained exosporium-like debris found in the *bclB* mutant also reacted with the anti-BclA antibodies, further suggesting that this debris was shed exosporia (Figure 10A).

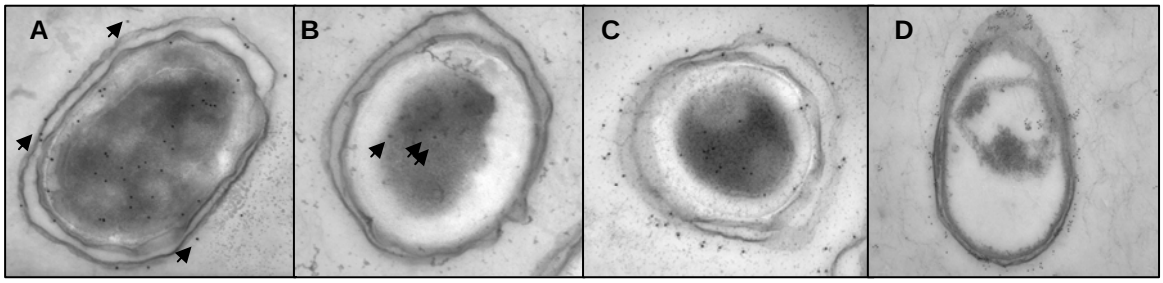

Figure 11: TEM immunogold labeled spores. A: ΔSterne spore labeled with anti-BclB polyclonal antisera and 15 nm colloidal gold beads. B: ΔSterne spore labeled with preimmune sera and 15nm gold beads. C: ΔSterne spore labeled with anti-BclA polyclonal antisera and 15 nm gold beads. D: MUS1692 labeled with anti-BclA antisera and 15 nm gold beads. Arrows denote presence of gold beads.

Changes in the outer surface of the BclB-negative spores were confirmed by scanning electron microscopy (Fig. 12). The majority of spores from the ΔSterne strain (Fig. 12A) exhibited a smooth raisin-like surface with characteristic ridges similar to those observed by atomic force microscopy (12, 157). Many of the *bclB*-negative spores displayed a rougher,

dimpled appearance (Fig. 12B). A subpopulation of the BclB-negative spores contained ridges and had a distinctly wild-type appearance. This rougher appearance could represent the changed appearance of the disorganized exosporium layer itself in the *bclB* mutant, or alternatively, may signify a disruption of the exosporium layer and visualization of the underlying spore coat layers. The sloughed off material in the *bclB* mutant may well be exosporium (Fig. 12C). The presence of ridges on the spores was reported to signify a lack of an exosporium (12). To determine if the exosporium was still present in the *bclB*-negative mutant spores, immunogold labeling of the spores using rabbit anti-BclA polyclonal sera was carried out. Since the BclA protein is surface exposed in the exosporium layer loss of the exosporium would eliminate binding of the anti-BclA antibodies. Immunolabeling demonstrated that the *bclB*-negative spores, despite their changed appearance, retained the exosporium as shown by the presence of surface-exposed BclA (Fig. 12D, E). There was a greater amount of debris associated with the mutant spores than was seen with the wild-type spores, presumably shed exosporium fragments. To further validate the presence of BclB in the exosporium of spores as was observed by TEM, immunolabeling of wild-type spores for visualization by SEM was accomplished using anti-BclB sera. The presence of immunogold label on the spore surface further supported BclB being present in the exosporium (Fig 12F). However, the BclB-labeling of the spores occurred at a reduced level relative to the immunogold labeling that of BclA. This supported the hypothesis that BclB is present on the spore surface at a substantially reduced level compared to that of BclA.

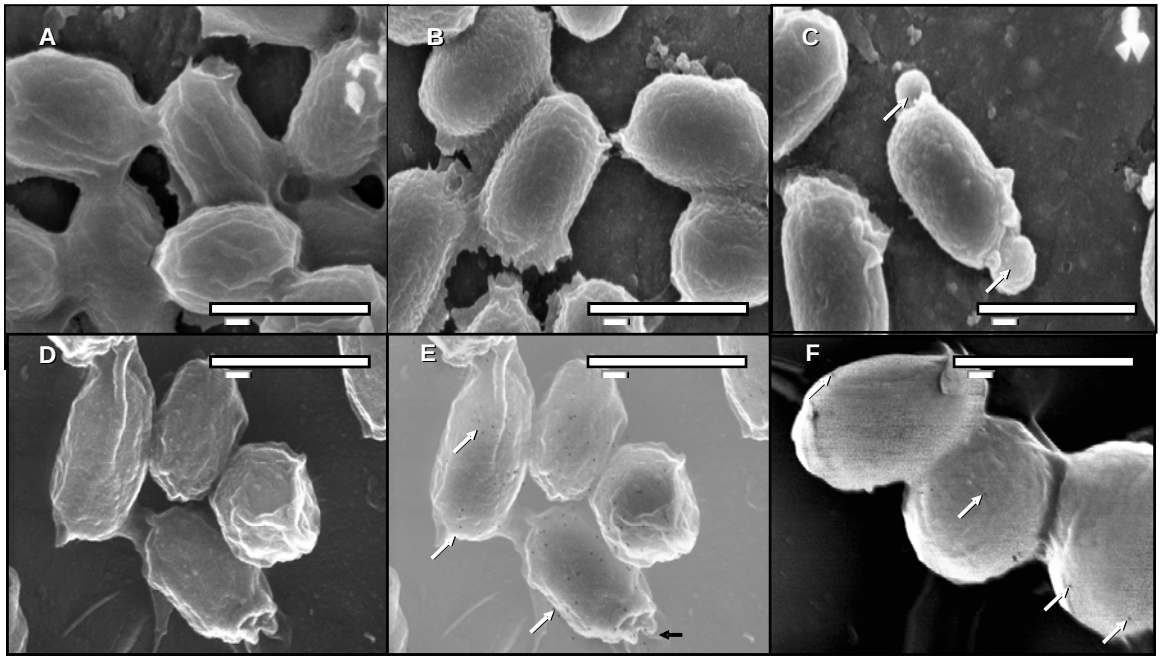

Figure 12: Scanning electron micrographs of the spores from ΔSterne (Panel A) and the *bclB*-deficient spores (B-F). Bars represents 1 micrometer. The appearance of material sloughing off mutant spores is marked in Panel C by the white arrows. Immunogold labeling of *bclB*-negative spores with anti-BclA antisera (D) and with overlaid backscatter image (E). White arrows denote some of the sites where 15 nm gold beads are evident. The black arrow in panel E points to gold bead labeling localized to sloughed off exosporium. Panel F depicts ΔSterne spores labeled with anti-BclB antibodies. Arrows denote some of the sites of surface-bound antibody.

Resistance Properties of the Mutant Spores.

The BclB-deficient spores were compared to the wild-type spores for resistance to heat (65˚C), ultraviolet irradiation (700 erg/mm^2), organic solvents (chloroform, 5% phenol), and disinfectants (bleach, 1:32 dilution; and 95% ethanol). No significant differences were observed in the resistance properties of the mutant versus wild-type spores except with chloroform, consistent with the resistance properties of the spores being a property of the spore coat layer (158), and the exosporium layer not substantially contributing to these resistance properties. (Figure 13) Bleach was found to be a very efficient disinfectant for the sterilization of *Bacillus anthracis* spores.

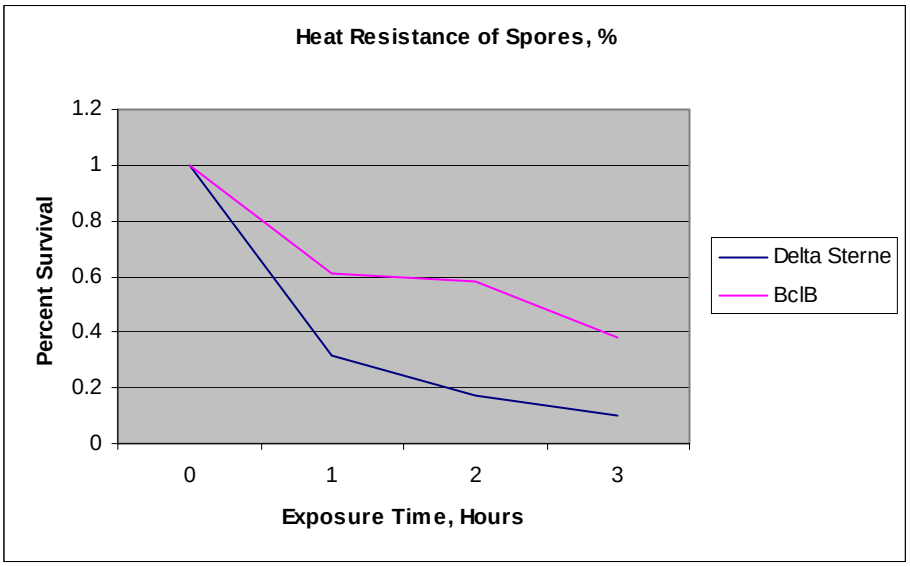

Figure 13A: The *bclB* mutant and wild-type ΔSterne spores and resistance to various insults.

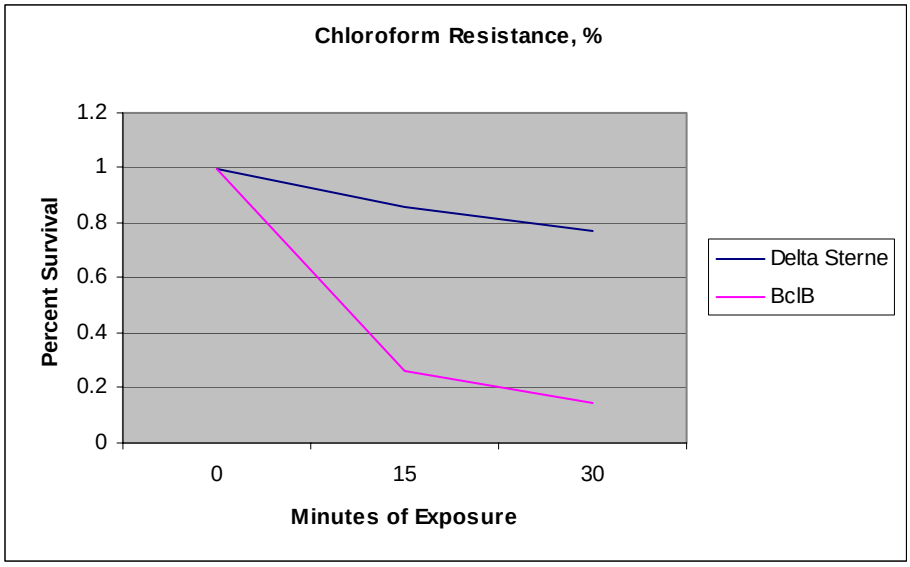

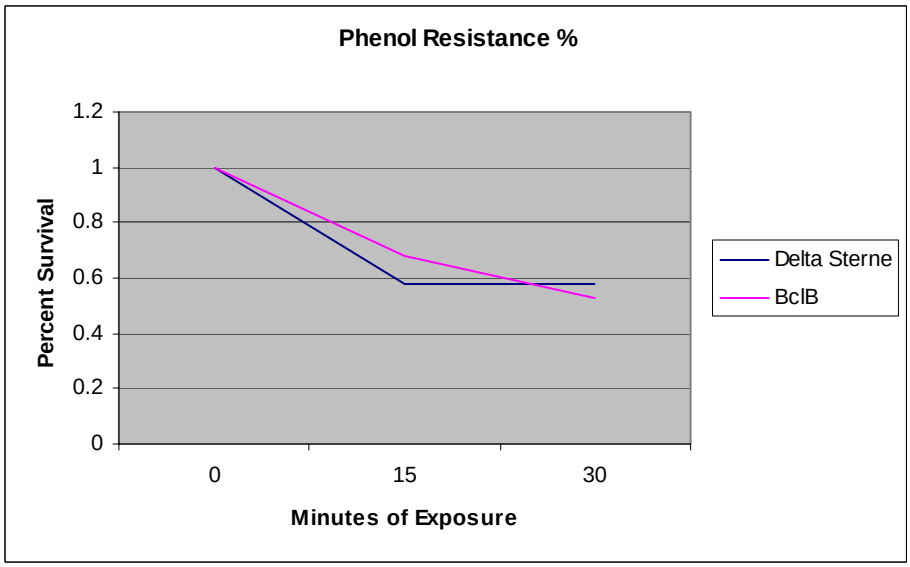

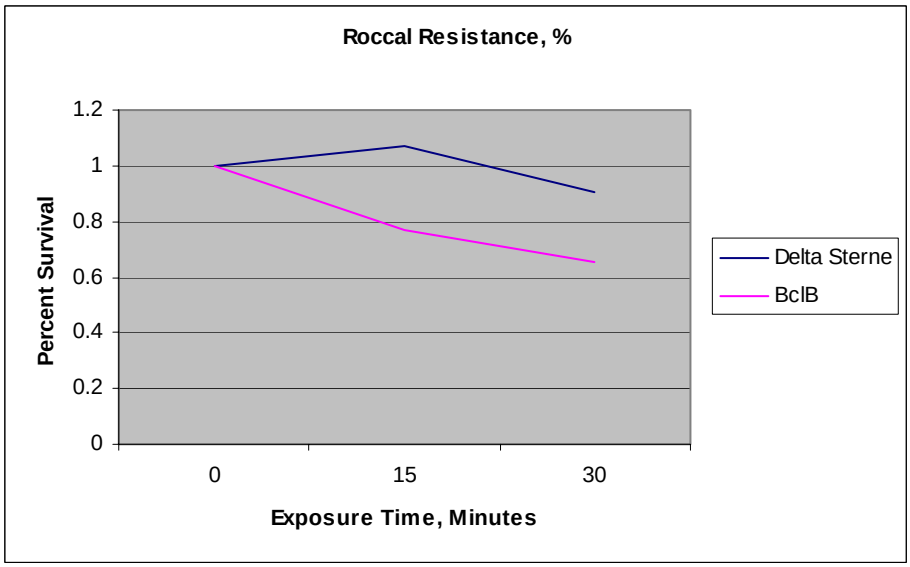

Figure 13B (Continued)

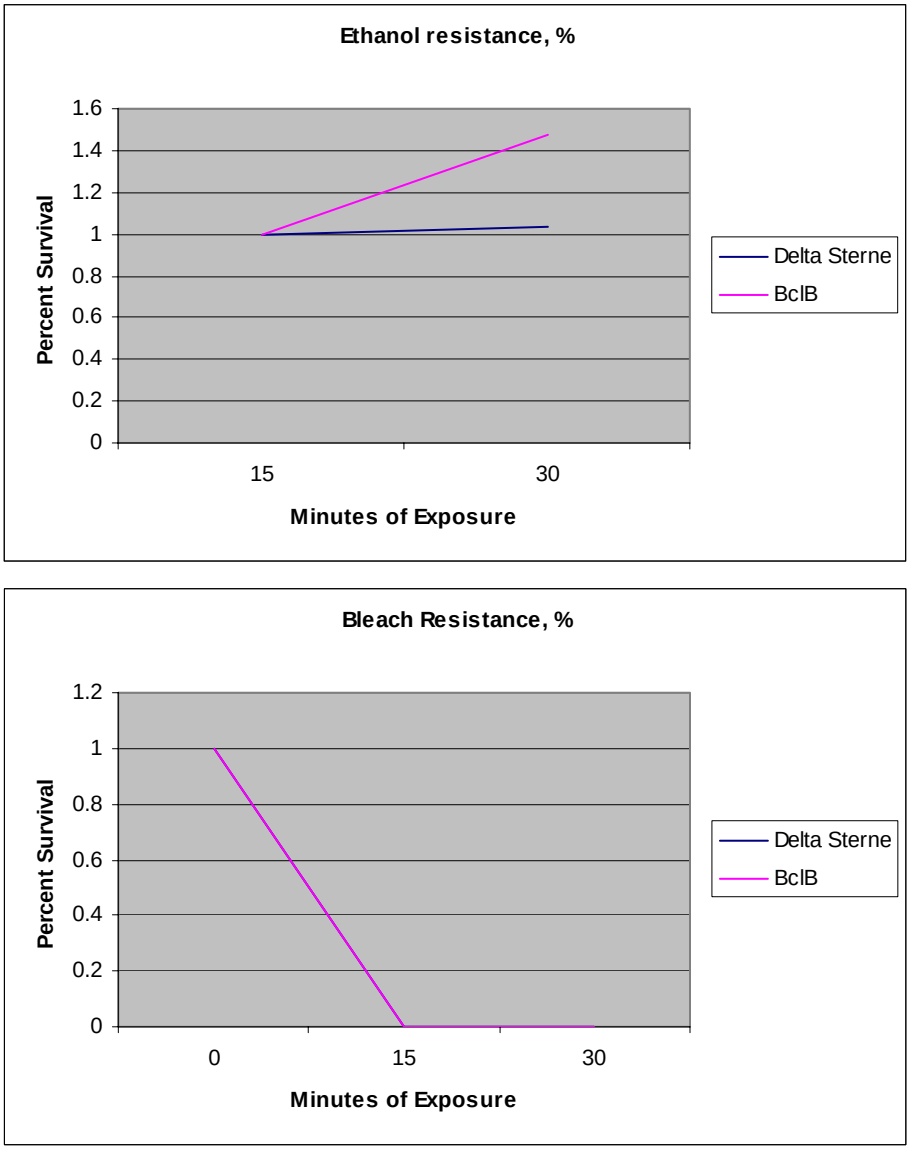

Figure 13C (Continued) The *bclB* mutant and wild-type ΔSterne spores and resistance to various insults.

Differential Protein Patterns in Spore Extracts from the *bclB* Mutant

Equal amounts of spores from the MUS1692 strain and the ΔSterne strain were boiled in SDS sample buffer for 10 minutes. The spores were pelleted by centrifugation, and the supernatant was collected. Proteins present in the supernatants were resolved by SDS PAGE on 4-20% Tris-HCl protein gels. The protein gels were stained with coomassie brilliant blue. Several unique bands differed in abundance between the extracts of the two strains. (Figure 14) Three protein bands were selected that differed between the two strains and cut from the gel and sent to the MU Proteomics core facility for MALDI-TOF MS/MS analysis and identification. The fourth high molecular weight band is presumed to be BclA, as this has been identified in many other studies (13, 15, 25, 80). The MUS1692 strain had a greater abundance of the presumed BclA band running at ~220 kDa. Results from the MALDI-TOF MS/MS protein identification are found in Figure 14. Band 1, migrating at about 105 kDa, is comprised of the surface layer protein EA1. This band has been shown to be a constant contaminate of spore preps, and despite extensive washing of the spores during purification, the presence of this protein persisted (13).

Band 2, migrating at approximately 30 kDa, was comprised of several spore coat proteins in complex with one another. Identified in the first band were the spore coat lytic enzyme CwlJ, the spore coat lytic enzyme SleB, and the germination protein GerQ. All three of these proteins are found in conjunction with one another, and gerQ is essential for the presence of CwlJ in the spore coat (9, 11). These proteins are essential for the degradation of the spore coat after spore association with a germination signal. The *bclB* mutant had a significant increase in the amounts of these proteins in the spore extract. These proteins were found in a series of heterogenous bands, due to their differing crosslinks between associated proteins (9, 11, 24). The increase in

this band may indicate that the BclB protein plays a role in stabilizing the spore coat, as has been reported for other exosporium proteins (81, 85, 86). This may explain the appearance of sloughed off spore coat in some of the TEM images of BclB-negative spores (Fig 10B).

Band 3, migrating at about 20 kDa, was identified as immune inhibitor A metalloprotease. This protein has been found in the exosporium of all members of the *Bacillus cereus* family, and plays a role in the escape of *Bacillus cereus* and *Bacillus thuringiensis* from macrophages. (18, 140) This protein was found to be greatly reduced in the *bclB* mutant spores. The protein migrates as a band of 86 kDa, but is often found proteolytically cleaved (18).

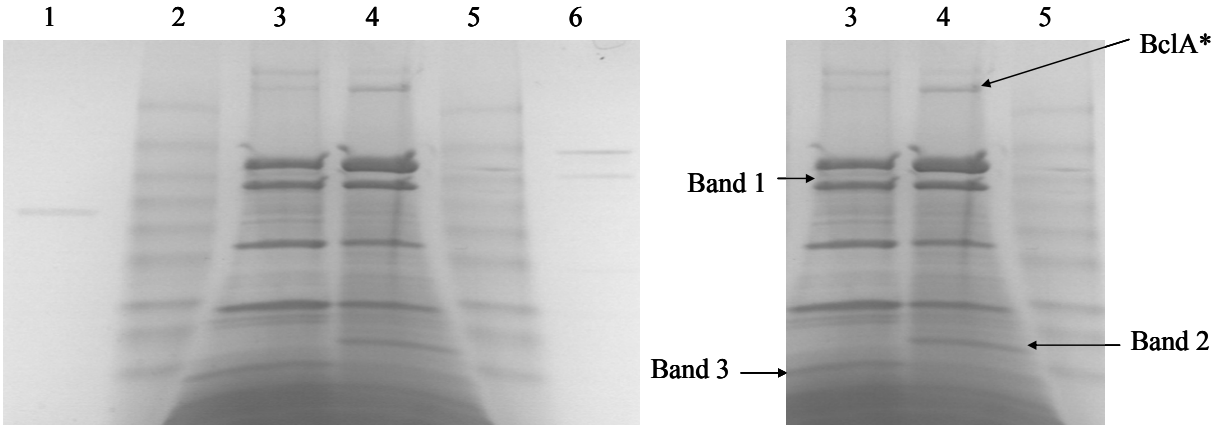

Figure 14. Left Panel: Coomassie-stained protein gel. Lane 1, rBclA protein; Lane 2, Prestained protein marker, top band 190 kDa; Lane 3, ΔSterne spore extract, Lane 4, MUS1692 spore extract, Lane 5, prestained protein marker; Lane 6, rBclB.

Right Panel: Protein gel with bands identified by MALDI-TOF MS/MS. The likely BclA protein band is marked**.** Band 1 – EA1 S-layer protein, Band 2 – SleB, CwlJ, and GerQ spore coat lytic enzymes and germination proteins, Band 3, Degraded InhA1 protein.

Glycoprotein and Phosphoprotein Analysis of Spore Extracts

Spore extracts of the MUS1692 and ΔSterne strains of *Bacillus anthracis* were made and resolved by SDS PAGE. Protein gels were collected and stained for either the presence of glycoproteins (Fig 15) using the Gel-Code Glycoprotein Staining kit (Pierce) or for phosphoproteins (Fig. 16) using the Pro-Q Diamond Phosphoprotein gel stain (Invitrogen). Presence of a high molecular weight band of about 220 kDa in both spore extracts was presumed to be the major glycoprotein in the exosporium, BclA. Once again, the *bclB* mutant spore extract contained an increased amount of this 220 kDa band than did the wild-type spore extract. Two minor glycoprotein bands appeared at 110 kDa and 90 kDa, which could either be the known exosporium glycoprotein ExsJ, (79), another exosporium glycoprotein, or partially glycosylated versions of BclA as seen in other studies (19). In the operon adjacent to *bclA*, along with the spore carbohydrate biosynthesis genes that are predicted to glycosylate BclA, there is a serine/threonine phosphatase. To determine if mature BclA or BclB is phosphorylated at their numerous threonine residues a phosphoprotein stain was performed on the spore extracts (Fig 16). There was a series of bands (approximately 43 kDa, 35 kDa, and 15 kDa) that appeared in the *bclB* mutant spore extract but not in the ΔSterne spore extract. The 35 kDa band most likely corresponds to the spore coat lytic enzyme proteins identified in Fig. 14. There appeared to be a smear of phosphoprotein containing protein migrating at >180 kDa in the *bclB* mutant, whether this band is reproducibly obtained and if it is partially glycosylated BclA awaits further investigation.

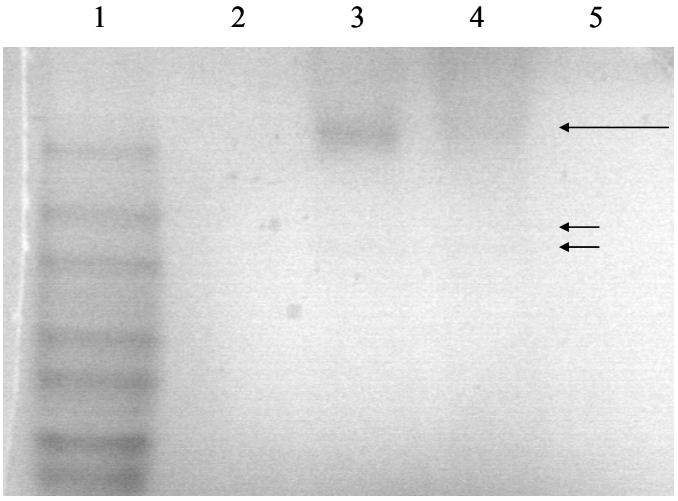

Figure 15: Glycoprotein stained protein gel of spore extracts. Lane 1, Prestained protein markers, top band 190 kDa. Lane 2, rBclB; Lane 3, MUS1692 spore extract, Lane 4, ΔSterne spore extract, Lane 5, rBclA. Long arrow denotes likely BclA band. Short arrows denote faint protein bands of approximately 90 and 110 kDa present in both spore samples.

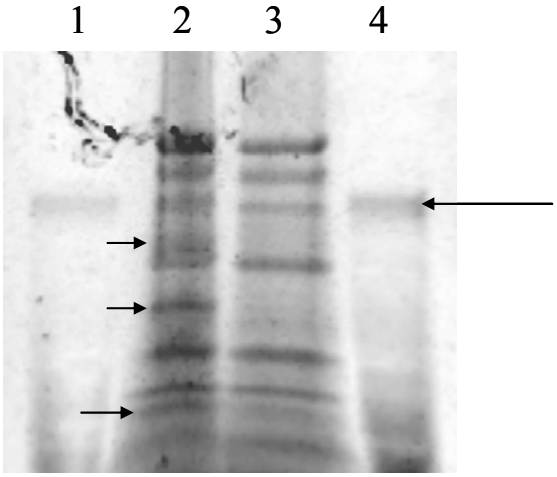

Figure 16: Pro-Q Diamond Phosphoprotein stained protein gel of spore extracts. Lane 1, protein marker with phosphoprotein at 60 kDa (long arrow). Lane 2, MUS1692 spore extract, Lane 3, ΔSterne spore extract, Lane 4, protein marker. (Differences in protein patterns are marked by small arrows.

Western Blot Analysis of the Mutant and Wild-Type Spore Extracts

Two chemical methods have been described for extracting exosporium proteins from intact spores of *B. anthracis*. The simplest method is to boil the spores in SDS PAGE buffer. The second method involves extraction of the spores with 8 M urea. Although both methods have been shown to be efficient at extracting BclA from the spores, we found that only the urea-extraction procedure reliably yielded the BclB protein from the wild-type spores (Fig. 17A, lane 3). SDS treatment resulted in lower recovery rates of BclB (data not shown). The BclB-reactive species were absent when the extracts were made from spores of MUS1692 (Fig 17A, lane 2), confirming the identity of the immunoreactive species in the ΔSterne spores as BclB. Western blot results further suggested that the BclB protein is present in the exosporium, or on the surface of the spore coat, in spores of *B. anthracis* but in a configuration that is less extractable from the spore then by simple SDS treatment. The BclB protein extracted from spores migrates in SDS PAGE as a high molecular weight heterogeneous population of bands. High molecular weight heteromers have been observed in spore extracts of *B. anthracis* and have been shown to consist of many exosporium-associated proteins that interact with BclA, BxpB, and ExsF (15, 19, and 75). The migration properties of BclB suggest it may be part of similar complexes. Most identified spore coat proteins are found as hetergenous species of molecular weights below 150 kDa (55). When anti-BclA antiserum was utilized to probe the spore lysates, the amount of BclA present in extracts from the *bclB* mutant spores was consistently greater (average of 2.3-fold based on 6 independent experiments) than the reactive material extracted from the wild-type spores. (Figure 18)

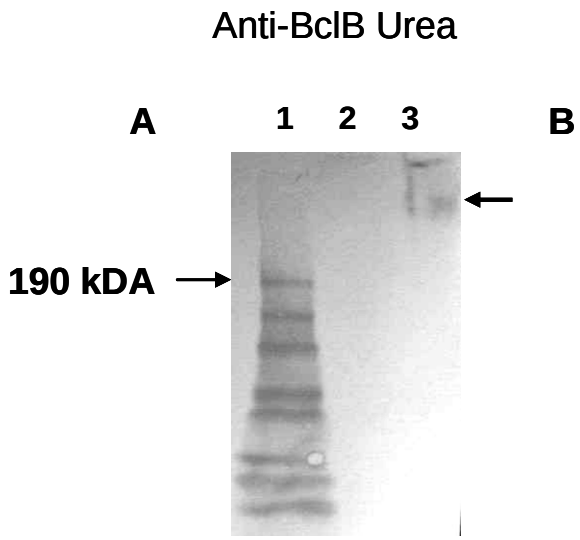

Figure 17: Western blot of spore extracts using rabbit anti-BclB polyclonal antiserum. Samples are: 1, protein standard markers; 2, urea extract from MUS1692; 3, urea extract from ΔSterne.

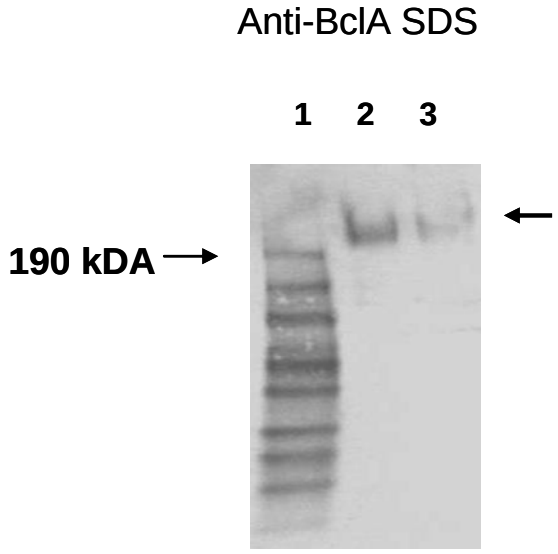

Figure 18: Western blot of spore extracts using rabbit anti-BclA polyclonal antiserum. Samples are: 1, protein standard markers; 2, SDS spore extract from MUS1692; and 3, SDS spore extract from ΔSterne.

Surface Exposure of BclB on *B. anthracis* Spores.

The anti-BclA and anti-BclB antisera were utilized to determine if the BclB protein is expressed on the surface of unfixed spores. Spores were incubated with the anti-BclA or anti-BclB antisera followed by incubation with FITC-labeled Protein A. The spores were then extensively washed and examined by epi-fluorescence microscopy. Results are shown in Fig. 19. Anti-BclA antibodies reacted strongly with the surface of the ΔSterne and BclB-negative spores, consistent with the known surface location of this glycoprotein (Fig 19D and 19F). The anti-BclA sera did not react with the BclA deletion strain CTL292 (Fig 19E). A fainter, but reproducible, signal was evident when the anti-BclB antiserum was incubated with wild-type spores (Fig 19G) but not with the *bclB* mutant spores (Fig. 19I). This suggested that the BclB protein is, at least in part, surface exposed in the spores of *B. anthracis*.

Anti-BclA antibodies reacted strongly to the spore surfaces of both the wild-type and *bclB* mutant spores (19D and 19F). Some spores in each population react strongly in this assay, whereas others displayed a uniform, but less intense, staining pattern. This pattern was consistently observed with antibodies in excess, suggesting limitation of antibodies available for binding to the spores was not responsible for the staining differences observed. Because the anti-BclA antiserum was raised against recombinant BclA, the antibodies do not recognize the carbohydrate moieties of the glycoprotein. Thus differences in glycosylation may explain the staining differences observed with individual spores. The western blot results described above consistently indicated that the *bclB* mutant spores contained either more BclA or a more easily extracted BclA configuration than did spores of the wild-type strain (Fig. 18).

If BclB is present in the basal layer of the exosporium, binding of the anti-BclB antibodies could be hindered by the presence of the BclA hair-like nap blocking access to the BclB epitopes. When the basal layer protein BxpB was identified, binding of the anti-BxpB antibodies was greatly increased when a *bclA* mutant strain was used (25). We used the BclA-deficient strain CLT292 to examine the binding of the anti-BclB antibodies (Fig 19H). When the CTL292 spores were analyzed for the presence of BclB, a minor increase was seen in the binding of the anti-BclB antibodies. More notably, the anti-BclB antibodies concentrated at a point at the pole of the spore (Fig 19H). This polar concentration was not evident with the ΔSterne spores (Fig. 19G).

In agreement with the findings of the *bclB* mutant under TEM and SEM, there was evidence of damage to the exosporium layer of the mutant when examined by immunofluorescence (Fig 19F). When the BclB-deficient spores were treated with anti-BclA antiserum, approximately 30-40% of the spores exhibited a lack of BclA-staining at one pole. This lack of BclA at one pole was most likely due to the damage of the exosporium layer at the pole, as was observed under TEM. These spores appear to be devoid of the exosporium polar cap. There was also evidence of the exosporium being sloughed off and some spores devoid of staining altogether (Fig. 19G and data not shown).

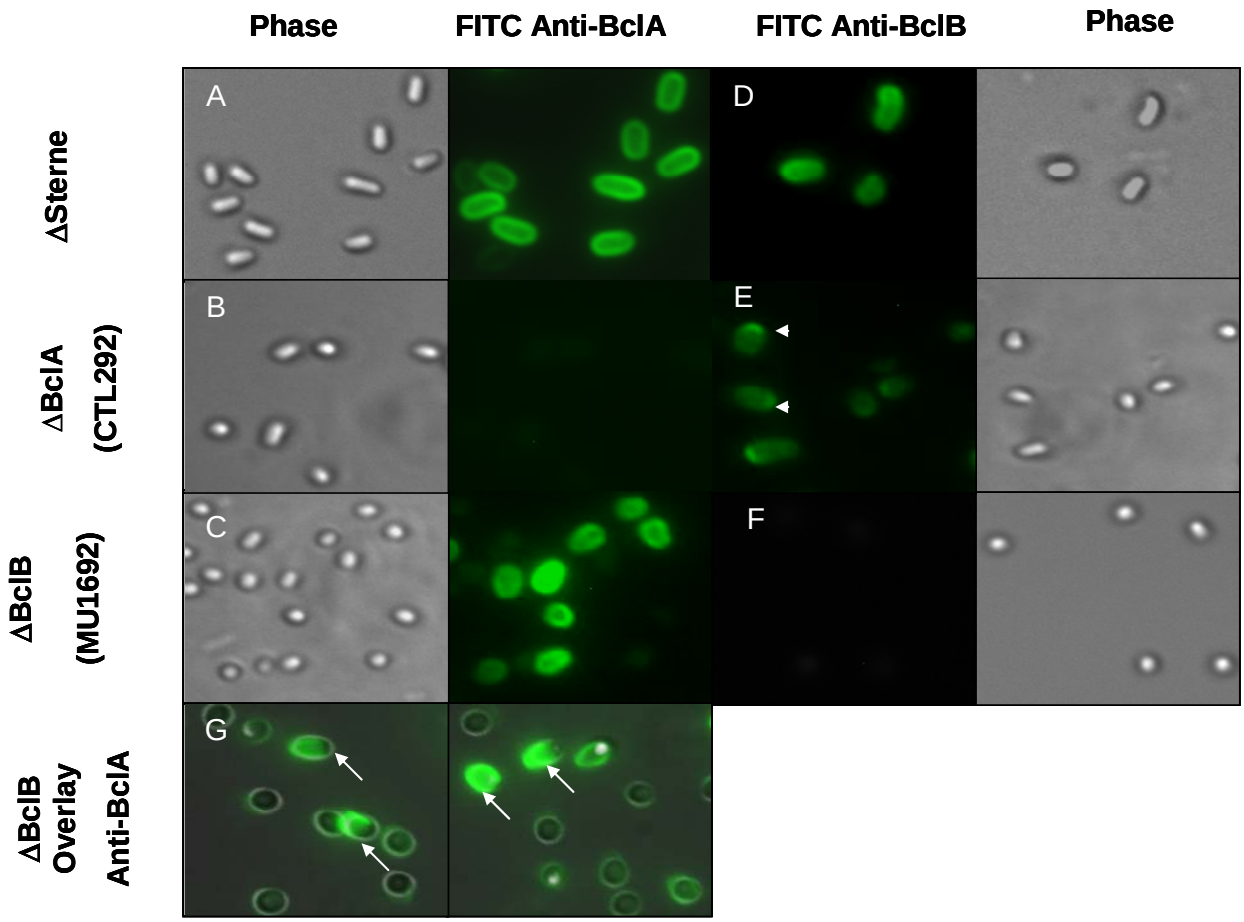

Figure 19: BclB is surface exposed in *B. anthracis*. Purified spores were treated with anti-BclA antiserum (panels A-C, and G) or anti-BclB antiserum (panels D-F) followed by FITC-protein A. Phase contrast images are shown adjacent to the fluorescence images (panels A-F). Panel G contains two merged anti-BclA fluorescence and phase contrast images to more clearly show the loss of fluorescence at one pole of certain spores. Spores were from the ΔSterne strain (panels A and D), the BclA mutant CTL292 (panels B and E) or the *bclB* mutant MUS1692 (panels C, F, and G). Image magnifications are 1000X. White arrowheads denote an increased concentration of the BclB protein at the pole of the spore. White arrows denote spores missing BclA at the cap or pole and sloughing of exosporium.

Flow Cytometric Analysis of Spores

The fluorescence micrographs provided only a qualitative assessment of surface exposure of the BclA and BclB proteins. For a quantitative determination of BclA and BclB protein exposure on the spore surfaces, spores were subjected to analysis by flow cytometry utilizing the anti-BclA and anti-BclB antisera. The results of these analyses are shown in Fig. 20. The results further demonstrated that BclB is surface exposed in the ΔSterne spores and is absent in the spores prepared from the *bclB*-deletion strain (Fig. 20A and 20B). Furthermore, the flow cytometry analyses indicated the levels of BclA detectable on the surface of the *bclB*-mutant spores was increased relative to that of the wild-type spores, consistent with the western blot results (Fig. 18). The mean fluorescence intensity for the spore samples with anti-BclA antibodies was higher with the BclB-deficient spores (mean fluorescence of 187 versus 106). The amount of BclB exposed on the surface of the spores was substantially less than that of BclA, with a mean fluorescence intensity of 42. Loss of the BclB glycoprotein and its associated sugars from the exosporium may have resulted in a compensatory increase in the presence of the BclA glycoprotein, or a change in the structure of the exosporium which allows greater access of the BclA epitopes to the anti-BclA antibodies.

A brief 10 minute exposure of spores from the *bclB*-deficient mutant to 50% ethanol followed by rehydration in PBS resulted in a shift in the staining with the anti-BclA antibodies (Fig. 20E), whereas this treatment had a negligible effect on the wild-type spores (Fig. 20F). The treatment of the mutant spores resulted in a small subpopulation of the spores showing increased fluorescence and a dramatic increase in the amount of material smaller in size than intact spores.

This BclA-reactive material appeared in a small size fraction, presumably representing free exosporium that had been stripped off of the mutant spores (lower left quadrant of Fig. 20E). Either the stress associated with the dehydration-rehydration cycle, or an effect of the solvent on the altered exosporium of the BclB-negative spores resulted in the physical removal of the exosporium material and its BclA nap from the spores.

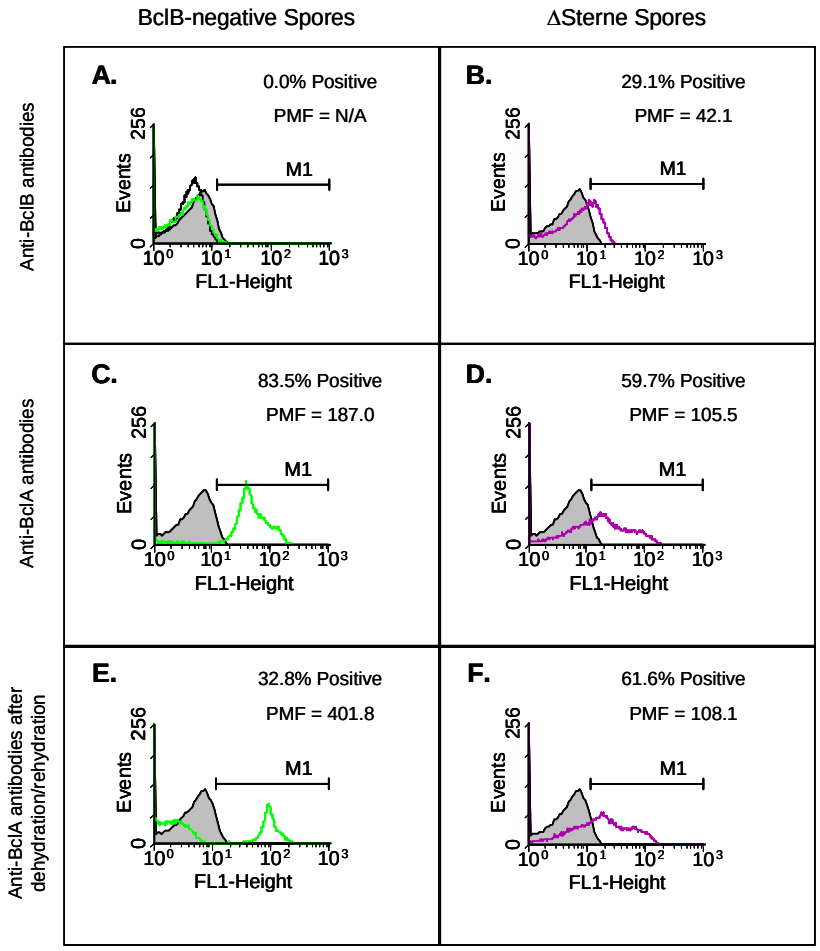

Figure 20: Flow Cytometry histograms. Paraformaldehyde-fixed spores stained with polyclonal rabbit antibodies and analyzed by flow cytometry. In all figures the gray curve represents a spore control that was treated without the primary antibody. Percentage positive is marked for each sample, as well as the mean fluorescence intensity of all positive samples (signified by PMF). A. The black line represents a spore control treated without the FITC-protein A conjugate. The green line represents the BclB-negative mutant treated with anti-BclB antiserum. B. The purple line represents ΔSterne spores treated with anti-BclB antiserum. C. The green line represents the BclB-negative mutant with anti-BclA antiserum. D. The purple line represents ΔSterne spores treated with anti-BclA antiserum. E. The green line represents the BclB-negative mutant spores treated with anti-BclA antiserum after dehydration in 50% ethanol and rehydration. F. The purple line represents ΔSterne spores treated with anti-BclA antiserum after dehydration in 50% ethanol and rehydration.

Effects of alcohol exposure and rehydration of spores is presented in Fig. 21, plotted to show size (forward scatter) along the x-axis and anti-BclA fluorescence along the y-axis. The BclB-negative spores are shown in panels A and C and the wild-type spores are in panels B and D. Examination of the wild-type spore patterns indicated the spores stain heterogeneously with the anti-BclA antiserum/protein A-FITC. Almost half of the alcohol-treated spore population stained poorly with the antiserum (Fig. 21C). This pattern was maintained when a 5-fold increase in the amount of antibody was included, indicating that this staining pattern is not the result of a limiting amount of antibodies being present. The antiserum was generated against recombinant BclA and the immunogen lacked the glycosylation found on native BclA. Differences in glycosylation as well as differences between exosporium assembly (and BclA accessibility) between spores may explain the heterogeneity in binding by the anti-BclA protein antibodies. The brief exposure to 50% ethanol followed by rehydration had no effect on the wild-type spore staining pattern with either the anti-BclA antiserum (Fig. 21D) or with the anti-BclB antiserum (not shown). However, ethanol-treatment of the BclB-negative spores resulted in the appearance of larger amounts of debris in the sample, as shown in the lower left quadrant of Fig. 21C. Because this was not associated with a substantial increase in an unstained spore-sized population, it is likely that the single alcohol exposure removed fragments of the exosporium, but not the entire exosporium layer in these spores.

The alcohol treatment may likely have accounted for the more dramatic change in appearance in the BclB-negative spores examined by scanning electron microscopy. A series of alcohol dehydration steps were involved in preparing the spores for SEM.

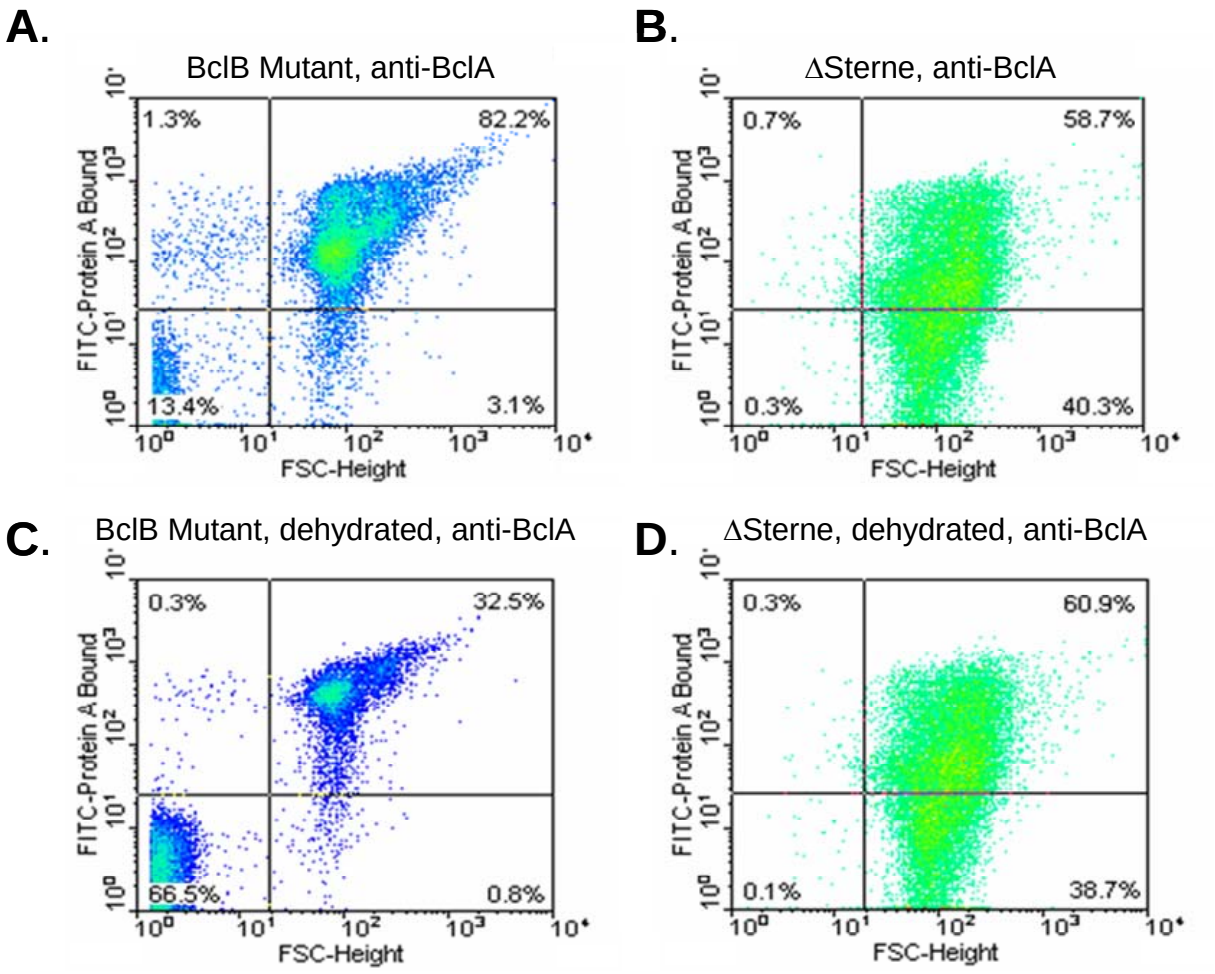

Figure 21: Flow Cytometry Density Plots. Paraformaldehyde-fixed spores stained with polyclonal rabbit antibodies and analyzed by flow cytometry. A. BclB-negative mutant spores treated with anti-BclA antiserum. B. ΔSterne spores treated with anti-BclA antiserum. C. BclB-negative mutant spores treated with anti-BclA antiserum after dehydration in 50% ethanol and rehydration. D. ΔSterne spores treated with anti-BclA antiserum after dehydration in 50% ethanol and rehydration

Spore-Macrophage Interactions.

The presence of the exosporium on the outermost part of the spore leads it to potentially play a role in the initial interactions with the host; including phagocytosis by host macrophages, as well as outgrowth and escape from the phagosomes (13, 22). The structural changes of the exosporium in the *bclB* mutant, and the loss of this spore-associated glycoprotein, may result in a change in the kinetics of survival of the mutated spores in macrophage cells. To assay uptake and infectivity of the *bclB* mutant spores vs. ΔSterne spores *in vitro*; RAW 264.7 murine macrophages were infected at MOIs of 10:1 and 1:1 (spores/macrophage). After treatment with gentamicin to kill off any free vegetative cells and inhibit growth of any unphagocytosed spores, samples were taken at timed intervals and plated for viable and heat-resistant colony counts. The total CFU would signify total phagocytosed and germinated spores and outgrown bacilli, while the heat-resistant viable count would signify ungerminated spores. Counts of heat-resistant CFU versus heat susceptible CFU reveals that greater than 99% of all spores added to the media were heat-susceptible at 1 hr (data not shown). At the first assayed time point of 1 hr, no significant difference was found between uptake efficiencies of the *bclB*-negative mutant spores versus ΔSterne spores. Examination of viable CFUs at 1, 2, 4, and 24 hours revealed no difference in viable counts between *bclB* mutant and ΔSterne spores. A representative experiment is shown in Fig. 22. Both strains were killed off with equal efficiency, with essentially zero viable cells remaining at 24 hours (based on 6 experiments). To assay the ability of ΔSterne and *bclB* mutant spores to escape from macrophages, a free spore count was undertaken at various time points throughout the infection process. Free spores appearing after gentamicin addition represent vegetative cells escaping from the macrophages, or more unlikely, slowly germinating spores.

Dixon *et al.* (39) reported that the presence of the pX01 plasmid is essential for escape from macrophages, but the results presented in Fig. 23 indicated that escape from macrophages occurred in both of our pX01-deficient strains, but at low amounts and these free cells were quickly killed off by the macrophages.

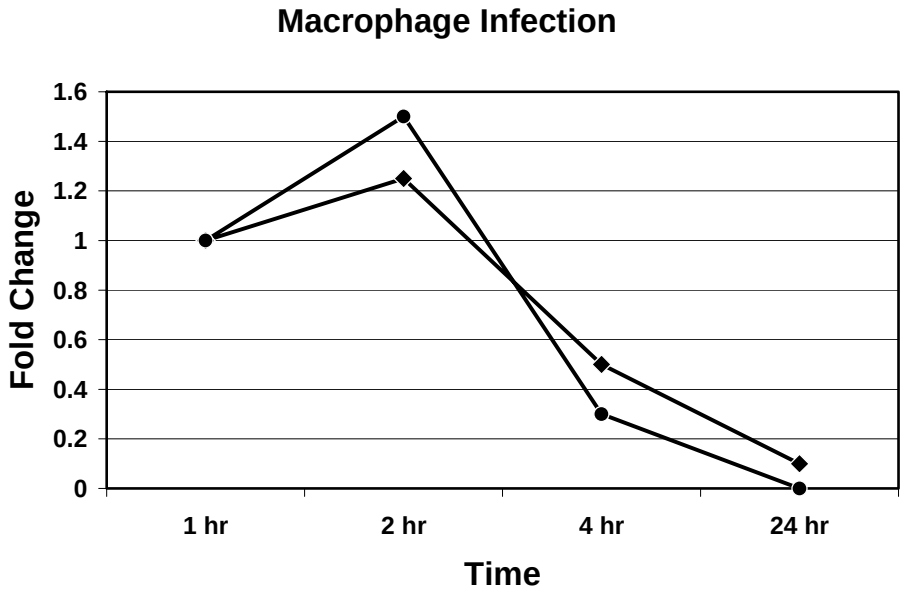

Figure 22: Plate counts of lysates of RAW 264.7 cells infected with spores of the ΔSterne strain (♦) or the *bclB* mutant spores (●). Values are expressed relative to the initial time point (1 hour post infection). Typical results of a 1:1 experiment are shown. Ratios of 1:1 and 10:1 (spores:macrophages) were utilized with the same results.

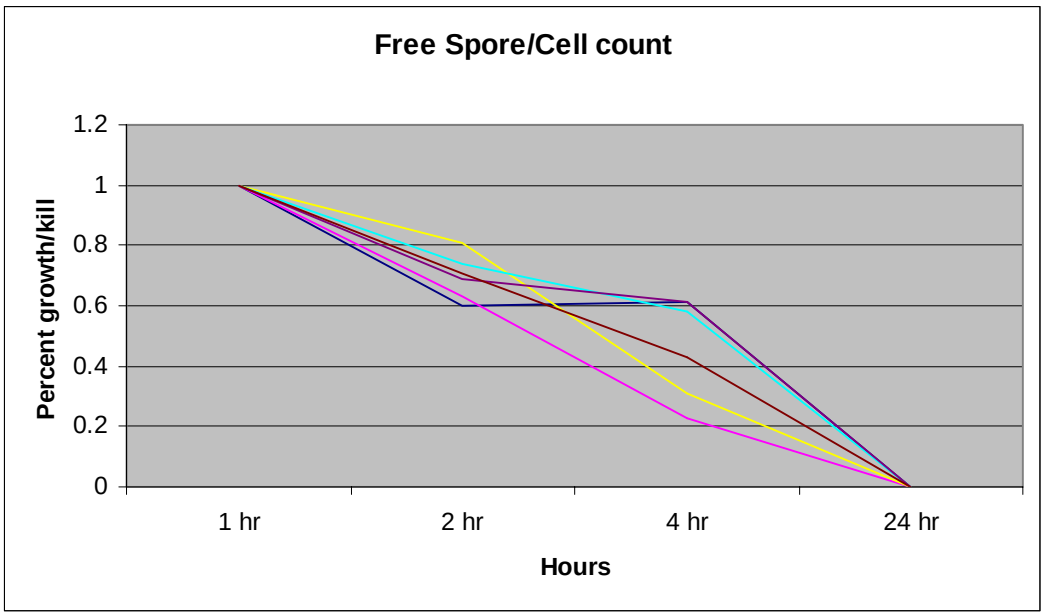

Figure 23: Plate counts of free vegetative cells from RAW 264.7 murine macrophages infected with spores of the ΔSterne strain (Pink, yellow, and dark blue lines) or the *bclB* mutant spores (brown, purple, and teal lines). Values are expressed relative to the initial time point (1 hour post infection). No significant differences in free spore counts were collected.

Additional Results

Expression of His-Tagged Bcl Proteins.

The *bclA* and *bclB* ORFs were PCR amplified with primers with a BamHI restriction site on the 5' primer and a SalI site on the 3' primer. (qbclA5pB cgggatccatgtcaaataataattatt and qbclA3pS agcgtcgacttaagcaacttttttcaat for *bclA*, qbclB5pB cgggatccatgaaacagaatgacaaattatg and qbclB3pS agcgtcgacttagacgatattaagacctgc for *bclB*). The PCR products were cloned into the pCR2.1 Topo TA cloning vector system (Invitrogen). After nucleotide sequencing to ensure the reading frame of the determinants was correct, the insert was digested and inserted into the pQE30 vector (Qiagen) utilizing the incorporated BamHI and SalI sites. The pQE30 plasmids encoding *bclA* (pBT3571) and *bclB* (pBT3642) were transformed into the M15 and AbleK *E. coli* strains harboring the pREP4 *lacI* repressor plasmid.

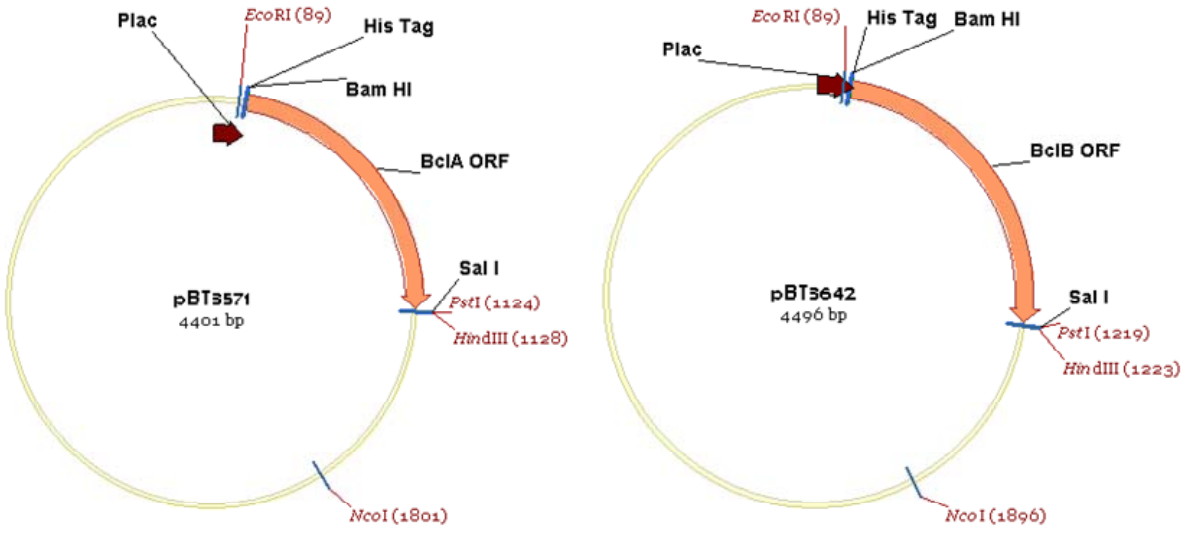

Figure 24: Plasmid maps of the BclA and BclB protein expression vectors.

IPTG-induced expression of the BclA and BclB His-tagged proteins was conducted for 3 hours, as suggested by the Qiagen protocol for optimal protein production. Yields of protein were, however, minimal. A growth curve was established for both the pBT3571 and pBT3642 plasmid-bearing strains in both the M15 and AbleK backgrounds (Figure 25). No growth difference was seen between the two plasmid-bearing strains. When the *E. coli* was induced by the addition of 1 mM IPTG to produce the recombinant proteins, a quick cessation in growth was observed within 30 minutes of induction. Growth of the cultures stalled indefinitely in both the M15 and AbleK strains. The M15 strain of *E. coli* reached the $O.D._{600}$ of 0.6 more quickly than the AbleK strain, potentially due to its higher plasmid copy number; but after induction the AbleK strain was able to reach a higher O.D. before stalling in growth. This slight increase in O.D. may explain the increased protein production obtained in the AbleK strain over the M15 strain. Only a modest inclusion body formation was seen in each strain (data not shown).

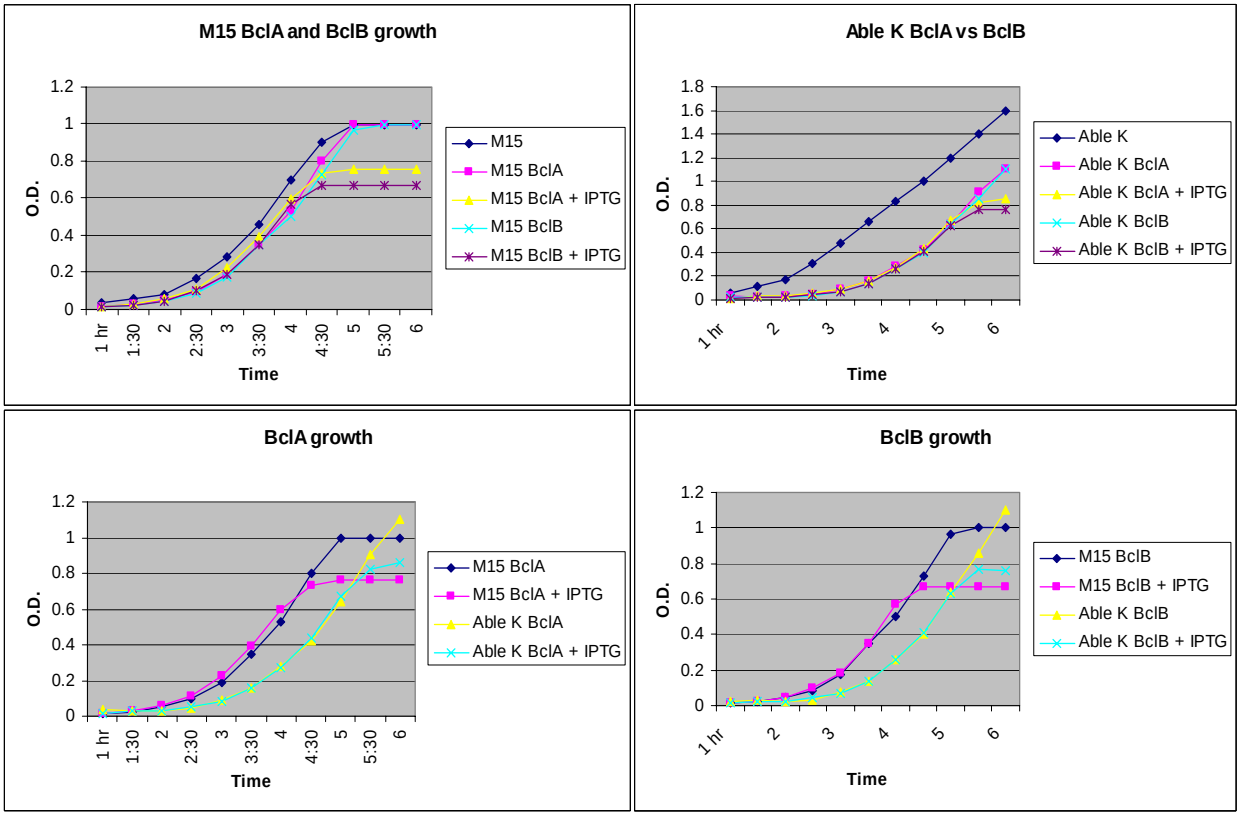

Figure 25: Growth curves of E. coli expressing rBclA and rBclB. Top Left Panel, Growth of the M15 strain with either: no construct, the BclA construct, or the BclB construct, with or without IPTG induction at OD 0.6. Top Right Panel, Growth of the Able K strain with either: no construct, the BclA construct, or the BclB construct respectively, with or without IPTG induction at OD 0.6. Bottom Left Panel, Comparison of growth between the M15 and Able K strains with the rBclA construct with or without IPTG induction. Bottom Right Panel, Comparison of growth between the M15 and Able K strains with the rBclB construct with or without IPTG induction. Note the cessation of growth after IPTG induction in all cases.

Proteins produced were analyzed by SDS PAGE, and migration rates were compared to expected sizes. Both rBclA and rBclB migrated as a species much greater than expected, but this has been seen in many bacterial proteins with high proline content (95, 96). The rBclB protein migrates as two bands (85 and 105 kDa). The reason for this is unknown at this time. rBclA migrates with a larger apparent molecular weight (65 kDa), as previously reported (15).

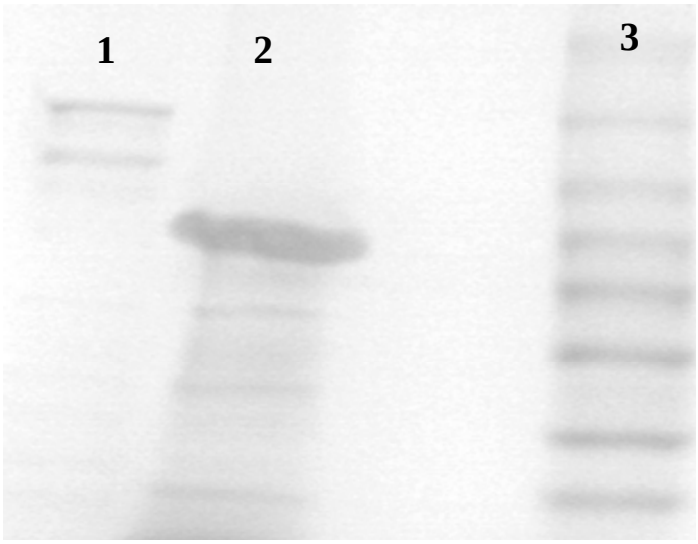

Figure 26: His-tag column purified proteins from Able K induced with IPTG for one hour. Lane 1, rBclB, Lane 2, rBclA, Lane 3, Protein Ladder (190 kDa, 100 kDa, 80 kDa, 70 kDa, 60 kDa, 50 kDa, 40 kDa, 30 kDa)

Sporulation Efficiencies.

To test the ability of the *bclB* mutant to sporulate, several sporulation assays were performed. Overnight cultures of live cells were inoculated into fresh BHI until the $O.D._{600}$ equaled 0.2. 500 ul of the cultures were used to inoculate Difco sporulation broth (into 9.5 ml) and allowed to go at 37°C.. The results are presented in Table 7. Two strains of *Bacillus anthracis* that either did not sporulated (spore -) or that sporulated rapidly (spore ++) were used as controls. There was a significant difference between the *bclB* mutant and the ΔSterne strain in sporulation efficiencies, with no released spores seen in the *bclB* mutant and full sporulation of cells seen in the ΔSterne strain at 5 days. This was tested by observation under light microscopy, as well as by heat resistance to 60°C to assay percent spores.

Media	ΔSterne Spore Broth	*bclB* mutant Spore Broth	Spore - Spore Broth	Spore ++ Spore Broth
24 Hours Sporulation Perecentage	**60.50%**	**0.10%**	**0%**	**45%**
48 Hours Sporulation Percentage	**63.40%**	**2.60%**	**7.60%**	**97.30%**

Table 7: Sporulation in spore broth, based on heat resistance at 65°C for 30 minutes

To further test this difference in sporulation efficiencies, fresh inoculums were used to test sporulation in different medias and at different temperatures, and micrographs taken at each timepoint to assay sporulation and release of spores. In Difco sporulation broth, the ΔSterne strain started sporulating in less than 24 hours, with the majority of spores being released between 48-72 hours, and consisted of greater than 95% free spores when observed at 5 days (Figure 27). In contrast, the *bclB* mutant did not start to sporulate at all, and started to lyse at the 72 hour time point, with death of the filaments and no spore production at 5 days. (Fig 27)

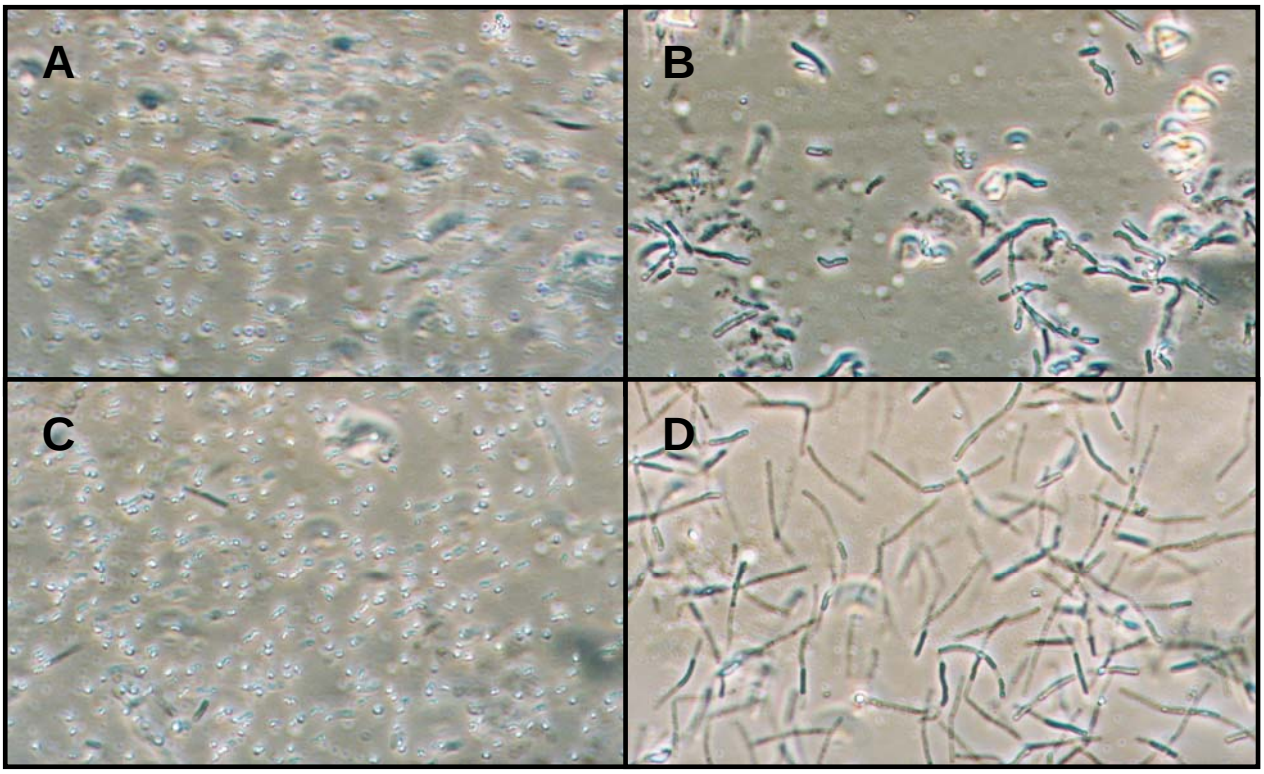

Figure 27: Sporulation in Difco sporulation broth, 5 days. Growth at 30°C (A and B) and 37°C (C and D) of ΔSterne (A and C) and MUS1692 (B and D). Phase bright spores are evident in the ΔSterne panels, but not in the MUS1692 panels. Evidence of cell lysis is present in the MUS1692 panels.

Another alternative to sporulation broth is nutrient broth. This low nutrient broth induces sporulation in little time in *Bacillus* species (data not shown). In nutrient broth the results were comparable with sporulation broth with ΔSterne completely sporulated at 5 days, and lysis of the *bclB* mutant strain at 48-72 hours. (Figure 28) In both of the broths more spores were produced at 37°C than at 30°C, potentially due to the higher O.D. reached before sporulation was initiated (data not shown).

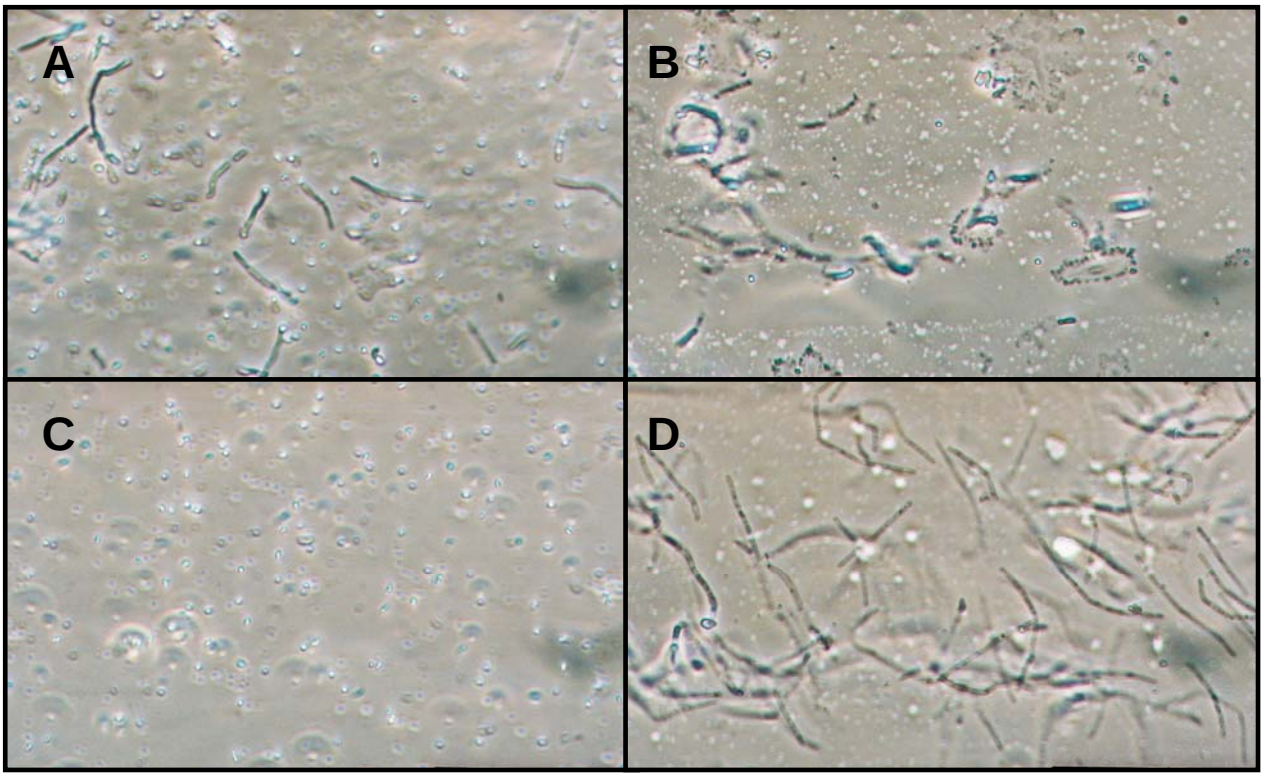

Figure 28: Sporulation in nutrient broth, 5 days. Growth at 30°C (A and B) and 37°C (C and D) of ΔSterne (A and C) and MUS1692 (B and D). Phase bright spores are evident in the ΔSterne panels, but not in the MUS1692 panels. Evidence of cell lysis is present in the MUS1692 panels.

A different phenotype was observed from analysis of spores that were streaked onto nutrient agar or sporulation agar plates. In both strains, under growth at 30°C, spores were observed as early as 24 hours. By 48 hours, more than half of the cells sporulated and released their spores. No conceivable difference was seen between the two strains through 5 days. (Figure 29) Interestingly, this was not the case when sporulation was induced at 37°C on agar plates. (Figure 29) The ΔSterne and *bclB* mutant strains appeared similar in both the broth sporulation assays, but with a decrease in free spore number seen in the ΔSterne strain. The *bclB* mutant once again lysed out at 48-72 hours with little to no spores produced. The summary of these results is shown in Table 8. Efficient sporulation in both strains was only induced by growth on nutrient or spore agar plates at 30°C. Sporulation in the *bclB* strain is dependent on temperature and on the media supplied. Part of this dependency is oxygen availability. When *bclB* mutant cells were inoculated in small volumes of broth in an oversized flask under high RPMs, to maximize exposure to oxygen, they sporulated with kinetics similar to ΔSterne. (Table 8)

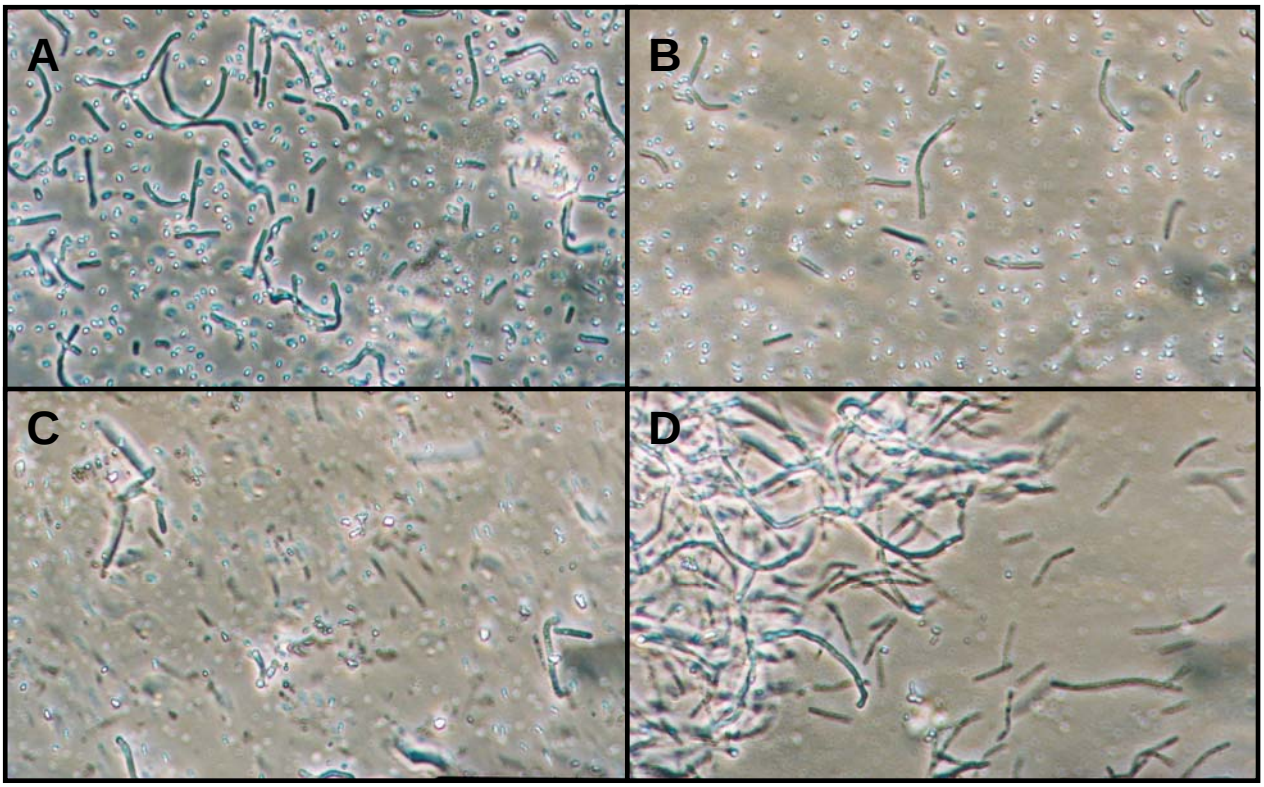

Figure 29: Sporulation on nutrient agar, 5 days. Growth at 30°C (A and B) and 37°C (C and D) of ΔSterne (A and C) and MUS1692 (B and D). Phase bright spores are evident in the ΔSterne panels and MUS1692 panel at 30°C, but not in the 37°C MUS1692 panel.

Media	ΔSterne Spore Broth	ΔSterne N Broth	ΔSterne N Agar	ΔSterne Spore Agar	*bclB* mutant Spore Broth	*bclB* mutant N Broth	*bclB* mutant N Agar	*bclB* mutant Spore Agar
24 Hours								
Sporulation Percentage 30°C	2%	2%	30%	40%	0%	0%	10%	40%
Sporulation Percentage 37°C	40%	15%	20%	20%	0%	0%	0%	20%
48 Hours								
Sporulation Percentage 30°C	15%	8%	40%	50%	0%	0%	35%	50%
Sporulation Percentage 37°C	30%	35%	40%	35%	0%	0%, lysis	0%	20%
72 Hours								
Sporulation Percentage 30°C	55%	30%	65%	95%	0%, lysis	0%, lysis	65%	95%
Sporulation Percentage 37°C	90%	95%	45%	70%	0%, lysis	0%, lysis	2%	20%
5 days								
Sporulation Percentage 30°C	95%	75%	95%	95%	0%, lysis	2%	95%	95%
Sporulation Percentage 37°C	95%	95%	80%	85%	0%, lysis	0%, lysis	5%	25%

Table 8: Sporulation efficiencies, assayed by visualization under light microscopy and observation of free, phase bright spores**.**

Infection Study Controls

Before undertaking the infection of macrophages with the spores, the ability of the spores to germinate in the media needed to be assayed. The spores in the presence of the cell culture media alone did not germinate. (Table 9) Further analysis of the defined cell culture media DMEM + low glucose (Eagle) revealed that the media did not contain any of the germinants necessary for proper germination and outgrowth of the spores. When the heat-inactivated FBS was added to a final concentration of 10%, the spores took off and multiplied rapidly, with >85% of the spores germinating within one hour, and a doubling time of roughly 30 minutes not including time allotted for outgrowth. Since germination occurs quickly in the DMEM + 10% heat-inactivated FBS, the spores were centrifuged down to rest upon the macrophages, and are

quickly engulfed within 5-10 minutes. (data not shown) To assay whether the gentamicin could efficiently kill any germinating and outgrown cells, a Minimum Inhibitory Concentration (MIC) of gentamicin was obtained by inoculating DMEM plus 10% FBS with serially increasing concentrations of gentamicin. The MIC of gentamicin under these conditions was 2.5 ug/ml. In the presence of media plus macrophages, the germination of spores was even greater, with almost all the spores germinating within one hour of inoculation. (Figure 30) Whether this was due to secretion of germinants by the macrophages, or by uptake of the spores into the macrophage where conditions are more suitable for germination is unknown.

Spores	Media alone	Media + FBS
Input spores	1000	1000
DS	1002	3698
DS ungerminated spores	1180	232
BclB	1587	4395
BclB ungerminated spores	1500	255

ΔSterne (2.5 ug/ml)
BclB (2.5 ug/ml)

Table 9: Germination efficiencies in DMEM media + low glucose, and DMEM + low glucose + 10% heat-inactivated FBS. Total CFU and heat resistant CFU (spores) as annotated separately. Input spores is an estimate**.** The MIC of gentamicin is indicated in the lower portion of the table in both strains.

Media	ΔSterne MOI 1:1	ΔSterne MOI 10:1	*bclB* mutant MOI 1:1	*bclB* mutant MOI 10:1
1 Hour Germination %	**99%**	**97%**	**95%**	**92%**
2 Hours Germination %	**99%**	**99%**	**99%**	**99%**

Figure 30: Germination of spores in DMEM + low glucose and 10% FBS in the presence of RAW 264.7 murine macrophages. Germination was determined by heat sensitivity to 65^{o}C for 30 minutes.

Nitric Oxide Release

Due to the success of the macrophages in elimination of spores, an assay was performed to test for whether the macrophages were being activated by the presence of the spores or potentially from contaminating LPS or residual activators. Activation of macrophages, due to signaling by TLRs, cytokine messages, or other stimuli leads to a dramatic increase the macrophages' ability to kill *Bacillus anthracis* spores (39). This activation leads to the upregulation of NO and related free radical species in the macrophage, and the NO can be assayed via the Greiss reaction. The disruptions in the exosporium in the bclB mutant spores, along with recent studies showing the protective effect of the exosporium in preventing access to stimulators of the immune system and secretion of cytokines by macrophages lead us to assay the NO concentration in the media around the macrophages (141). Ratios of spores:macrophages greater than 10:1 are required for NO release in the avirulent ΔSterne and MUS1692 strains. The

only increase in NO production was seen at a MOI of 100:1 after 24 hours. The addition of Nystatin or gentamicin had no effect on NO production (data not shown)

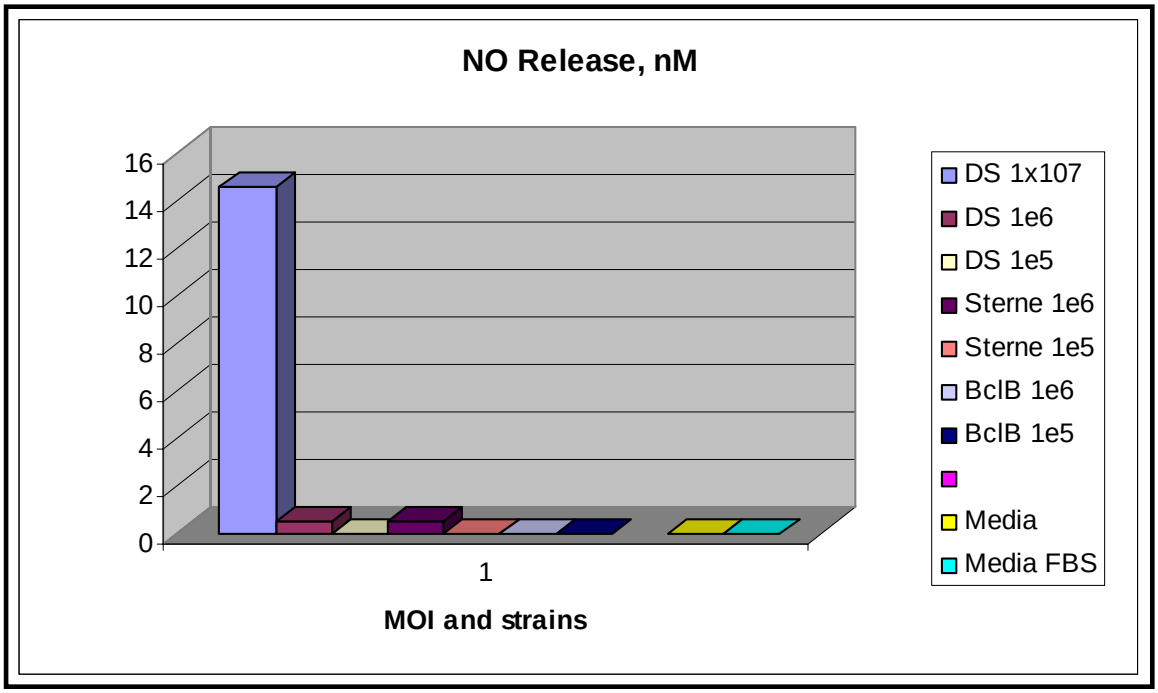

Figure 31: NO release by macrophages under different MOIs of ΔSterne and MUS1692 spores for 24 hours. Total spore CFU is denoted to the right of the strain, infecting $1x10^6$ macrophages per well.

Promoter Analysis

The promoter for both *bclA* and *bclB* were collected from the TIGR Microbe Genome Database. Selection of the promoters was accomplished by analyzing the region between the start codon of each gene and the region upstream until the next ORF was met. The selected putative promoter regions were analyzed for the presence of the well characterized *Bacillus subtilis* late sporulation gene and other sigma factor binding sites. Both genes had several putative σ^K-like promoter elements, comparable to analysis of the promoters of other late sporulation genes in *Bacillus anthracis* (ExsF, ExsY, CotY). A recent genome wide microarray data set (54) was analyzed for the upregulation of late sporulation genes, many in adjacent operons to *bclA*. *bclA* and *bclB*, as well as several other related late sporulation genes were upregulated concurrently with σ^K. (Figure 31, 32)

BAS1130 promoter sequence (BclA)

TAATC**AC**CCTCTTCCA**AA**TCAAT**CATATGTTA**TA**CATATACTA**AACTTTCCATTTTTTTA
AATTGTTCAAGTAGTTTAAGATTTCTTTTCAATAATTCAAATGTCCGTGTCATTTTCTTTC
GGTTTTGCATCTACTATATAATGAACGCTTTATGGAGGTGAATTT**ATG**TC

RED- PERFECT MATCH
BLUE – ONE OFF, -35
GREEN-RBS

BAS2281 promoter sequence (BclB)

ATTAGAACGTA**AC**CAATTTAG**TA**TTTTGA**AATAGAGCTA**T**CATTTTATA**ATATGAATA
CTACTAGTTATAGAAACGGCAAAAAGTTTAATATATGTAAAAATCATT**TG**GATATGAAA
AAAGTAGC**CATAGATTT**TTTCGAAATGATAAATGTTTTATTTTGTTAATTAGGAAACAA
AAATGTGGAAT**GAGGG**GGATTTAA**TTG**AAACAGAA

RED-THREE OFF
BLUE – THREE OFF, OR TWO OFF WITH 16 SPACER
TWO OTHERS WITH THREE OFF
GREEN-RBS

Figure 32: Promoter analysis of *bclA* and *bclB*. The putative σ^K binding sites are denoted in various colors with the number of imperfect matches to the Bacillus subtilis consensus sequence.

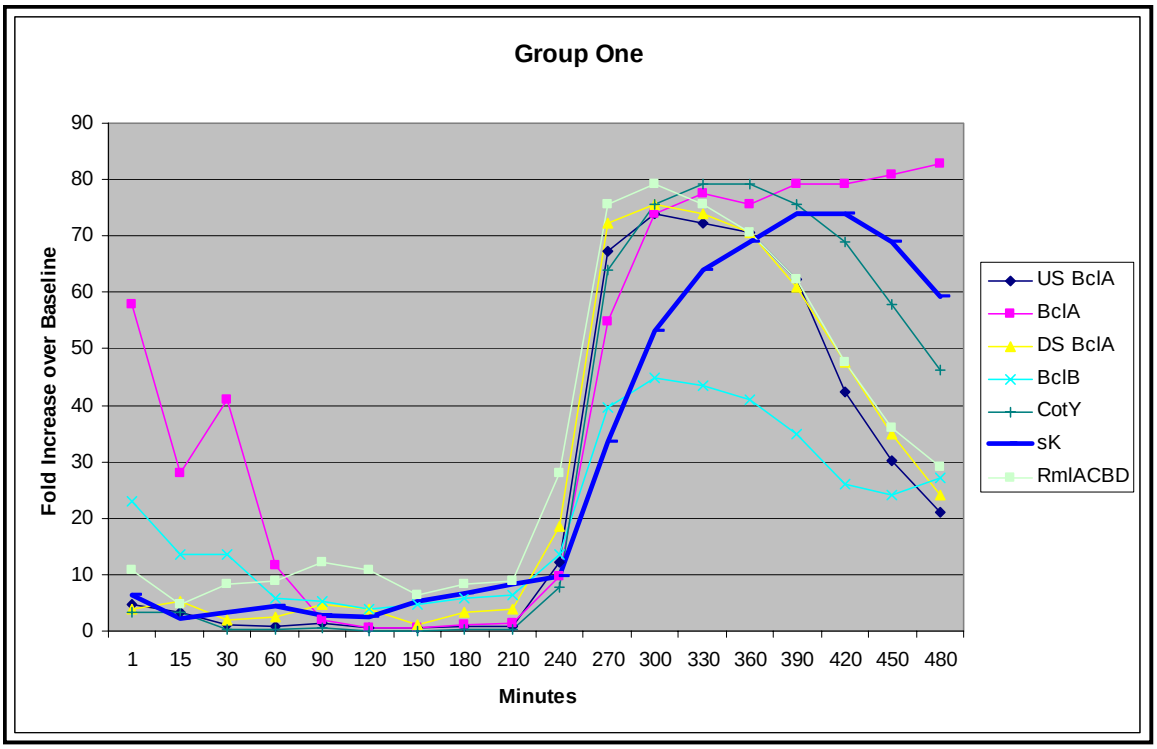

Figure 33: Transcription profiling of the *bclA* and *bclB* genes, as well as the operons adjacent to *bclA*. Adapted from Bergman *et al.* (54)

TEM in vegetative cells

Sporulating cells were analyzed by TEM in the process of sporulation to look for defects in the appearance of the exosporium inside the developing cell. Preliminary results show no discernable difference in the exosporiums of developing spores.

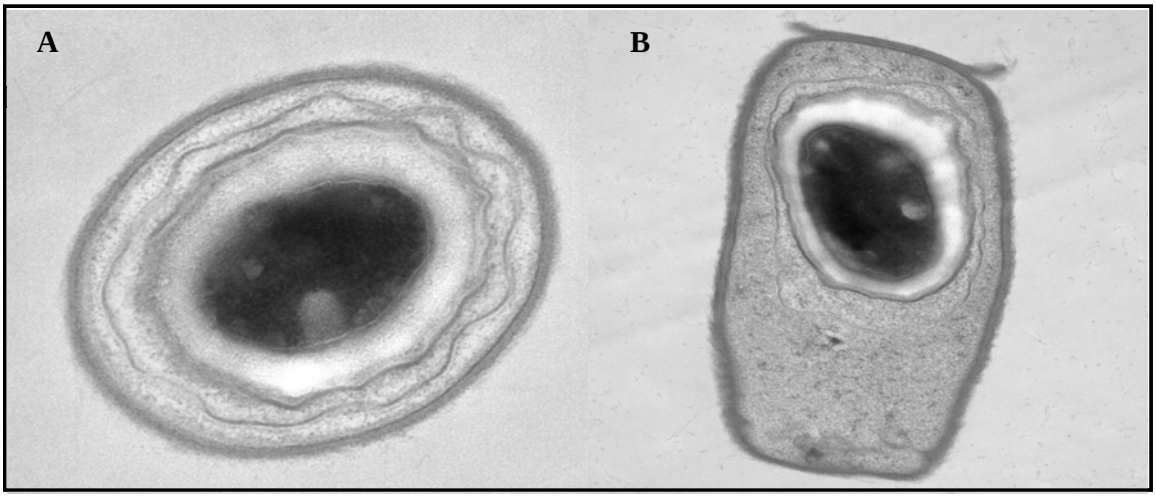

Figure 34: TEM Micrographs of developing spores. A: ΔSterne spores. B: MUS1692 spores.

Urea vs. SDS

Analyses of the two methods for extraction of proteins from the exosporium were analyzed. First, western blots were performed on ΔSterne spores and *bclB* mutant spores that had been boiled in either urea extraction buffer or SDS sample buffer. Results using anti-BclA antisera are presented in Figure 35. There was an increase in both the BclB and BclA proteins extracted using the urea buffer extraction technique (Figure 35 and data not shown). Interestingly, the migration rate of BclA differs significantly between the two methods, with an increase seen when BclA was extracted with urea (figure 35). One explanation is that the treatment of spores with urea may enable BclA to keep incorporated with BclA-associated proteins, but under treatment with SDS, the BclA comes off as clean trimers.

Spores that had been boiled in either buffer were washed several times in PBS, and analyzed using both immunofluorescence (Figure 36) or by examination by TEM (Figure 37). After boiling of spores in SDS, no discernable damage was evident on the spores, but a general loss of fluorescence was observed (Figure 36 A-D). After boiling in urea buffer, the spores took on a fuzzy appearance, with a halo of fluorescent material coming off many of the spores (Figure 34 E and F). This fuzzy appearance was more dramatic under TEM, and the appearance of the nap and exosporium changed dramatically after urea treatment (Figure 35). SDS treatment had minor effects of the exosporium.

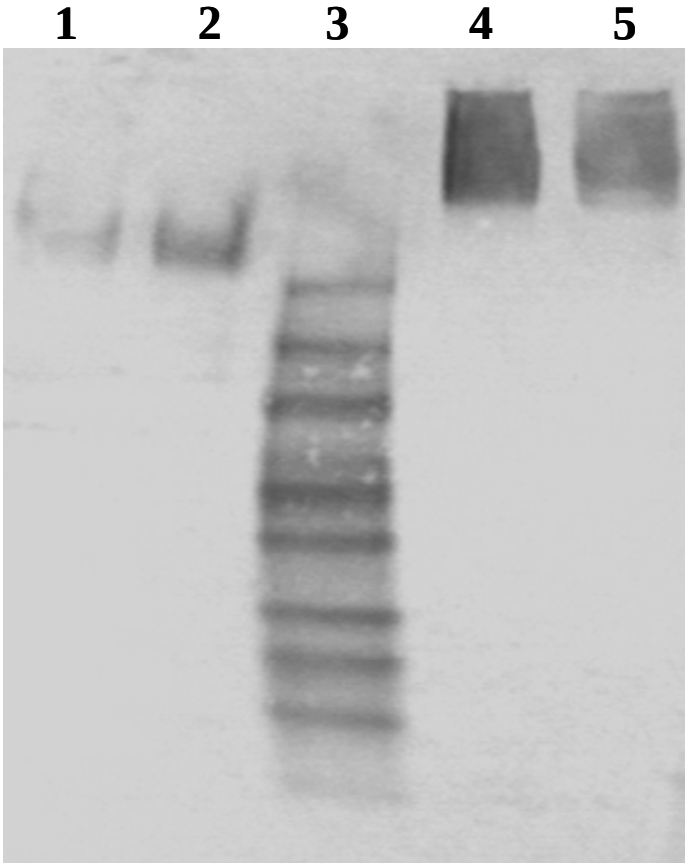

Figure 35: Western blot using anti-BclA antisera. Lane 1, ΔSterne spores boiled in SDS sample buffer, Lane 2, MUS1692 spores boiled in SDS sample buffer, Lane 3, protein marker, Lane 4, MUS1692 spores boiled in urea buffer, Lane 5, ΔSterne spores boiled in urea buffer.

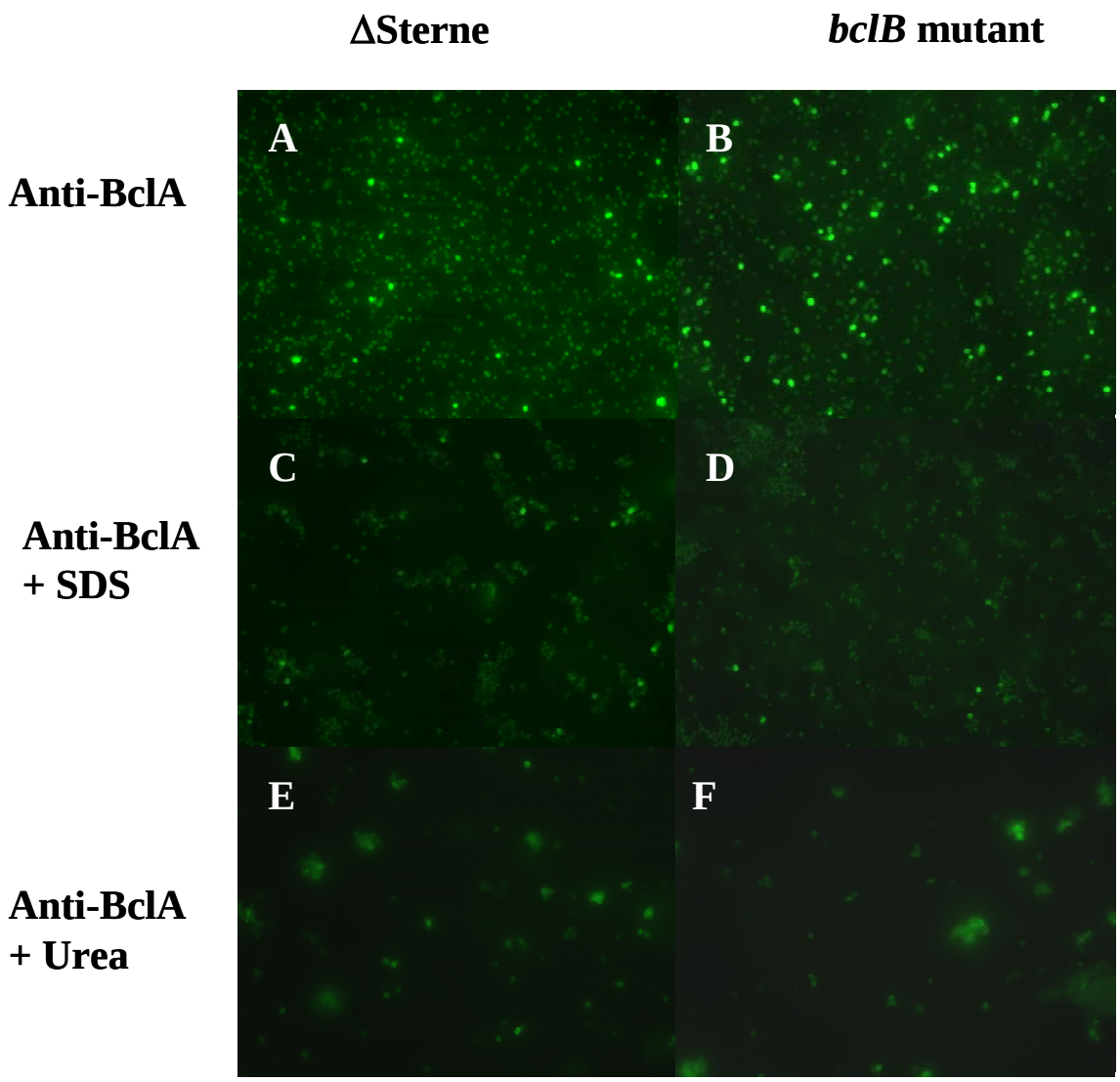

Figure 36: Immunofluorescence of spores with anti-BclA antisera before (A and B) or after boiling in SDS (C and D) or Urea buffers (E and F). Samples are ΔSterne (A, C, and E) or MUS1692 spores (B, D, and F).

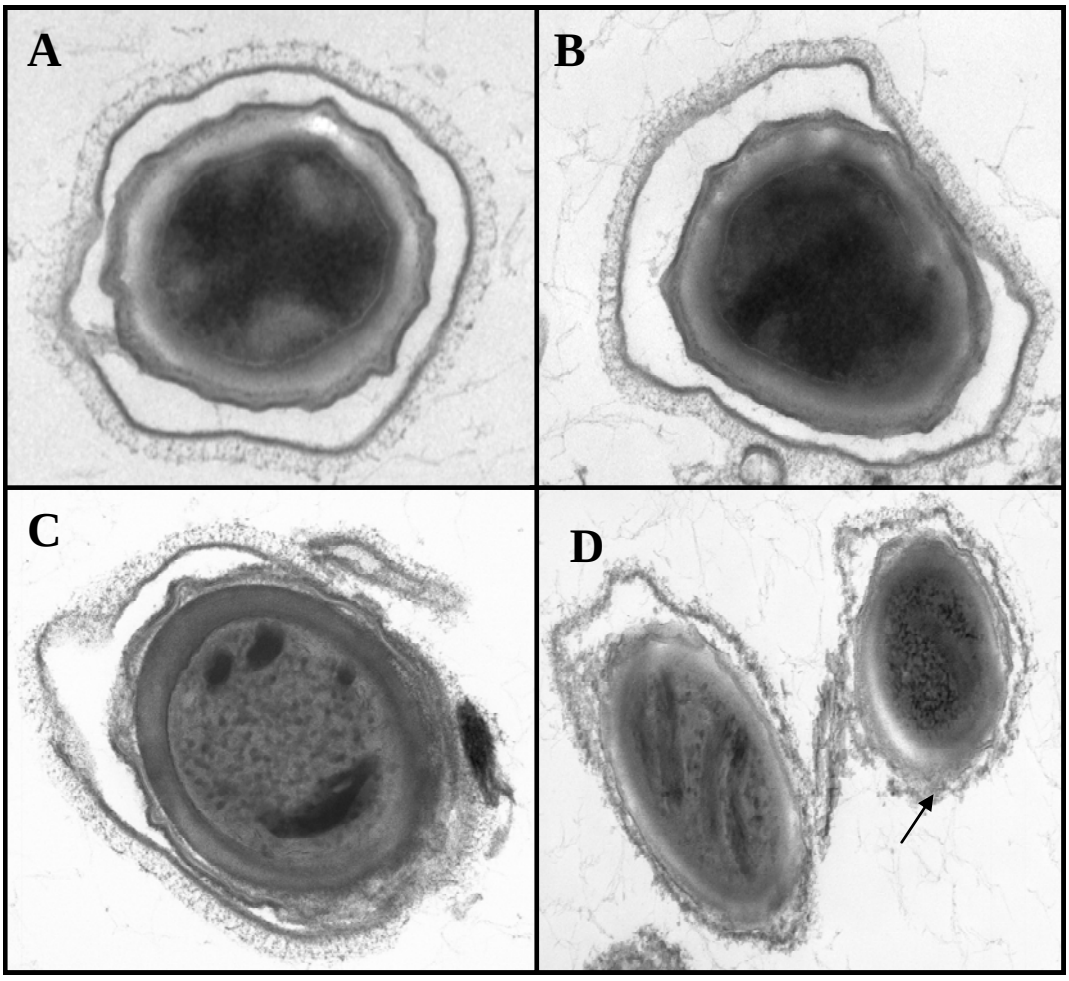

Figure 37: TEM of spores untreated (Panels A and B) or treated with SDS (Panel C) or Urea buffer (Panel D). An arrow denotes the fuzzy, modified appearance of the exosporium after boiling in urea buffer.

DISCUSSION

Much of what we know about spore maturation was learned from studies with *Bacillus subtilis* and its well defined genetic systems. However, *B. subtilis* does not possess either a distinct exosporium layer or BclA- or BclB-like proteins. Thus no information is available from the *B. subtilis* literature to extrapolate to the assembly of this outermost spore layer in *B. anthracis*. The exosporium is a prominent spore feature of organisms of the *B. cereus* family, a group comprised of animal and insect pathogens. The exosporium layer may therefore be important for spore interactions with host cells.

BclB has many similarities to the well-characterized exosporium glycoprotein BclA. Like BclA, it also contains an internal collagen-like tandem repeat (GITGVTGAT). As in BclA, the repeated threonines in the BclB repeat are the likely sites of glycosylation, and the BclB-associated sugars rhamnose, 3-*O*-methyl rhamnose, and galactosamine have been identified. Recent microarray data showed that both *bclA* and *bclB* are transcribed simultaneously during sporulation (54). The *bclA* and *bclB* determinants are both preceded by σ^K-like promoter sequences and expression of these genes initiates late in sporulation (54). Both glycoprotein determinants are expressed in conjunction with the rhamnose determinants in the operon adjacent to *bclA*, also containing a σ^K-like promoter element. This expression pattern is consistent with expression from promoters regulated by this late mother-cell-specific sigma factor and is consistent with the placement of BclB in the outer spore layers.

Under SEM, the *bclB* mutant appears to have a more dimpled appearance, with a decrease in the presence of the pronounced ridges found in the wild-type spores. Chada and coworkers utilized atomic force microscopy to characterize spore surfaces and suggested that the presence of ridges in spores signifies the loss of the exosporium layer (12). Using anti-BclA sera, our immunogold-labeled spores appeared to be encased within an exosporium as evidenced by the presence of the surface-exposed BclA. The presence of the BclA-containing exosporium was independent of the appearance of the ridges on the spore surface. Loss of the BclB protein has an impact on both the integrity and stability of the exosporium, as well as modifying the appearance of the exosporium under SEM.

Examination of material extracted from spores further supports our conclusion that BclB is associated with the exosporium. Other exosporium-associated proteins when extracted and subjected to SDS PAGE analysis have been found to co-migrate with BclA in a heterogenous band of >200 kDa. The presence of BclB migrating in similarly sized complexes further suggests its association in similar complexes. The decreased yield of BclB from spores suggests that it is present at a lower concentration then BclA, or is more securely anchored than BclA.

We have found that BclB is surface exposed on the spores of *B. anthracis*. It has been shown that antibodies can not cross the exosporium, suggesting that BclB is in the exosporium and not residual fluorescence from the spore coat (159). By immunofluorescence we have shown a consistent binding of our anti-BclB antibodies to the surface of spores. The intensity of the binding is less than that observed with anti-BclA antibodies. The heterogeneity of the

fluorescence of the spores with anti-BclA antibodies could be explained by the differing accessibilities of the antibodies to the protein backbone epitopes of BclA due to the differing glycosylation patterns, or may support a nonuniform assembly of the exosporium, as recently described (97).

The length of the surface filaments on the exosporium surface correlates with BclA repeat number and *bclA*-negative spores possess no visible hair-like nap layer, indicating that the nap is largely composed of this protein (15, 19). Immunofluorescence studies reported herein indicate that the BclB glycoprotein is also surface exposed on the spore and plays a role in the structural integrity of the exosporium layer as indicated by the increased fragility of this layer in spores lacking this protein. The fact that the *bclA* mutant spores are devoid of a noticeable nap does not rule out the possible presence of BclB in the nap. The lower content of BclB expressed on the exosporium may not produce visible filaments without the presence of BclA. Loss of BclB and its associated sugars could leave architectural voids within the exosporium nap layer that are selectively filled with BclA and may lead to an increase in BclA incorporation and the relative increase in BclA as seen on western blots and immunofluorescence. Alternatively, loss of BclB could also open up gaps in the nap that better allow antibodies access to BclA epitopes or could orient the BclA protein in a way that can be more easily extracted from the exosporium.

The loss of the BclB glycoprotein from the exosporium and possibly from other sites within mutant spores leads to a more fragile exosporium layer. Examination of the BclB-negative spores under TEM and by immunofluorescence demonstrated that often this fragility is at one pole of the spore. BclB was found to localize in greater amounts at one pole of the cells in the

CTL292 *bclA* deletion strain, suggesting that BclB accumulates at the pole of the spore, or potentially in the cap structure described by Turnbough and coworkers (75, 97). If the BclB protein has a structural role at the pole of the exosporium, lack of BclB at this site may lead to the polar damage seen in the TEM and immunofluorescence micrographs. Stress of the exosporium may lead to breakage at the pole. The exosporium cap has been reported to be a weakened spot in the exosporium where newly germinated cells emerge (97). BclB may play a role in strengthening or anchoring the cap, and lack of BclB could lead to a weaker cap that pops off more easily. When BclB-negative spores were stained with anti-BclA sera, many of the spores exhibited no staining at one pole. We interpreted this as a lack of exosporium at the pole and not a lack of antibody staining, consistent with the damage seen in the TEM micrographs. The percentage of spores with damage seen under TEM is roughly equal to the percentage of mutant spores seen under Immunofluorescence without polar staining or a cap. Without the exosporium at the cap or pole, the exosporia may slough off, as is evident under TEM. These sloughed off exosporia may be more susceptible to extraction, leading to the increased amount of BclA found in the BclB-negative spores by western blot.

The effects of ethanol exposure and presumably the dehydration/rehydration process may underscore the significant role of BclB in the architecture of the exosporium. Since BclB may play also play a role in the flexibility of the exosporium, the ΔBclB mutant may lose this flexibility causing increased breakage of the exosporium when stressed by the dehydration/rehydration of the spore.

BclB plays a role in the structural integrity of the exosporium. The influence of BclB on the incorporation of the BclA protein and on the overall architecture of the spore, directly or indirectly, is one of the keys in the formation or maintenance of a rigid and complete exosporium structure in *B. anthracis*.

Bibliography

1. **Gould GW**. History of Science – Spores. J. Applied Microb. 2006;101:507-523

2. **Pickering AK, Osorio M, Lee GM, Grippe VK, Bray M, Merkel TJ.** Cytokine response to infection with *Bacillus anthracis* spores. Infect Immun. 2004;72(11):6382-6389

3. **Brossier F, Levy M, Mock M.** Anthrax spores make an essential contribution to vaccine efficiency. Infect Immun 2000;68(10):5731-5734.

4. **Kiel JL, Parker JE, Alls JL, Kalns J, Holwitt EA, Stribling LJ, Morlaes PJ, Bruno JG**. Rapid recovery and Identification of Anthrax bacteria from the environment. Ann N Y Acad Sci. 2000;916:240-252

5. **Mesnage S, Tosi-Couture E, Gounon P, Mock M, Fouet A**. The Capsule and S-Layer: Two Independent and Yet Compatible Macromolecular Structures in *Bacillus anthracis*. J Bacteriol 1998;180(1):52-58

6. **Mignot T, Mock M, Fouet A**. Developmental Switch of S-layer protein synthesis in *Bacillus anthracis*. Mol. Microbiology. 2002;43(6):1615-1628

7. **Couture-Tosi E, Delcroix H, Mignot T, Mesnage S, Chami M, Fouet A, Mosser G.** Structural Analysis and Evidence for Dynamic emergence of *Bacillus Anthracis* S-layer Networks. J Bacteriol 2002;184(23):6448-6456

8. Nessi C, Jedrzejas MJ, Setlow P. Structure and mechanism of action of the protease that degrades small acid soluble spore proteins during germination of spores of *Bacillus* species. J Bacteriol. 1998;180(19): 5077-5084

9. Moir A. Spore Germination. Cell. Mol. Life Sci. 2002;59:403-409

10. Setlow P. Spores of *Bacillus subtilis*: their resistance to and killing by radiation, heat, and chemicals. J. Appl. Microb. 2006;101(3):514-525

11. Moir A. How do spores germinate? J Appl Microb 2006;101(3):526-530

12. Chada VG, Sansted EA, Wang R, Driks A. Morphogenesis of *Bacillus* spore surfaces. J. Bacteriology. 2003;185(21):6255-6261

13. Redmond C, Baillie LW, Hibbs S, Moir AJ, Moir A. Identification of proteins in the exosporium of *Bacillus anthracis*. Microbiology. 2004;150:355-363

14. Plomp M, Leighton TJ, Wheller KE, Malkin AJ. The high-resolution architecture and structural dynamice of *Bacillus* spores. Biophys J 2005;88(1):603-606

15. Steichen C, Chen P, Kearney JF, Turnbough CL. Identification of the immunodominant protein and other proteins of the *Bacillus anthracis* exosporium, J. Bacteriol 2003;185(6):1903-1910

16. Ireland JA, Hanna PC. Amino acid- and purine ribonucleoside-induced germination of *Bacillus anthracis* Delta sterne endospores: gerS mediated responses to aromatic ring structures. J. Bacteriol. 2002;184(5):1296-303

17. Cabrera-Martinez RM, Tovar-Rojo F, Vepachedu VR, Setlow P. Effects of overexpression of nutrient receptors on germination of spores of *Bacillus subtilis*. J Bacteriol 2003;185(8):2457-2464

18. Charlton S, Moir AJ, Baillie L, Moir A. Chacterization of the exosporium of *Bacillus cereus*. J Appl. Micro. 1999;87(2):241-245

19. Sylvestre P, Couture-Tosi E, Mock M. A collagen-like surface glycoprotein is a structural component of the *Bacillus anthracis* exosporium. Mol. Microbiol. 2002;45(1):169-178

20. Welkos SL, Cote CK, Rea KM, Gibbs PH. A microtiter fluorometric assay to detect the germination of *Bacillus anthracis* spores and the germination inhibitory effects of antibodies. J. Microb. Methods. 2004;56(2):253-65

21. Weiner MA, Read TD, Hanna PC. Identification and Characterization of the gerH operon of *Bacillus anthracis* endospores: a differential role for purine nucleosides in germination. J.Bacteriol. 2003;185(4):1462-1464

22. Weiner MA, Hanna PC. Macrophage-mediated germination of *Bacillus anthracis* endospores requires the GerH operon. J Bacteriol 2003;71(7):3954-3959

23. Daubenspeck JM, Zeng H, Chen P, Dong S, Steichen CT, Krishna NR, Pritchard DG, Turnbough CL Jr. Novel Oligosaccharide side chains of the collagen-like region of BclA, the major glycoprotein of the *Bacillus anthracis* exosporium. J. Biol. Chem. 2004;279(30):30945-30953

24. Kim HS, Sherman D, Johnson F, Aronson AI. Characterization of a major *Bacillus anthracis* spore coat protein and its role in spore inactivation. J.Bacteriol. 2004;186(8):2413-2417

25. Steichen CT, Kearney JF, Turnbough CL. Characterization of the exosporium basal layer protein BxpB of *Bacillus anthracis*. J. Bacteriol. 2005;187(17):5868-5876

26. Acha, Pedro and Szyfres, Boris. Zoonoses and communicable diseases common to man and animals. 3rd edition. 2003, Renouf Publishing Co. Ltd, Ogdensburg, NY 13669

27. Hasegawa M, Yang K, Hashimoto M, Park JH, Kim YG, Fujimoto Y, Nunez G, Fukase K, Inohara N. Differential release and distribution of NOD1 and NOD2 immunostimulatory molecules among bacterial species and environments. J. Biol. Chem. 2004;281(39):29054-29063

28. Basu S, Kang TJ, Chen WH, Fenton MJ, Baillie L, Hibbs S, Cross AS. Role of *Bacillus anthracis* (BA) spore strutures in macrophage cytokine responses. Infect. Immun. 2007;75(5):2351-2358

29. Oncu S, Oncu S, Sakarya S. Anthrax – an overview. Med Sci Monit. 2003;9(11):276-283

30. Mock M, Fouet A. Anthrax. Annu Rev Microbiol. 2001;55:647-671

31. Baillie LWJ. Past, imminent, and future human medical countermeasures for anthrax. J.Appl Microb 2006;101(3):594-606

32. Xu Q, Hesek ED, Zeng M. Transcriptional stimulation of anthrax toxin receptors by anthrax edema toxin and *Bacillus anthracis* Sterne spores. Microb Pathog 2007;43(1):37-45

33. Zhong W, Shou Y, Yoshida TM, Marrone BL. *Bacillus anthracis*, *B. cereus*, and *B. thuringiensis* differentiation using pulse field gel electrophoresis. Appl. Env. Micro. 2007;73(10):3446-3449

34. Russell B.H., Yasan R., Keene DR., and Xu Y. *Bacillus anthracis* internalization by human fibroblasts and epithelial cells. Cell Microb. May 2007;(5):1262-1274.

35. Heffernan BJ, Thomason B, Herring-Palmer A, and Hanna P. *Bacillus anthracis* anthrolysin O and three phospholipases C are functionally redundant in a murine model of inhalational anthrax. FEMS Microb Lett. Jun 2007:(1)98-105

36. Heffernan BJ, Thomason B, herring-Palmer A, Shaughnessy L, McDonald R, Fisher N, Huffnagle GB, Hanna P. *Bacillus anthracis* phospholipases C facilitate macrophage-associated growth and contribute to virulence in a murine model of inhalation anthrax. Infect Immun. Jul 2006;(7):3756-3764

37. Zink S, and Burns DL. Importance of SrtA and SrtB for growth of *Bacillus anthracis* in macrophages. Infect Immun. Aug 2005;73(8):5222-5228

38. Cendrowski S, MacArthur W, and Hanna P. *Bacillus anthracis* requires siderophore biosynthesis for growth in macrophages and mouse virulence. Mol Microb. 2004;51(2):407-417

39. Dixon TC, Fadl AA, Koehler TM, Swanson JA, and Hanna, PC. Early *Bacillus anthracis*-macrophage interactions: intracellular survival and escape. Cell. Microb 2000;2(6):453-463

40. Sirard JC, Guidi-Rontani C, Fouet A, Mock M. Characterization of a plasmid region involved in *Bacillus anthracis* toxin production and pathogenesis. Int. J. Med. Microb. 2000;290(4-5)313-316.

41. Guidi-Rontani C, Weber-Levy M, Labruyere E, Mock M. Germination of *Bacillus anthracis* spores within alveolar macrophages. Mol Microb. 1999 Jan;31(1):9-17

42. Guidi-Rontani C, Levy M, Ohavon H, Mock M. Fate of germinated *Bacillus anthracis* spores in primary murine macrophages. Mol Microb 2001 Nov;42(4):931-8

43. Cote CK, Rossi CA, Kang AS, Morrow PR, Lee JS, Welkos SL. The detection of protective antigen (PA) associated with spores of *Bacillus anthracis* and the effects of anti-PA antibodies on spore germination and macrophages interactions. Microb Pathog. 2005 May-Jun;38(5-6):209-225

44. Welkos S, Little S, Friedlander A, Fritz D, Fellows P. The role of antibodies to *Bacillus anthracis* and anthrax toxin components in inhibiting the early stages of infection by anthrax spores. Microbiology. 2001 Jun;147(6):1677-1685

45. Guidi-Rontani C, Pereira Y, Ruffie S, Sirard JC, Weber-Levy M, Mock M. Identification and characterization of a germination operon on the virulence plasmid pX01 of *Bacillus anthracis*. Mol Microb. 1999 Jul;33(2):407-414

46. Lee JY, Janes BK, Passalacqua KD, Pfelger BF, Bergman NH, Liu H, Hakansson K, Somu RV, Aldrich CC, Cendrowski S, Hanna PC, Sherman DH. Biosynthetic analysis of the petrobactin siderophore pathway from *Bacillus anthracis*. J. Bacteriol. 2007 Mar;189(5):1698-1710

47. Daniel R. Caldwell. Microbial Physiology and Metabolism. W.M. Brown Communications, Inc. 1995. Star Publishing Company (Belmont, CA)

48. Kozuka S, and Tochikubo K. Properties and origin of filamentous appendages on spores of *Bacillus cereus*. Microbiol. Immunol. 1985;29(1):21-37

49. Ruthel G, Ribot WJ, Bavari S, and Hoover, TA. Time-Lapse Confocal Imaging of Development of *Bacillus anthracis* in macrophages. J. Inf. Dis. 2004;189:1313-1316

50. Qi Y, Patra G, Liang X, Williams LE, Rose S, Redkar RJ, and DelVecchio VG. Utilization of the *rpoB* gene as a specific chromosomal marker for real-time PCR detection of *Bacillus anthracis* Appl. Envi. Micro. 2001;67(8):3720-3727

51. Helgason E, Okstad OA, Caugant DA, Johansen HA, Fouet A, Mock M, Hegna I, and Kolsta AB. *Bacillus anthracis*, *Bacillus cereus*, and *Bacillus thuringiensis* – one species on the basis of genetic evidence. Appl. Environ. Microbiol. 2000;66:2627-2630

52. Xu Y, Liang X, Chen Y, Koehler TM, Hook M. Identification and Biochemical characterization of two novel collagen binding MSCRAMMs of *Bacillus anthracis*. J. Biol. Chem. 2004;279(50)51760-51768

53. Hahn UK, Boehm R, and Beyer W. DNA vaccination against anthrax in mice-combination of anti-spore and anti-toxin components. Vaccine 2005;24(21):4569-4571

54. Bergman NH, Anderson EC, Swenson EE, Niemeyer MM, Miyoshi AD, and Hanna, PC. Transcriptional Profiling of the *Bacillus anthracis* Life Cycle *In Vitro* and an Implied Model for Regulation of Spore Formation. J. Bacteriol. 2006;188(17)6092-6100.

55. Lai E, Phadke ND, Kachman MT, Giorno R, Vazquez S, Vazquez JA, Maddock JR, and Driks A. Proteomic Analysis of the spore coats of *Bacillus subtilis* and *Bacillus anthracis*. J. Bacteriol 2003;185(4):1443-1454

56. Firoved AM, Miller GF, Moayeri M, Kakkar R, Shen Y, Wiggins JF, McNally EM, Tang W, and Leppla SH. *Bacillus anthracis* Edema Toxin Causes Extensive Tissue Lesions and Rapid Lethality in Mice. Amer. J. Path. 2005;167(5)1309-1320

57. Rampersad J, Khan A, and Ammons D. A *Bacillus thuringiensis* isolate possessing a spore-associated filament. Curr. Microbiol. 2003 Oct;47(4):355-357

58. Setlow P. Spores of *Bacillus subtilis*: their resistance to and killing by radiation, heat, and chemical. J. Appl. Microbiol. 2006;101:514-525

59. Hart SJ, Terray A, Leski TA, Arnold J, Stroud R. Discovery of a significant optical chromotagraphic difference between spores of *Bacillus anthracis* and its closest relative, *Bacillus thuringiensis*. Anal. Chem 2006;78:3221-3225

60. Dai L, and Zimmerly S. Compilation and analysis of group II intron insertions in bacterial genomes: evidence for retroelement behavior. Nuc. Acids Res. 2002;30(5)1091-1102

61. Chitlaru T, Ariel N, Zvi A, Lion M, Velan B, Shafferman A, and Elhanany E. Identification of chromosomally encoded membranal polypeptides of *Bacillus anthracis* by a proteomic analysis: Prevelance of proteins containing S-layer homology domains. Proteomics 2004;677(4):677-691

62. Klichko VI, Miller J, Wu A, Popov SG, and Alibek K. Anaerobic induction of *Bacillus anthracis* hemolytic activity. Bioch. Biophys. Res. Comm. 2003;303:855-862

63. Agaisse H, Gominet M, Okstaf OA, Kolsto AM, and Lereclus D. PlcR is a pleiotrophic regulator of extracellular virulence factor gene expression in *Bacillus thuringiensis*. Mol. Microb. 1999;32:104310-104353

64. Mignot T, Mock M, Robichon D, Landier A, Lerechis D, and Fouet A. The incompatability between PlcR- and AtxA-controlled regulons may have been selected a nonsense mutation in *Bacillus anthracis*. Mol. Microb. 2001;42:1189-1198

65. Pomerantsev AP, Kalnin KV, Osorio M, and Leppla SH. Phosphotidylcholine-specific Phospholipase C and Sphingomyelinase activities in bacteria of the *Bacillus cereus* group. Infect. Immun. 2003;71(11):6591-6606

66. Drysdale M, Bourgogne A, and Koehler TM. Transcriptional Analysis of the *Bacillus anthracis* capsule regulators. J. Bacteriol. 2005;187(15):5108-5114

67. Bourgogne A, Drysdale M, Hilsenbeck SG, Peterson SN, and Koehler TM. Global effects of virulence gene regulators in a *Bacillus anthracis* strain with both virulence plasmids. Infect. Immun. 2003;71:2736-2743

68. Saile E, and Koehler T. *Bacillus anthracis* multiplication, persistence, and genetic exchange in the rhizosphere of grass plants. Appl. Env. Micro. 2006;72:3168-3174

69. Rety S, Salamitou S, Garcia-verdugo I, Hulmes DJS, Le Hegerat F, Chaby R, and Lewit-Bentley A. The crystal structure of the *Bacillus anthracis* spore surface protein BclA shows remarkable similarity to mammalian proteins. J. Biol. Chem. 2005;280(52):43073-47078

70. Saksena R, Adamo R, and Kovac P. Synthesis of the tetrasaccharide side chain of the major glycoprotein of the *Bacillus anthracis* exosporium. Bioorg. Med. Chem. Lett. 2006;16:615-617

71. Adamo R, Saksena R, and Kovac P. Synthesis of the β-anomer of the spacer-equipped tetrasaccharide side chain of the major glycoprotein of the *Bacillus anthracis* exosporium. Carbohydrate Res. 2005;340:2579-2582

72. Salamitou S, Rety S, Le Hegarat F, Leblon G, and Lewit-Bentley A. The use of high halide-ion concentrations and automated phasing procedures fro the structural analysis of BclA, the major component of the exosporium of *Bacillus anthracis* spores. Acta Cryst. 2005;61:344-349

73. Abachin E, Poyart C, Pellegrini E, Milhanic E, Fiedler F, Berche P, and Cuot P. Formation of D-alanyl-lipotechoic acid is required for adhesion and virulence of *Listeria monocytogenes.* Mol. Microb. 2002;43:1-14

74. Daubenspeck JM, Zeng H, Chen P, Dong S, Steichen CT, Krishna NR, Pritchard DG, and Turnbough CL. Novel Oligosaccharide side chains of the collagen-like region of BclA, the major glycoprotein of the *Bacillus anthracis* exosporium. J. Biol. Chem. 2004;279(30):30945-30953

75. Boyston JA, Chen P, Steichen CT, and Turnbough CL. Orientation within the exosporium and structural stability of the collagen-like glycoprotein BclA of *Bacillus anthracis*. J. Bacteriol. 2005;187(15):5310-5317

76. Mehta AS, Saile E, Zhong W, Buskas T, Carlson R, Kannenberg E, Reed Y, Quinn CP, and Boons G. Synthesis and antigenic analysis of the BclA glycoprotein oligosaccharide from the *Bacillus anthracis* exosporium. Chemistry. 2006;;12(36):9136-9149

77. Bozue J, Cote CK, Moody KL, and Welkos SL. Fully virulent *Bacillus anthracis* does not require the immunodominant protein BclA for pathogenesis. Infect. Immun. 2007;75(1):508-511

78. Koshikawa T, Yamazaki M, Yoshimi M, Ogawa S, Yamada A, Watabe K, and Torii M. Surface hydrophobicity of spores of *Bacillus* spp. J. Gen. Microbiol. 1989;135(10):2717-2722.

79. Todd SJ, Moir AJG, Johnson MJ, and Moir A. Genes of *Bacillus cereus* and *Bacillus anthracis* encoding proteins of the exosporium. J. Bacteriol. 2003;185(11):3373-3378

80. Sylvestre P, Couture-Tosi E, and Mock M. Contribution of ExsFA and ExsFB proteins to the localization of BclA on the spore surface and to the stability of the *Bacillus anthracis* exosporium. J. Bacteriol. 2005;187(15):5122-5128

81. Bailey-Smith K, Todd SJ, Southworth TW, Proctor H, and Moir A. The ExsA protein of *Bacillus cereus* is required for assembly of coat and exosporium onto the spore surface. J. Bacteriol. 2005;187(11):3800-3806

82. Werz DB, and Seeberger PH. Total synthesis of antigen *Bacillus anthracis* tetrasaccharide-Creation of an anthrax vaccine candidate. Angew. Chem. Int. Ed. 2005;44:6315-6318

83. Sylvestre P, Couture-Tosi E, and Mock M. Polymorphism in the collagen-like region of *Bacillus anthracis* BclA protein leads to variation in exosporium filament length. J. Bacteriol 2003;185(5):1555-1563

84. Swiecki MK, Lisanby MW, Shu F, Turnbough CL, and Kearney, JF. Monoclonal antibodies for *Bacillus anthracis* spore detection and functional analyses of spore germination and outgrowth. J. Immun. 2006 6076-6084

85. Boydston JA, Yue L, Kearney JF, and Turnbough CL. The ExsY protein is required for complete formation of the exosporium of *Bacillus anthracis*. J. Bacteriol. 2006;188(21):7440-7448

86. Johnson MJ, Todd SJ, Ball DA, Shepard AM, Sylvestre P, and Moir A. ExsY and CotY are required for the correct assembly of the exosporium and spore coat of *Bacillus cereus*. J. Bacteriol. 2006;188(22):7905-7913

87. Giorno R, Bozue J, Cote C, Wenzel T, Moody KS, Mallozi M, Ryan M, Wang R, Zielke R, Maddock JR, Friedlander A, Welkos S, and Driks A. Morphogenesis of the *Bacillus anthracis* spore. J. Bacteriol. 2007;189(3):691-705

88. Liu H, Bergman NH, Thomason B, Shallom S, Hazen A, Crossno J, Rasko DA, Ravel J, Read TD, Peterson SN, Yates III J, and Hanna, P. Formation and composition of the *Bacillus anthracis* endospore. J. Bacteriol. 2004;186(1):164-178

89. Waller LN, Stump MJ, Fox KF, Harley WM, Fox A, Stewart GC, and Shahgholi M. Identification of a second collagen-like glycoprotein produced by *Bacillus anthracis* and demonstration of associated spore-specific sugars. J. Bacteriol. 2005;187(13):4592-4597

90. Collins LV, Kristian SA, Weidenmaier C, Faigle M, Kessel KP, Strijp JA, Gotz F, Neumeister B, and Peschel A. *Staphylococcus aureus* strains lacking D-alanine modification of teichoic acids are highly susceptible to human nuetrophil killing and are virulence attenuated in mice. 2002 J. Inf. Disease 186:214-219

91. Williams DD and Turnbough CL. Surface layer protein EA1 is not a component of *Bacillus anthracis* spores but is a persistent contaminant in spore preperations. J. Bacteriol. 2004;186(2):566-569

92. Bozue JA, Parthasarathy N, Phillips LR, Cote CK, Fellows PF, Mendelson I, Shafferman A, and Friedlander AM. Construction of a rhamnose mutation in *Bacillus anthracis* affects adherence to macrophages but not virulence in guinea pigs. Microb. Patho. 2005;38:1-12

93. Fisher N, Sherton-Rama L, Herring-Palmer A, Heffernan B, Bergman N, and Hanna P. The dltABCD operon of *Bacillus anthracis* Sterne is required for virulence and resistance to peptide, enzymatic, and cellular mediators of innate immunity. J. Bacteriol. 2006;188(4):1301-1309

94. Rasmussen M, Jacobsson M, and Bjorck L. Genome-based identification and analysis of collagen-related structural motifs in bacterial and viral proteins. J. Biol. Chem. 2003;278(34):32313-32316

95. Karlstrom A, Jacobsson K, and Guss B. SclC is a member of a novel family of collagen-like proteins in *Streptococcus equi* subspecies *equi* that are recognized by antibodies against SclC. Vet. Microbiol. 2006;114:72-81

96. Humtsoe JO, Kim JK, Xu Y, Keen DR, Hook M, Lukomski S, and Wary KK. A streptococcus collagen-like protein interacts with the $\alpha 2\beta 1$ integrin and induces intracellular signaling. J. Biol. Chem. 2005;289(14):13848-13857

97. Steichen CT, Kearney JF, and Turnbough CL. Non-uniform assembly of the *Bacillus anthracis* exosporium and a bottle cap model for spore germination and outgrowth. Mol. Microb. 2007;64(2):359-367

98. Williamson ED, Hodgson I, Walker NK, Topping AW, Duchars MG, Mott JM, Estep J, LeButt C, Flick-Smith HC, Jones HE, Li H, and Quinn CP. Immunogenecity of recombinant protective antigen and efficacy against aerosol challenge with anthrax. Infect. Immun. 2005;73(9):5978-5987

99. Castanha ER, Swiger RR, Senior B, Fox A, Waller LN, Fox KF. Strain discrimination among *B. anthracis* and related organisms by characterization of BclA polymorphisms using PCR coupled with agarose gel or microchannel fluidics electrophoresis. J. Microbiol Methods. 2006;64(1):27-45

100. Mohamed N, Clagett M, Li J, Jones S, Pincus S, D'Alia G, Nardone L, Babin M, Spitalny G, and Casey L. A High-affinity Monoclonal Antibody to Anthrax Protective Antigen Passively Protects Rabbits before and after Aerosolized *Bacillus anthracis* spore Challenge. Infect. Immun. 2005;73(2):795-802

101. Xie H, Gursel I, Ivins BE, Singh M, O'Hagan DT, Ulmer JB, and Klinman DM. CpG Oligodeoxynucleotides Adsorbed onto Polyactide-Co-Glycolide Microparticles Improve the Immunogenecity and Protective Activity of the Licensed Anthrax Vaccine. Infect. Immun. 2005;73(2):828-833

102. Lee JS, Hadjipanayis AG, and Welkos SL. Venezuelan Equine Encephalitis Virus-Vectored Vaccines Protect Mice against Anthrax Spore Challenge. Infect. Immun. 2003;71(3):1491-1496

103. Schneerson R, Kubler-Kielb J, Liu T, Dai Z, Leppla SH, Yergey A, Backlund P, Shiloach J, Majadly F, and Robbins JB. Poly(gamma-D-glutamic acid) protein conjugates induce IgG antibodies in mice to the capsule of *Bacillus anthracis*: A potential addition to the anthrax vaccine. PNAS 2003;100(15):8945-8950

104. Kudva IT, Griffin RW, Garren JM, Calderwood SB, and John M. Identification of a Protein Subset of the Anthrax Spore Immunome in Humans Immunized with the Anthrax Vaccine Adsorbed Preparation. Infect. Immun. 2005;73(9):5685-5696

105. Turnbull, PC. Anthrax Vaccines: past, present, and future. Vaccine 1986;9:533-539

106. Broster MG, and Hibbs SE. Protective efficacy of anthrax vaccines against aerosol challenge. Salisbury Med. Bull. Sp. Suppl. 1990 68:91-92

107. Welkos SL, Keener TJ, and Gibbs PH. Differences in susceptibility of inbred mice to *Bacillus anthracis*. Infect. Immun. 1986;51:795-800

108. **Little SF, Knudson GB**. Comparative efficacy of Bacillus anthracis live spore vaccine and protective antigen vaccine against anthrax in the guinea pig. Infect Immun. 1986 May;52(2):509-512

109. Iber D, Clarkson J, Yudkin MD, and Campbell ID. The mechanism of cell differentiation in *Bacillus subtilis*. Nature Letters. 2006;441:371-374

110. Haldenwang, WG. The Sigma Factors of *Bacillus subtilis*. Microb. Reviews. 1995;59(1):1-30

111. Hilbert DW, and Piggot PJ. Compartmentalization of Gene Expression during *Bacillus subtilis* Spore Formation. Microb. Mol. Biol. Rev. 2004;68(2):234-262

112. Cui X, Li Y, Laird MW, Subramanian M, Moayeri M, Leppla SH, Fitz Y, Su J, Sherer K, and Eichacker PQ. *Bacillus anthracis* Edema and Lethal Toxin Have Different Hemodynamic Effects but Function Together to Worsen Shock and Outcome in a rat model. J. Inf. Dis. 2007;195:572-579

113. Hadjifrangiskou M, Chen Y, and Koehler TM. The alternative sigma factor SigH is required for toxin gene expression by *Bacillus anthracis*. J. Bacteriol. 2007 Mar;189(5):1874-1883

114. Tournier J, Quesnel-Hellmann A, Cleret A, and Vidal DR. Contribution of toxins to the pathogenesis of inhalational anthrax. Cell. Microb. 2007 1-11

115. Brittingham KC, Ruthel G, Panchal RG, Fuller CL, Ribot WJ, Hoover TA, Young HA, Anderson AO, and Bavari S. Dendritic cells endocytose *Bacillus anthracis* spores:implications for anthrax pathogenesis. J. Immuno. 5545-5552

116. Pickering AK, Osorio M, Lee GM, Grippe VK, Bray M, and Merkel TJ. Cytokine Response to Infection with *Bacillus Anthracis* Spores. Infect. Immun. 2004;72(11):6382-6389

117. Cordoba-Rodriguez R, Fang H, Lankford CSR, and Frucht DM. Anthrax Lethal Toxin Rapidly Activates capsase-1/ICE and induces extracellular release of Interleukin IL-1B and IL-18. J. Biol. Chem. 2004;279(20):20563-20566

118. Bergman NH, Passalacqua KD, Gaspard R, Sherton-Rama LM, Quackenbush J, and Hanna PC. Murine Macrophage transcriptional responses to *Bacillus anthracis* infection and intoxification. Infect. Immun. 2005;73(2):1069-1080

119. Drysdale M, Heninger S, Hutt J, Chen Y, Lyons CR, and Koehler TM. Capsule Biosynthesis by *Bacillus anthracis* is required for dissemination in murine inhalational anthrax. EMBO 2005;24:221-227

120. Agrawal A, Lingappa J, Leppla SH, Agrawal S, Jabbar A, Quinn C, and Pulendran B. Impairment of dendritic cells and adaptive immunity by anthrax lethal toxin. Nature Letters. 2003;424:329-334

121. Salles II, Tucker AM, Voth DE, and Ballard JD. Toxin-induced resistance in *Bacillus anthracis* lethal toxin-treated macrophages. PNAS 2003;100(21):12426-12431

122. Welkos S, Friedlander A, Weeks S, Little S, and Mendelson I. *In vitro* characterization of the phagocytosis and fate of anthrax spores in macrophages and the effects of anti-PA antibody. J. Med. Microb. 2002;51:821-831

123. Kirby, JE. Anthrax lethal toxin induces human endothelial cell apoptosis. Infect. Immun. 2004;72(1):430-439

124. Cote CK, Rea KM, Norris SL, Van Rooijen N, and Welkos SL. The use of *in vivo* macrophage depletion to study the role of macrophages during infection with *Bacillus anthracis* spores. Microb. Patho. 2004;37:169-175

125. Kaufmann, AF, Meltzer, MI, and Schmid, GP. The Economic Impact of a Bioterrorist Attack: Are Prevention and Postattack Intervention programs Justifiable? Emerging Infectious diseases, 1997;3(2): 83-94.

126. Hoffmaster AR, Ravel J, Rasko DA, Chapman GD, Chute MD, Marston CK, De BK, Sacchi CT, Fitzgerald C, Mayer LW, Maiden MCJ, Priest FG, Barker M, Jiang L, Cer RZ, Rilstone J, Peterson SN, Weyant RS, Galloway DR, Read TD, Popovic T, and Fraser CM. Identification of anthrax toxin genes in a *Bacillus cereus* associated with an illness resembling inhalation anthrax. PNAS. 2004;101(22):8449-8454

127. Hoffmaster AR, and Koehler TM. Control of virulence gene expression in *Bacillus anthracis*. J. Appl. Microb. 1999;87:279-281

128. Koehler TM, Dai Z, and Kaufman-Yarbray M. Regulation of the *Bacillus anthracis* protective antigen gene: CO2 and a trans-acting element activate transcription from one of two promoters. J. Bacteriol. 1994:176(3):586-595

129. Drysdale M, Bourgogne A, Hilsenbeck SG, and Koehler TM. AtxA controls *Bacillus anthracis* capsule synthesis via acpA and a newly discovered regulator acp*B.* J. Bacteriol. 2004:186(2):307-315

130. Mignot T, Mock M, and Fouet A. A plasmid-encoded regulator couples the synthesis of toxins and surface structures in *Bacillus anthracis*. Mol. Microb. 2003;47(4):917-927

131. Bourgogne A, Drysdale M, Hilsenbeck SG, Peterson SN, and Koehler TM. Global effects of virulence gene regulators in a *Bacillus anthracis* strain with both virulence plasmids. Infect. Immun. 2003:71(5):2736-2743

132. Abrami L, Liu S, Cosson P, Leppla SH, and Van Der Goot FG. Anthrax toxin triggers endocytosis of its receptor via a lipid raft-mediated clathrin-dependent process. J. Cell Biol. 2003;160(3):321-328

133. Kurzchalia T. Anthrax toxin rafts into cells. J. Cell. Biol. 2003:160(3):295-296

134. Pellizzari R, Guidi-Rontani C, Vitale G, Mock M, and Montecucco C. Anthrax lethal factor cleaves MKK3 in macrophages and inhibits the LPS/IFN-gamma release of NO and TNF alpha. FEBS Letters 1999;462:199-204

135. Park JM, Greten FR, Li Z, and Karin M. Macrophage apoptosis by anthrax lethal factor through p38 MAP kinase inhibition. Science 2002;297:2048-2051

136. Moayeri M, Haines D, young HA, and Leppla SH. *Bacillus anthracis* lethal toxin induces TNF-alpha-independent hypoxia-mediated toxicity in mice. J. Clin. Invest. 2003;112(5):670-682

137. Stranbacj MN and Collier RJ. Anthrax delivers a lethal blow to host immunity. Nature Med. 2003;9(8):996-997

138. Wu AG, Alibek D, Li YL, Bradburne C, Bailey CL, and Alibek K. Anthrax toxin induces hemolysis: an indirect effect through polymorphonuclear cells. J. Inf. Disease 2003;188:1138-1141

139. Gold JA, Hoshino Y, Hoshino S, Jones MB, Nolan A, and Weiden MD. Exogenous gamma and alpha/beta interferon rescues human macrophages from cell death induced by *Bacillus anthracis*. Infect. Immun. 2004;72(3):1291-1297

140. Ramarao N and Lereclus D. The InhA1 metalloprotease allows spores of the *B. cereus* group to escape macrophages. Cell. Microb. 2005;7(9):1357-1364

141. Raines KW, Kang TJ, Hibbs S, Cao G, Weaver J, Tsai P, Baillie LW, Cross AS, and Rowen GM. Importance of Nitric Oxide Synthase in the control of infection of *Bacillus anthracis*. Infect. Immun. 2006;74(4):2268-2276

142. Beaman TC, Pankratz HS, and Gerhardt P. Paracrystalline sheets reaggregated from solubilized exosporium of *Bacillus cereus*. J. Bacteriol. 1971;107(1):320-324

143. Beaman TC, Pankratz HS, and Gerhardt P. Ultrastructure of the exosporium and underlying inclusions in spores of *Bacillus megaterium* strains. J. Bacteriol 1972;109(3):1198-1209

144. HachisukaY, Kojima K, and Sato T. Fine filaments on the outside of the exosporium of *Bacillus anthracis* spores. J. Bacteriol 1966;91(6):2382-2385

145. Martinex-Pomares L, wienke D, Stillino R, McKenzie EJ, Anronl JN, Harris J, McGreal E, Sim RB, Isacke CM, and Gordon S. Carbohydrate-independent recognition of collagens by the macrophage mannose receptor. Eur. J. Immun. 2006;36:1074-1082

146. Jedrzejas MJ and Huang WJM. *Bacillus* species proteins involved in spore formation and degradation: from identification in the genome, to sequence analysis, and determination of function and structure. Crit. Rev. Bioch. Mol. Biol. 2003;38(3):173-198

147. Priest FG, Barker M, Baillie LWJ, Holmes EC, and Maiden MCJ. Population Structure and Evolution of the *Bacillus cereus* group. J. Bacteriol. 2004;186(23):7959-7970

148. Mosser Em and Rest RF. The *Bacillus anthracis* cholesterol-dependent cytolysin, anthrolysin O, kills human neutrophils, monocytes, and macrophages. BMC Microb. 2006;56(6):

149. Birnboim HC and Doly J. A rapid alkaline extraction procedure for screening of recombinant plasmid DNA. Nuc. Acid Res. 1979;7(6):1513-1523

150. Ho, S. N., H. D. Hunt, R. M. Horton, J. K. Pullen, and L. R. Pease. 1989. Site-directed mutagenesis by overlapping extension using the polymerase chain reaction. Gene **77**:51-59.

151. Horton, R. M., H. D. Hunt, S. N. Ho, J. K. Pullen, and L. R. Pease. 1989. Engineering hybrid genes without the use of restriction enzymes: gene splicing by overlap extension. Gene **77**:61-68.

152. Perez-Casal, J., M. G. Caparon, and J. R. Scott. 1991. Mry, a *trans*-acting positive regulator of the M protein gene of *Streptococcus pyogenes* with similarity to the receptor proteins of two-component regulatory systems. J. Bacteriol. **173**:2617–2624.

153. Chen, Y., F.C. Tenover, and T.M. Koehler. 2004. ß-lactamase gene expression in a penicillin-resistant *Bacillus anthracis* strain. Antimicrob. Ag. Chemother. **48**:4873-4877.

154. Green, B. D., L. Battisti, T. M. Koehler, C. B. Thorne, and B. E. Ivins. 1985. Demonstration of a capsule plasmid in *Bacillus anthracis*. Infec. Immun. **49**:291-297

155. Saile E., and T. M. Koehler. 2002. Control of anthrax toxin gene expression by the transition state regulator *abrB*. J Bacteriol **184**:370–380

156. Waller L., K. F. Fox, A. Fox, and R. L. Price. 2004. Ruthenium red staining for ultra-structural visualization of a glycoprotein layer surrounding the spore of *Bacillus anthracis* and *B. subtilis*. J. Microbiol. Meth. **58**:23-30.

157. Zolock, R. A., Li, G, Bleckman, C, Burggraf, L, and Fuller, D. 2006. Atomic force microscopy of *Bacillus* spore surface morphology. Micron **37**:363-369

158. Riesenman, P. J. and W. L. Nicholson. 2000. Role of the spore coat layers in *Bacillus subtilis* spore resistance to hydrogen peroxide, artificial UV-C, UV-B and solar UV radiation. Appl. Env. Micro. **66**:620-626.

159. Gerhardt P. Cytology of *Bacillus anthracis*. Fed. Proc. 1967;26(5):1504-1517

160. Hart CA and Beeching NJ. A spotlight on anthrax. Clin. Dermat. 2002;20(4):365-375

161. Cieslak TJ and Eitzen EM Jr. Clinical and epidemiological principles of anthrax. Emerg Inf. Dis. 1999;5(4):552-555

162. Bradley KA, Mogridge J, Mourez M, Collier RJ, Young JA. Identification of the cellular receptor for anthrax toxin. Nature. 2001 Nov 8;414(6860):225-229.

163. Hanna P. Lethal toxin actions and their consequences. J Appl Microbiol. 1999 Aug;87(2):285-287.

164. Leppla SH. Purification and characterization of adenylyl cyclase from *Bacillus anthracis*. Methods Enzymol. 1991;195:153-168.

165. O'Brien J, Friedlander A, Dreier T, Ezzell J, Leppla S. Effects of anthrax toxin components on human neutrophils. Infect Immun. 1985 Jan;47(1):306-310.

166. Wright GG, **Mandell GL**. Anthrax toxin blocks priming of neutrophils by lipopolysaccharide and by muramyl dipeptide**.** J Exp Med. 1986 Nov 1;164(5):1700-1709

167. Vancurik J. Causes of the failure of antibiotic prophylaxis of inhalation anthrax and clearance of the spores from the lungs.Folia Microbiol (Praha). 1966;11(6):459-464.

168. Bradaric N, Punda-Polic V. Cutaneous anthrax due to penicillin-resistant *Bacillus anthracis* transmitted by an insect bite. Lancet. 1992 Aug 1;340(8814):306-307.

169. Lalitha MK, Thomas MK. Penicillin resistance in *Bacillus anthracis*. Lancet. 1997 May 24;349(9064):1522.

170. Friedlander AM, Welkos SL, Pitt ML, Ezzell JW, Worsham PL, Rose KJ, Ivins BE, Lowe JR, Howe GB, Mikesell P Postexposure prophylaxis against experimental inhalation anthrax. J Infect Dis. 1993 May;167(5):1239-1243.

171. Hu H, Sa Q, Koehler TM, Aronson AI, Zhou D. Inactivation of *Bacillus anthracis* spores in murine primary macrophages. Cell Microbiol. 2006 Oct;8(10):1634-1642.

172. Alileche A, Serfass ER, Muehlbauer SM, Porcelli SA, Brojatsch J. Anthrax lethal toxin-mediated killing of human and murine dendritic cells impairs the adaptive immune response. PLoS Pathog. 2005 Oct;1(2):e19.

173. Gimenez AP, Wu YZ, Paya M, Delclaux C, Touqui L, Goossens PL. High bactericidal efficiency of type iia phospholipase A2 against *Bacillus anthracis* and inhibition of its secretion by the lethal toxin. J Immunol. 2004 Jul 1;173(1):521-530.

174. Batty S, Chow EM, Kassam A, Der SD, Mogridge J. Inhibition of mitogen-activated protein kinase signalling by *Bacillus anthracis* lethal toxin causes destabilization of interleukin-8 mRNA. Cell Microbiol. 2006 Jan;8(1):130-138.

175. Kassam A, Der SD, Mogridge J. Differentiation of human monocytic cell lines confers susceptibility to Bacillus anthracis lethal toxin. Cell Microbiol. 2005 Feb;7(2):281-292.

176. Fang H, Xu L, Chen TY, Cyr JM, Frucht DM. Anthrax lethal toxin has direct and potent inhibitory effects on B cell proliferation and immunoglobulin production.
J Immunol. 2006 May 15;176(10):6155-6161.

177. Fang H, Cordoba-Rodriguez R, Lankford CS, Frucht DM. Anthrax lethal toxin blocks MAPK kinase-dependent IL-2 production in CD4+ T cells. J Immunol. 2005 Apr 15;174(8):4966-4971.

178. Paccani SR, Tonello F, Ghittoni R, Natale M, Muraro L, D'Elios MM, Tang WJ, Montecucco C, Baldari CT. Anthrax toxins suppress T lymphocyte activation by disrupting antigen receptor signaling. J Exp Med. 2005 Feb 7;201(3):325-331.

179. Duverger A, Jackson RJ, van Ginkel FW, Fischer R, Tafaro A, Leppla SH, Fujihashi K, Kiyono H, McGhee JR, Boyaka PN. *Bacillus anthracis* edema toxin acts as an adjuvant for mucosal immune responses to nasally administered vaccine antigens.
J Immunol. 2006 Feb 1;176(3):1776-1783.

180. Warfel JM, Steele AD, D'Agnillo F. Anthrax lethal toxin induces endothelial barrier dysfunction.Am J Pathol. 2005 Jun;166(6):1871-1881.

181. Gozes Y, Moayeri M, Wiggins JF, Leppla SH. Anthrax lethal toxin induces ketotifen-sensitive intradermal vascular leakage in certain inbred mice. Infect Immun. 2006 Feb;74(2):1266-1272.

182. Kau JH, Sun DS, Tsai WJ, Shyu HF, Huang HH, Lin HC, Chang HH. Antiplatelet activities of anthrax lethal toxin are associated with suppressed p42/44 and p38 mitogen-activated protein kinase pathways in the platelets. J Infect Dis. 2005 Oct 15;192(8):1465-1474.

183. Alam S, Gupta M, Bhatnagar R. Inhibition of platelet aggregation by anthrax edema toxin. Biochem Biophys Res Commun. 2006 Jan 6;339(1):107-114.

184. Stewart GS, Eaton MW, Johnstone K, Barrett MD, Ellar DJ. An investigation of membrane fluidity changes during sporulation and germination of *Bacillus megaterium* K.M. measured by electron spin and nuclear magnetic resonance spectroscopy. Biochem Biophys Acta. 1980 Aug 4;600(2):270-290

185. Cowan AE, Olivastro EM, Koppel DE, Loshon CA, Setlow B, Setlow P. Lipids in the inner membrane of dormant spores of *Bacillus* species are largely immobile. Proc Natl Acad Sci U S A. 2004 May 18;101(20):7733-7738.

186. Clements MO, Moir A. Role of the gerI operon of *Bacillus cereus* 569 in the response of spores to germinants. J Bacteriol. 1998 Dec;180(24):6729-6735

187. Titball RW, Manchee RJ. Factors affecting the germination of spores of *Bacillus anthracis*. J Appl Bacteriol. 1987 Mar;62(3):269-273

188. Chen Y, Fukuoka S, Makino S. A novel spore peptidoglycan hydrolase of *Bacillus cereus*: biochemical characterization and nucleotide sequence of the corresponding gene, *sleL*. J Bacteriol. 2000 Mar;182(6):1499-1506.

189. Cohen S, Mendelson I, Altboum Z, Kobiler D, Elhanany E, Bino T, Leitner M, Inbar I, Rosenberg H, Gozes Y, Barak R, Fisher M, Kronman C, Velan B, Shafferman A. Attenuated nontoxinogenic and nonencapsulated recombinant *Bacillus anthracis* spore vaccines protect against anthrax. Infect Immun. 2000 Aug;68(8):4549-58.

190. Matz LL, Beaman TC, Gerhardt P. Chemical composition of exosporium from spores of *Bacillus cereus*. J Bacteriol. 1970 Jan;101(1):196-201

191. DesRosier JP, Lara JC. Isolation and properties of pili from spores of *Bacillus cereus*. J Bacteriol. 1981 Jan;145(1):613-619

192. Hunter ME, DeLamater ED. Observations on the nuclear cytology of spore germination in *Bacillus megaterium*. J Bacteriol. 1952 Jan;63(1):23-31

193. Cole HB, Ezzell JW Jr, Keller KF, Doyle RJ. Differentiation of *Bacillus anthracis* and other *Bacillus* species by lectins. J Clin Microbiol. 1984 Jan;19(1):48-53.

194. Timpl R, Beil W, Furthmayr H, Meigel W, Pontz B. Characterization of conformation independent antigenic determinants in the triple-helical part of calf and rat collagen. Immunology. 1971 Dec;21(6):1017-1030.

195. Mann K, Mechling DE, Bachinger HP, Eckerskorn C, Gaill F, Timpl R. Glycosylated threonine but not 4-hydroxyproline dominates the triple helix stabilizing positions in the sequence of a hydrothermal vent worm cuticle collagen. J Mol Biol. 1996;261(2):255-66.

196. Chopra AP, Boone SA, Liang X, Duesbery NS. Anthrax lethal factor proteolysis and inactivation of MAPK kinase. J Biol Chem. 2003 Mar 14;278(11):9402-6

197. Glomski IJ, Corre JP, Mock M, Goossens PL. Cutting Edge: IFN-gamma-producing CD4 T lymphocytes mediate spore-induced immunity to capsulated Bacillus anthracis. J Immunol. 2007 Mar 1;178(5):2646-50